NASA CR-
141795

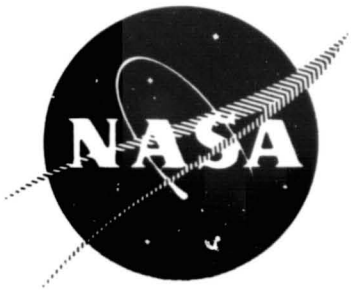

R-9690

HYDRAZINE GAS GENERATOR PROGRAM

Final Report

by

L. Kusak
R. Marcy

ROCKETDYNE
A DIVISION OF ROCKWELL INTERNATIONAL
6633 CANOGA AVENUE, CANOGA PARK, CALIFORNIA

Prepared for

NATIONAL AERONAUTICS AND SPACE ADMINISTRATION

Lyndon B. Johnson Space Center
Houston, Texas

FOREWORD

This report was submitted by the Rocketdyne Division of Rockwell International, 6633 Canoga Avenue, Canoga Park, California 91304, under Contract NAS9-13003 with the Lyndon B. Johnson Space Center, Houston, Texas.

Mr. R. Villemarette was the NASA program monitor for this program which was performed by Messrs. L. Kusak and R. Marcy of Rocketdyne. Mr. J. Speeds was the principal investigator under this contract.

CONTENTS

Introduction and Summary 1
Conclusions 2
Phase I: Gas Generator Design and Life Demonstration. 5
  Discussion 5
  Materials 5
  Stress Analysis 13
  Design/Operational Relationships 15
  Performance Characteristics 34
  Life Test 37
Phase II: Performance Tests 51
  Acceptance Tests 51
  Helium Saturation Study 54
  Off-Nominal Temperature Tests 61
  Altitude Start Study 64
  Duty Cycle Insensitivity Tests 69
  Start Sequence Varification 70
Phase III Program 73
  Introduction 73
  Experimental Program 74
  Test Setup 74
  Test Procedures 90
  Data and Results 94
Discussion of Results 113
  Gas Generator Operational Mode Efficiencies 113
  Gas Generator Response Characteristics 119
  Hot Restarts 120
  Thermal Bed Preheating 120
Conclusions 124
References 126

Appendix A

Performance Degradation of a Monopropellant Gas Generator in a Pulse Rate Modulated Mode of Operation A-1

Appendix B

Thermal Bed Packing Procedure B-1

Appendix C

Gas Generator Design Evolution C-1

Appendix D

Throttle Valve D-1

ILLUSTRATIONS

1. Gas Generator Assembly - SSAPU 6
2. Gas Generator - GGT-268-560 7
3. Gas Generator 8
4. Gas Generator Model GGT-191-460, External Radiation Heat Flux . . . 11
5. Wall Temperature vs Insulation External Temperature, Model GGT-191-460 12
6. Bed Characteristic Effects - GG Design - GGT-191-460 17
7. Bed Loading Effects on Temperature Distribution - Model GGT-268-460 21
8. Bed Loading Effects on Temperature Distribution - Model GGT-268-460 22
9. Effect of G/P_c on Gas Generator Operation 23
10. Effect of G/P_c on Gas Generator Operation 24
11. Mathematical Model of GG Decomposition Process 26
12. Model GGT-268-560-E, Test Run 10B-5, March 1973 28
13. Model 268-560-E, Test Run 11A-5 (d), March 1973 29
14. Stability Criteria 31
15. Gas Generator Stability Criteria Based on Analog Model Analysis (Flowrate = 0.372 lb/sec) 32
16. Stability Correlation, Test Data on GGT-191-460 33
17. Pressure Budget - Model GGT-268-560 35
18. Stability Correlation - Test Data on GGT-268-460 36
19. Gas Generator Test Installation 38
20. Gas Generator Test Installation 39
21. Approximate Flowrate Schedule (Half Mission Duty Cycle) 43
22. Life Test Results, 10 MDC's + 500 Seconds Sustained Maximum Power 45
23. Life Test - Exit Gas Temperature Variation 47
24. Life Test - Chamber Pressure Characteristics 48
25. Life Test - Bed Characteristics 50
26. Test Stand Installation Used for Gas Generator Characterization Under Nominal Operating Conditions 52

27. Test Stand Installation Used for Gas Generator Tests Under Nominal Operating Conditions 53
28. Test Stand Installation Used to Perform Tests with Helium Saturated Hydrazine 58
29. Test Stand Configuration Used for Heated Hydrazine Gas Generator Tests 63
30. View of Gas Generator Installed Within Vacuum Chamber for Heat Soakback and Altitude Start Evaluation 65
31. View of Altitude Chamber Showing Exhaust Port Closure Plate in the Open Position 66
32. Details of Test Stand Installation with Thermal Bed Heater Reactor for Preheating Main Gas Generator 75
33. Overall View of Test Installation Showing Auxiliary Fuel Tank and Electrically Powered GN_2 Heaters 77
34. Auxiliary Fuel Tank Installation 78
35. Thermal Bed Heater Reactor 79
36. Modified Throat Section 81
37. Gas Generator Installation 83
38. Gas Generator Instrumentation 86
39. Chamber Pressure and Temperature as a Function of Flowrate . . . 96
40. Fraction "On" Time for Low Inertia Machine 100
41. Fraction "On" Time for High Inertia Machine 101
42. Typical Oscillograph Trace for Pulse Operation 102
43. Test Conditions of τ and f for High and Low Inertia Machines. . . 103
44. Power Level as a Function of Machine Inertia and τ 104
45. Pulse Efficiency 107
46. Pilot Heater Gas Generator After Explosion 110
47. SPC as a Function of Power Control-Pulse vs Throttling and Machine Inertia 114
48. Pressure vs Pulse Modulated Relationship at Varying Power Levels 115
49. SPC Penalty Associated with Pressure Modulation as a Function of Power Level 117

TABLES

1. Temperature Distributions Model GGT-268-560 10
2. Thermal Bed Screen Design 13
3. Delivered Gas Characteristics 37
4. Sugar Stand 2 Instrumentation List 40
5. Mission Duty Cycle Schedule 42
6. Performance Tests 55
7. Instrumentation 87
8. Pulse Mode Tests 95
9. High Inertia Machine Schedule Test 98
10. Low Inertia Machine Schedule Tests 99
11. 100 Percent Power Level (High Inertia Machine) Stabilized Test Data 106

INTRODUCTION AND SUMMARY

The requirements for the Space Shuttle APU dictated the use of a hydrazine gas generator to drive the turbine and associated machinery. Because of the long duration requirement for the Space Shuttle APU, the technology of hydrazine gas generators did not provide sufficient background for accurate prediction of the life capability of such a gas generator. For this reason, the Lyndon B. Johnson Space Center initiated a technology program monitored by Mr. R. J. Villemarette.

The objective of this technology program was to establish the necessary base for the design and fabrication of a flight gas generator for the Space Shuttle APU. This objective was approached by evaluating critical performance parameters and stability criteria as well as scaling laws that could be applied in designing the flight gas generator. The analytical gas generator performance evaluation was coupled with a test program to provide the necessary design information. The primary experimental effort in support of the analysis was performed on an IR&D program. Based on these results a structural design, including thermal and stress analysis, as well as material evaluation was made and two gas generators were fabricated.

These two gas generators were alternately used to evaluate the various critical parameters including, flight type gas generator performance, thermal distribution within the gas generator and of the structural members, response, life tests including ten mission duty cycles and a comparative evaluation between pulse modulated and pressure modulated performance of the gas generator.

Successful completion of all of the above tasks has provided a comprehensive basis for the design and fabrication of a thermal bed gas generator meeting the Space Shuttle APU flight requirements and the two gas generators having completed these tests have been delivered to the Lyndon B. Johnson Space Center for further testing, if desired.

CONCLUSIONS

A flight type, thermal bed, hydrazine gas generator has successfully been designed, fabricated, evaluated, and subjected to ten mission duty cycles as well as a series of pulse and pressure modulated comparison tests. This fully tested gas generator has been prepared for delivery to the Lyndon B. Johnson Space Center.

An analysis and design study was successfully completed providing critical parameters for scaling of thermal bed gas generators as well as predicting stability criteria and all other pertinent geometric configurations.

An extensive material evaluation program was completed to establish the effect of a nitriding atmosphere on high temperature high strength materials. Based on these tests, Inco 617 was selected for the high temperature, high strength material, but due to unavailability, Haynes 188 (second choice) was used and Inconel 600 was selected for the thermal bed as well as the sleeve containing it.

Design of the injector and thermal bed resulted in a low total gas generator fractional pressure drop of 22.8 percent at maximum power level while maintaining stability beyond the required 10 to 1 throttle range, 33 to 1 ranges were achieved successfully.

The gas generator did not show any degradation in performance, stability, or response after being subjected to a 10 mission duty cycle life test followed by a five hundred second full power burn. In fact, the same gas generator was used to perform pulse and pressure modulated comparison tests and was shipped to the Lyndon B. Johnson Space Center for further testing, if desired.

Extensive testing of the gas generator under conditions of ramp and step functions from 10 percent power level to 100 percent power level have shown that there is neither over nor undershoot of the chamber pressure and that the roughness of the gas generator is below the level that could be measured.

A series of off-design performance tests was conducted to demonstrate the sensitivity of the gas generator to specific conditions that might arise in a vehicle application. The gas generator was totally insensitive to helium saturation of the propellant which might occur during long term pressurization of the use tank. The gas generator was also operated with hydrazine propellant at 50 and 180 F. The gas generator operated smoothly at these inlet temperatures over the entire range of power levels. Simulation of altitude starting capabilities were made by placing the gas generator in a vacuum chamber and initiating firing under vacuum conditions. During these tests heat soakback to the injector manifold was monitored and the gas generator was restarted at altitude successfully with a manifold temperature of 464 F. To provide confidence in the operation of the gas generator beyond the four different power levels, 10, 30, 50, and 100 percent, the gas generator was successfully operated over the entire power level spectrum which was varied continuously from 0 to 100 percent. The gas generator was totally impervious to any power level or rate of change of power level insofar as operation was concerned and ran smoothly regardless of conditions imposed. The final test series of this portion of the program consisted of verifying the start sequence required for the gas generator. Temperature profiles of the gas generators were obtained during the 30 minute heat up cycle while heated GN_2 flow was monitored. No attempt was made to minimize the heat up cycle time of 30 minutes, however, a similar gas generator was started in 18 seconds by different start up techniques which were developed on an IR&D program.

Test with contaminated propellants, water, UDMH, and MMH demonstrated the thermal bed design, unlike the catalytic design, to be insensitive to these contaminants.

The gas generator used for the 10 mission duty cycles was also used to perform experimental evaluations in the performance characteristics between a pulse modulation and a pressure modulated mode of operation. Comprehensive and high response instrumentation and was used for this test series and established the advantages of pulse modulation over pressure modulation from a Specific Propellant Consumption (SPC) point of view. After completing the comparative SPC

tests, the gas generator was used to establish acceptable limits of the injector manifold temperature for restarting purposes. The gas generator was successfully restarted with the manifold temperature at 548 F, but higher temperatures resulted in a small overshoot in the manifold temperature after restart. When the gas generator was shutdown after this temperature overshoot, a pressure spike occurred, however there was no damage to the hardware. From this it can be concluded that manifold temperatures above 500 F, for purgeless restarting, represent a risk factor which must be investigated experimentally and analytically before exposing the gas generator to these conditions.

The total accumulated operating time for this gas generator was 21.9 hours including 4790 ON-OFF pulses. The gas generator performance does not show any change relative to its last use in preceding phases of this program. Furthermore, there is no indication of any deterioration which would preclude the probability of meeting a 1000-hour life requirement.

PHASE I: GAS GENERATOR DESIGN AND LIFE DEMONSTRATION

During this phase of the program, the flight design of the SS/APU gas generator was used as the basis for the design and fabrication of a prototype gas generator. Two gas generators of this design were fabricated to perform the various tests for this program.

DISCUSSION

Design - Description

The Rocketdyne proposed gas generator assembly for the Space Shuttle APU is shown in Fig. 1. The assembly consists of four components: a model GGT-171-1000 thermal gas generator, a model GGC-105-320 catalytic initiator, and two JPC P/N VC4076-T-ZAH shutoff valves.

The thermal gas generator is scaled from a Rocketdyne model GGT-268-560 which is shown in Fig. 2 and 3. The design incorporates a dual element screen pack, regenerative flow dual wall, shower head injector, standoff inlet manifold and adiabatic insulation.

MATERIALS

Material selection for the gas generator assembly was based upon results of a 1000 hour nitriding environment, material evaluation program. This program determined the effects of nitriding on strength and ductility properties after exposure to a 1800 F ammonia gas environment, and included high temperature tensile tests, bend tests, hardness penetration and microstructure analysis. It was concluded that none of the high strength materials (yeild strength in excess of 8000 psi and 50-hour rupture strength in excess of 5000 psi) would

WEIGHT	
SOLENOID VALVES (2)	0.70
VALVE MANIFOLDS	1.50
INITIATOR ASSY	0.60
REACTOR ASSY	3.40
SCREEN PACK	2.10
BLANKET	1.70
TOTAL	10.00 LB

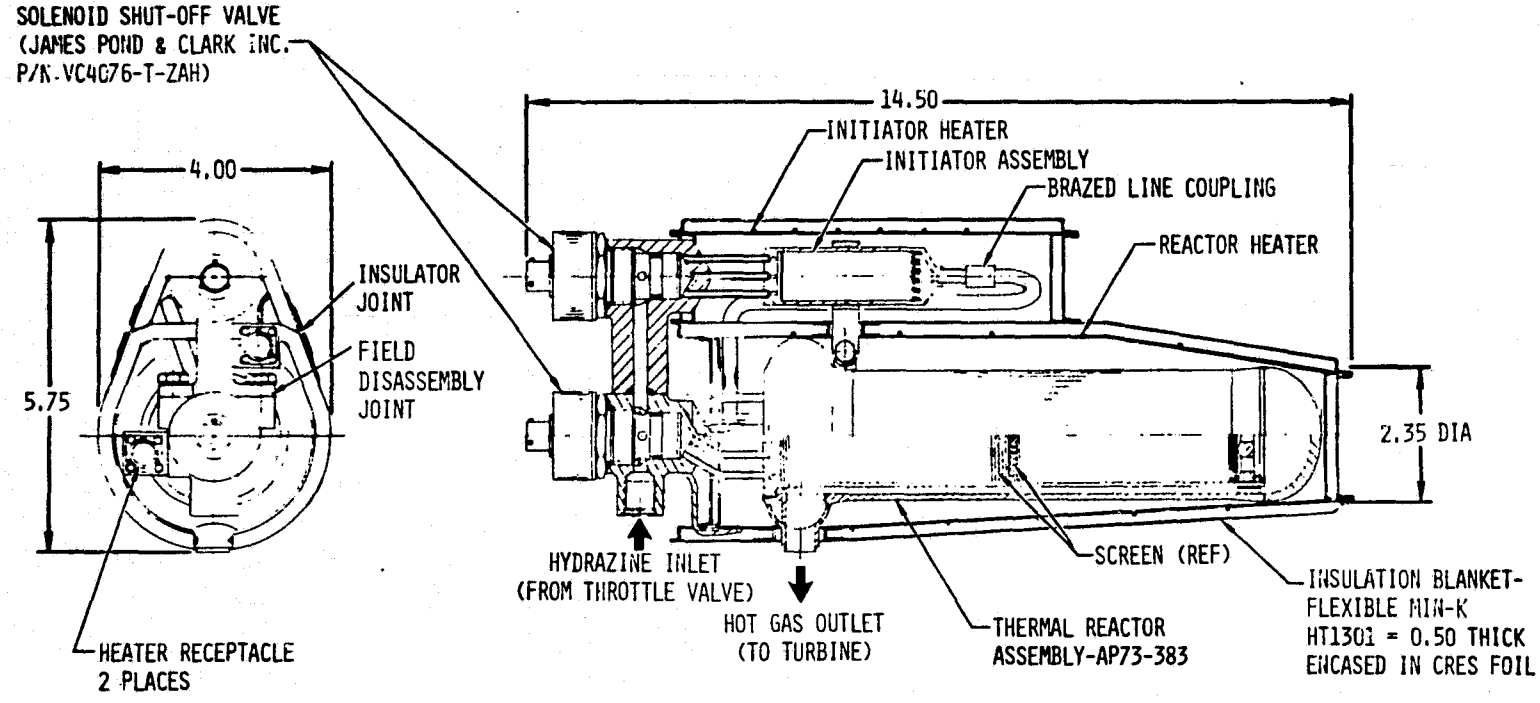

Figure 1. Gas Generator Assembly - SSAPU

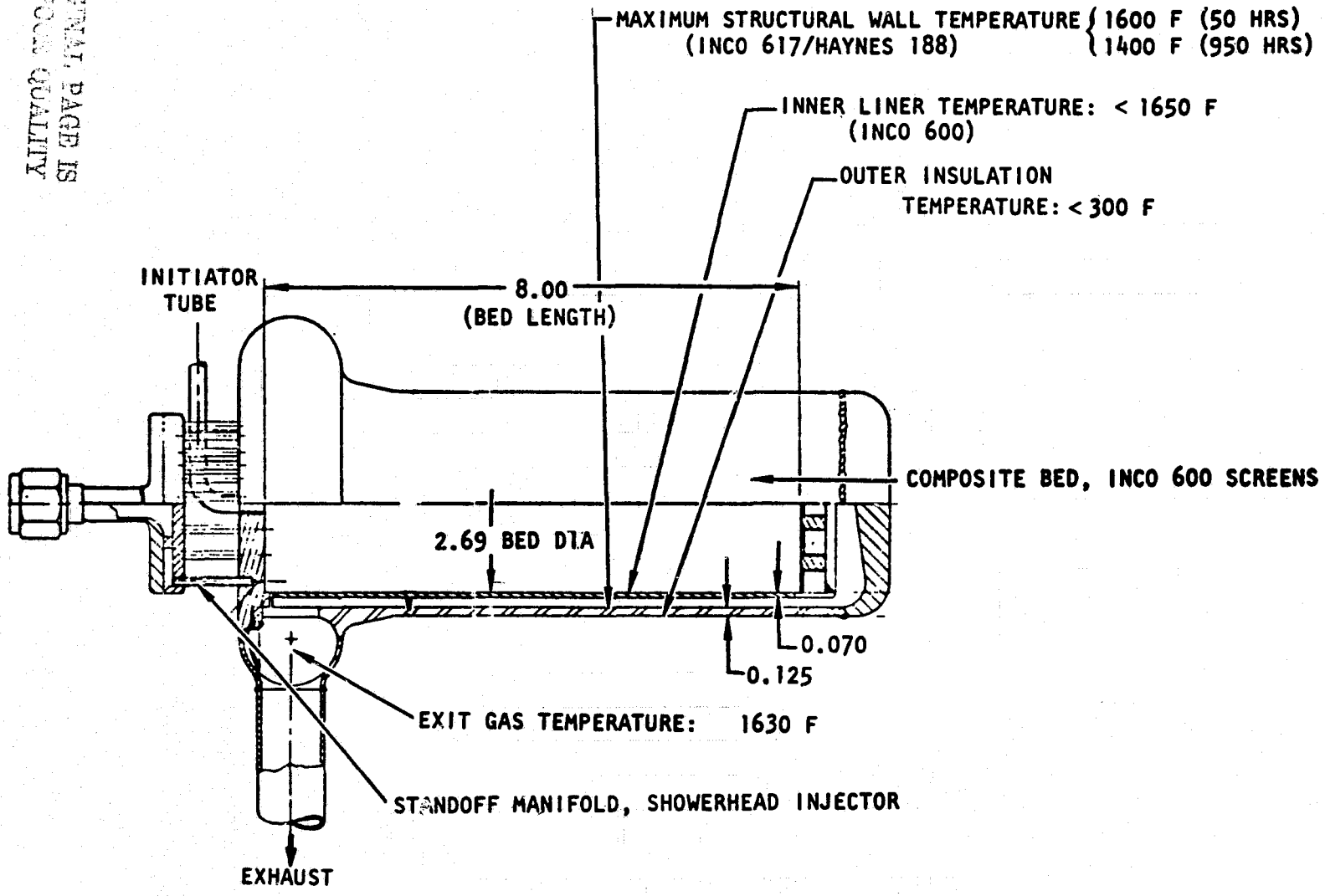

Figure 2. Gas Generator - GGT-268-560

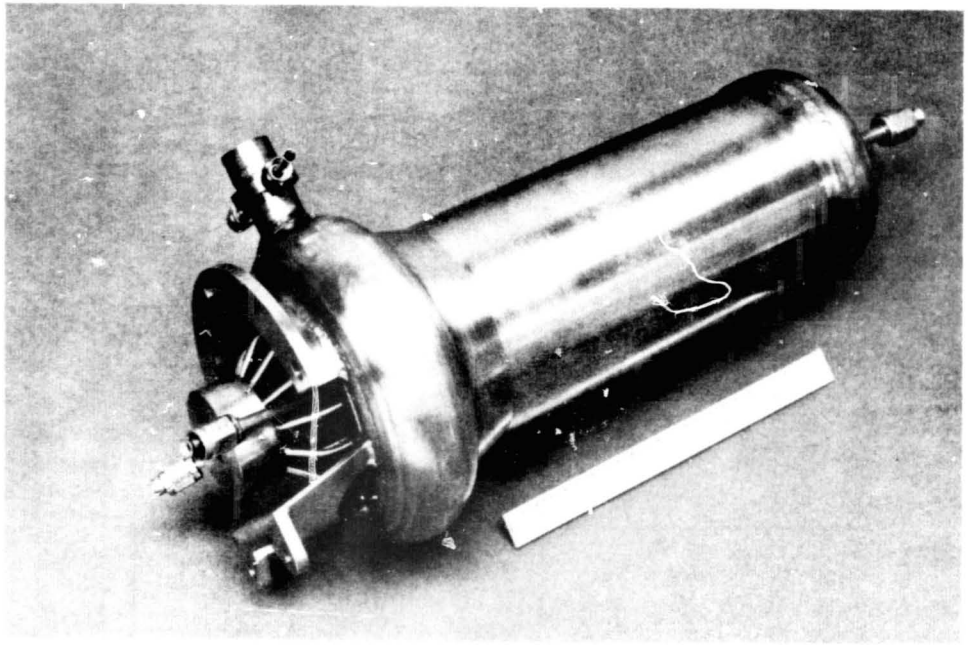

GGT 268-560

TECHNOLOGY
CONTRACT
NAS9-13003

OBJECTIVES

- 10:1 TURN DOWN RATIO
- RAPID RESPONSE
- LONG LIFE
- MINIMUM EXTERNAL HEAT FLUX
- FULL RANGE STABILITY
- LOW ΔP

ACHIEVEMENTS

- 50:1; ROUGHNESS < 1%
- 45 MSEC (90% Pc CHANGE), ZERO Pc OVERSHOOT
- 19 HRS: INCLUDING 10 MDC'S, 500 SEC. SUSTAINED MAXIMUM POWER MATERIALS BASED ON 1000 HOUR TEST
- REGENERATIVE DESIGN PERMITS ACCEPTABLE WALL TEMPERATURE AND FULL INSULATION
- STABILITY CRITERIA ESTABLISHED AND PROVEN FOR
- ~ 20% $\Delta P/Pc$ GG PRESSURE LOSS

Figure 3. Gas Generator

provide a suitably high confidence level for long duration use in an 1800 F nitriding environment. This necessitated a design which reduced the maximum structural wall temperature to 1600 F, and thereby minimized material property degradation. In order to simultaneously achieve a near adiabatic insulation, a dual wall exhaust gas regenerative design was indicated. Inco 617 was selected for the structural chamber wall and injector with Hayes 188 as a second choice. Inco 600 (the least degraded material by the 1800 F nitriding environment) was selected for the low-stressed thermal bed screens and screen liner. The standoff injector manifold and tubes are constructed of 304 stainless, the insulation blanket is flexible MIN-K, HT 1301 x 0.5 inch encased in cresfoil.

Thermal Control

Thermal characteristics of the gas generator establish steady state and transient temperature distrubitions which, in addition to affecting material strength and expansion, influences material property degradation due to nitriding (a temperature dependent process). Thermal characteristics also affect heat soak-back following shutdown which may result in excessive injector manifold temperatures (a safety hazard due to potential local decomposition) and an excessive environment for a close-coupled valve. Finally, heat loss to the environment and external surface temperatures are thermal considerations which must be limited by the design.

Rocketdyne's gas generator thermal model, utilizing the DEAP digital program was used to calculate transient and steady state temperature profiles and heat flux. This program was used to design the model GGT 268-560 gas generator and has been correlated against test data to adjust heat transfer coefficients and other program constants.

A single-wall gas generator design was discarded for the more complex dual wall construction on the basis of the thermal analysis results, material

nitriding program, and gas generator test data. It was concluded that a single wall construction with controlled insulation, could not maintain maximum structure wall temperatures below the critical range of 1700-1750 F, without introducing excessive external surface temperatures together with high heat flux to the environment. Figures 4 and 5 show the thermal analysis results, for the single wall model GGT-191-460, which incorporated a radiation shield outside the chamber wall covered by an insulation blanket. Maintaining external surface temperatures below 600 F would result in a chamber wall temperature in excess of 1730 F. On the other hand, chamber wall temperatures below 1700 F would require a thin insulation with external surface temperatures in excess of 700 F and heat flux in excess of 1600 Btu/hr. A regenerative dual wall design permits near adiabatic insulation with 1600 F structural wall temperatures, and held the low stressed inner liner temperatures below 1700 F. Temperature distribution data for the dual wall model GGT-268-560 design during mission duty cycle endurance testing is shown in Table 1.

TABLE 1. TEMPERATURE DISTRIBUTIONS MODEL GGT-268-560

	100% Flow		10% Flow	
	MDC No. 1	MDC No. 10	MDC No. 1	MDC No. 10
Exit Gas Temperature, F	1624	1630	1440	1433
Wall, 1.5 inches from Injector Face, F	1607	1616	1466	1465
Wall, 3.5 inches from Injector Face, F	1605	1612	1453	1475
Wall, 5.5 inches from Injector Face, F	1612	1621	1450	1462
Injector Manifold, F	168	123	142	147

MDC = Mission Duty Cycle
MDC No. 1 (Run 48A June 2, 1973)
MDC No. 10 (Run 57B June 6, 1973)

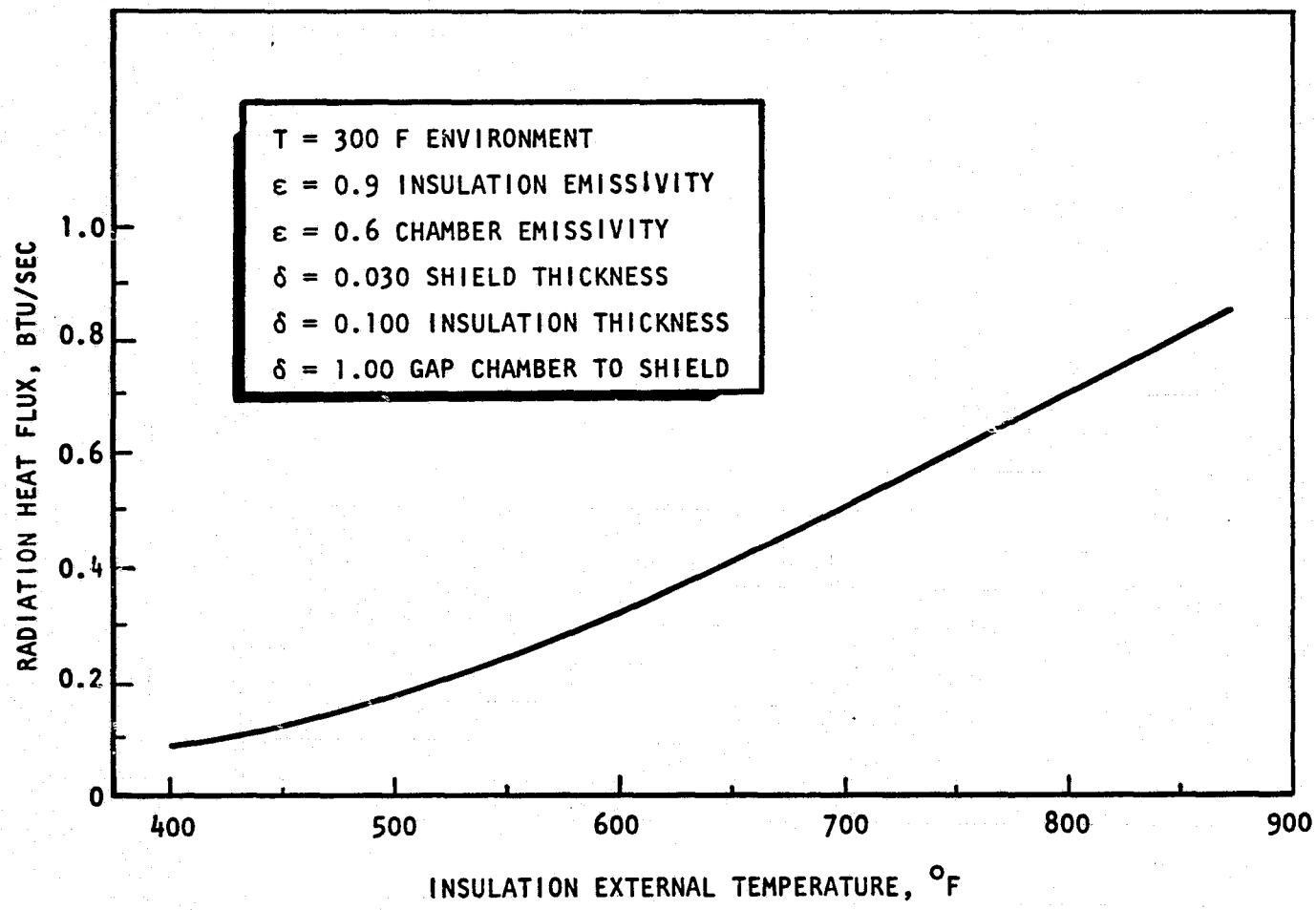

Figure 4. Gas Generator Model GGT-191-460,
External Radiation Heat Flux

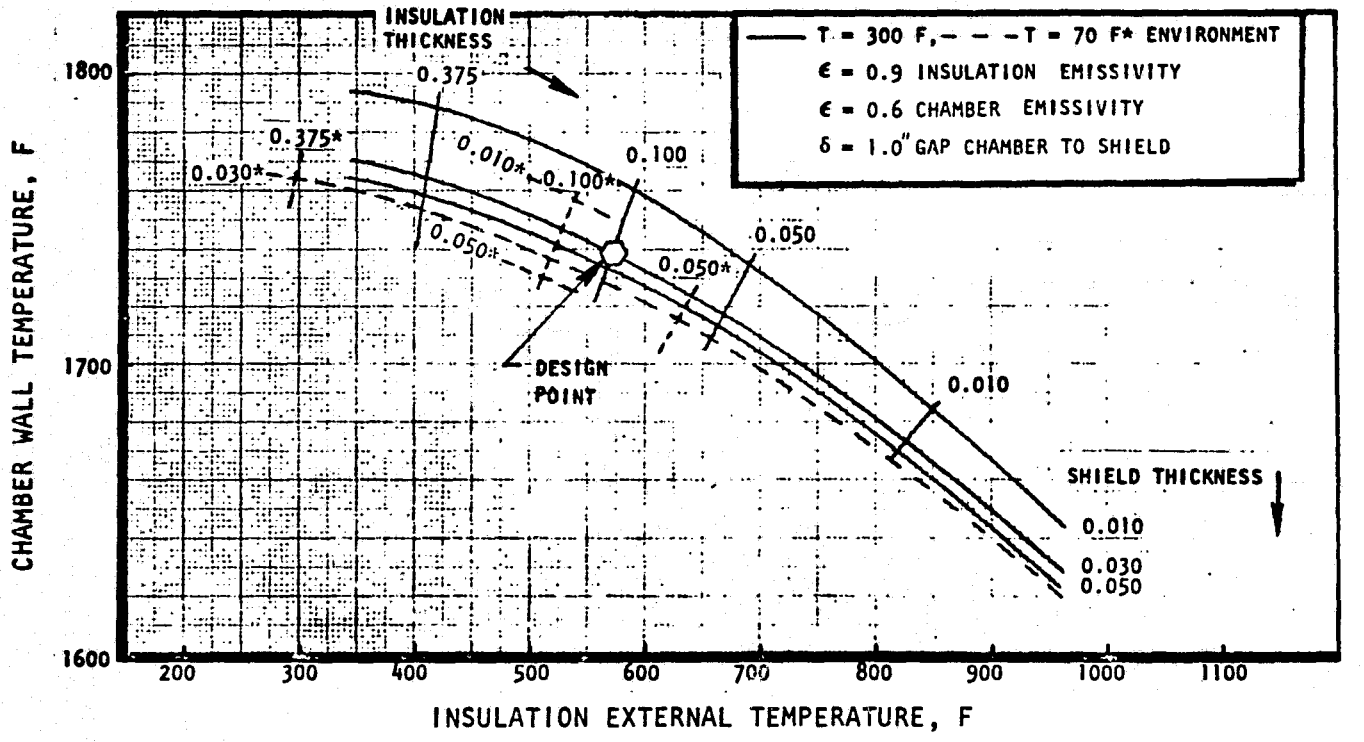

Figure 5. Wall Temperature vs Insulation External Temperature, Model GGT-191-460

STRESS ANALYSIS

A Rocketdyne digital stress analysis program was employed in the design of the model GGT-268-560 gas generator. This program calculates displacements, stresses, and strains, enabling calculation of fatigue and creep damage fractions. These results together with thermal and materials analysis information were used to extablish satisfactory design criteria.

A preliminary analysis was performed for the proposed SS-APU gas generator assembly (Fig. 1) to check feasibility of design and calculate minimum wall thickness at critical areas. Analysis results indicate a structurally sound design, with adequate life to attain 100 missions for both a pulse and pressure modulated control mode.

Thermal Bed

The thermal bed performs two primary functions in a thermal gas generator: (1) provides a thermal capacitance which is drawn upon for hydrazine decomposition when hot decomposed gas products are not present in sufficient quantity; (2) provides a large surface area for ammonia dissociation following hydrazine decomposition, which lowers both temperature and molecular weight of the exhaust products. Packed screens are used to form the bed which consists of a dual screen pack, the details of which are shown in Table 2.

TABLE 2. THERMAL BED SCREEN DESIGN

Screen Geometry Mesh x Diamter	Number of Screens	Actual Stack Height, Inches	Ideal Stack Height, Inches	Pack Factor, Percent	Void Fraction	Free Flow Area
16 x 0.035	53	4.05	3.71	91.6	0.56	0.194
26 x 0.015	128	3.81	3.84	101.0	0.69	0.372

The upper screen pack, in the decomposition zone, consists of 4 inches of 16 mesh, 0.35-inches -diameter wire screens; the lower screen pack contains 3.8 inches of 26 mesh, 0.15-inches -diameter wire screens. The packing factor is defined as the ratio of ideal to actual stack height; the void fraction, $\theta = 1 - M/4\,\pi d$, where M = mesh and d = wire diameter (inches); the free flow area, $\alpha = (1\text{-}Md)^2$.

Injector-Manifold Assembly

Function of the shower head injector is to distribute the liquid hydrazine evenly over the cross sectional area of the gas generator, and thereby promote heat transfer with the recirculating hot gas products in the upper bed section, rapid vaporization and decomposition.

The GGT-268-560 gas generator contains a 24-hole shower head injector. Hole diameter is 0.0225 in., providing a total area of 0.00954 in^2. The hole length-to-diameter ratio is 9.3, and the holes are arranged in three concentric rings. The outer ring, on a 2.33-inch diameter, contains 12 holes; the middle ring, on a 1.55-inch diameter, 8 holes; and the inner ring on a 0.776-inch diameter, 4 holes. The flow coefficient of the injector, determined from the relation:

$$\dot{w} = Cd\ Ai\ 5.31\ \sqrt{\Delta P}$$

where

Cd = flow coefficient
Ai = total area, 0.00954 in^2
ΔP = injector pressure drop, psi

was measured to be 0.797. The injector manifold is stood off from the injector face a distance of 3 inches and connected by means of individual tubes to each orifice.

DESIGN/OPERATIONAL RELATIONSHIPS

During the period from 1971 to 1973, Rocketdyne was engaged in both IR&D programs and this NASA contractual program (NAS9013003) to investigate design/operational relationships of a hydrazine monopropellant gas generator. The following discussion describes the restults of both the test and analytical investigations, and the conclusions drawn regarding critical design parameters of the gas generator.

Thermal Bed

Operational characteristics of a screen packed bed GG are influenced by the following critical design parameters: wire material, size, mesh and packing factors, which govern fractional flow area, void fraction and surface area. There parameters influence certain critical operational characteristics such as hot gas recirculation in the upper bed section and over all flow resistance. Hot gas recirculation of the decomposed N_2H_4 products (also influenced by the injector design) is essential for satisfactory heat transfer to incoming liquid hydrazine and affects decomposition delay. Overall flow resistance affects the pressure budget and plays a role in hydrazine stability.

The Rocketdyne design incorporates a dual section bed; an upper section (closest to the injector) designed to promote hot gas recirculation with sufficient thermal capacitance, and a lower section to provide sufficient surface area with minimum pressure drops. Thermal bed fractional pressure drop, P/P_c, is the pressure loss, P as a fraction of chamber pressure P_c:

$$\frac{P}{P_c} = R_s \, L(G/P_c)^2$$

where

R_s = unit screen resistance, $sec^2/in.$
L = bed length, in.

G = bed loading, lb/sec-in.^{2}

P_c = chamber pressure, lb/in.^{2} (downstream of bed)

The unit screen resistance, R_s, is a function of screen geometry, Reynolds number, the integrated average gas temperature over the bed, and the packing factor (or ratio of ideal to actual bed length). The specific bed loading, G/P_c, is related to the gas generator exit throat to flow area ratio and, is a near constant over the operational range.

Test experience indicates that GG operation is strongly sensitive to screen geometry at the upper bed section, as it affect the decomposition process. This is demonstrated by Fig. 6, in which gas temperature, close to the injector, is plotted as a function of bed loading. In all cases shown, only the gas generator bed packing has been changed. For configurations A and B of Fig. 6, a "wash-out" (loss of decomposition process) at low flowrates occurred, due to the use of high resistance, calendered screens, with a packing factor greater than 1.4 in the decomposition region; i.e., first 4 inches of bed. Satisfactory operation was attained with Configuration C utilizing uncalendered, lower resistance screens, more lightly packed for the upper 4 inches of bed.

The exit gas temperature of a gas generator varies as a function of bed loading, G, and typically will vary approximately 200 F over a 10:1 flow range. When flow is rapidly varied, the exit gas temperature response will lag the exit pressure variation due to the thermal capacitance of the bed. This thermal response of the bed may be described by the relation:

$$\tau = \frac{C_p W}{hA}$$

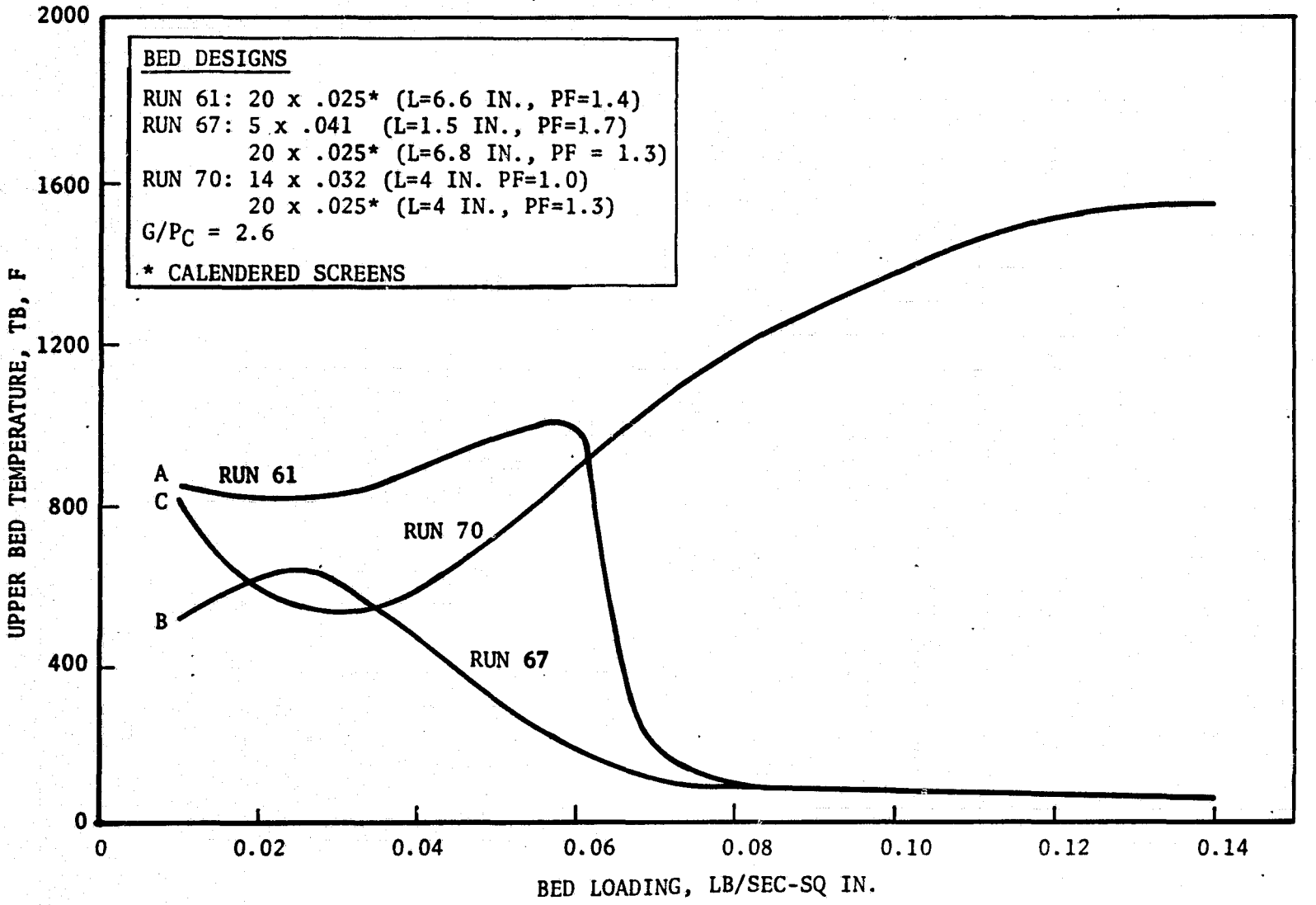

Figure 6. Bed Characteristic Effects - GG Design - GGT-191-460

where

τ = first order time constant
C_p = screen specific heat
W = weight of screens
h = heat transfer coefficient
A = heat transfer area

Since the heat transfer coefficient, h, varies approximately linearly with flowrate, the thermal time constant decreases with increasing power level. A typical value of τ at 100 percent power level is 2.0 seconds (compared with a pressure response of 0.030 seconds).

Injector

Injector geometry strongly affects both the decomposition process and flow stability of the gas generator. The critical geometric parameters are flow resistance, orifice length-to-diameter ratio, orifice density, and orifice arrangement.

$$\text{Flow Resistance, } R = \frac{\Delta P_i}{\dot{W}^2},$$

where

ΔP_i = injector drop, and
$\dot{W}$ = flowrate;

$$\text{Orifice Density, } \rho_i = \frac{N_o}{A_c},$$

where

N_o is number of injector orifices,
A_c is chamber cross sectional area

The relation between injector resistance and flow stability has been well established analytically and verified by test. On the other hand, empirical relationships have not clearly been defined for the effects of injector geometry on the decomposition process, even though satisfactory designs have been formulated over a flowrange from 0.006 lb/sec to 15 lb/sec, using experience factors and trial and error approach.

Bed Loading

In addition to the critical design parameters associated with the thermal bed and injector geometry, additional factors such as bed loading, G, and specific bed loading, G/P_c, influence gas generator operation:

$$\text{bed loading, } G = \dot{W}/A_c$$

$$\text{Specific bed loading, } G/P_c = g/C^* \ (A_t/A_c)$$

where

$\dot{W}$ = flowrate, lb/sec

A_c = GG cross sectional area, $in.^2$

$C^* = \frac{PA_tG}{\dot{W}}$ ft/sec

A_t = exit throat area, $in.^2$

g = acceleration of gravity, ft/sec^2

Bed loading influences gas temperatures throughout the gas generator. Increased bed loading increases the peak decomposition temperature at the upper bed section due to a decrease in the initial ammonia dissociation which accompanies the decomposition process. A variation as much as 450 F may result from a 10:1 flow variation. The location of the peak temperature, generally moves upstream with increasing bed loading. For example, a 10:1 flow variation might result in a two to four inch movement of the peak temperature location, with the maximum flow location as close as 1 inch downstream of the injector. Finally, bed loading influences the extent of ammonia dissociation following initial hydrazine decomposition. At maximum flowrate, a 250 to 500 F temperature drop, from peak to exit temperature, may result from the endothermic NH_3 dissociation process, depending upon Mach number and bed geometry. At low flows, this temperature drop decreases, however, the resultant exit gas temperature is still approximately 200 F lower, than at maximum flow, due to the reduced peak temperatures. The effect of bed loading on temperature distribution through the gas generator is shown in Fig. 7 and 8.

Specific bed loading, G/P_c, is a function of gas generator geometry and is proportional to the gas Mach number through the bed, which remains nearly constant over the operational range. Fractional bed pressure drop, $\Delta P/P_c$, varies as the square of G/P_c, as previously shown. Specific bed loading also influences the decomposition process at the upper bed sections; a high Mach number tends to reduce peak temperatures, especially at the high flow levels. This is demonstrated by the curves in Fig. 9 and 10, which shows a substantial decrease in both the injector face and upper bed temperature; 1.0 in. downstream of the face, due to a doubling of the Mach number in otherwise identical gas generator configurations.

Response to Load Transients

The overall response of a gas generator generally refers to the elapsed time from receipt of a valve actuation signal to development of 90 percent of the resultant change in chamber pressure or flowrate. Neglecting the valve response,

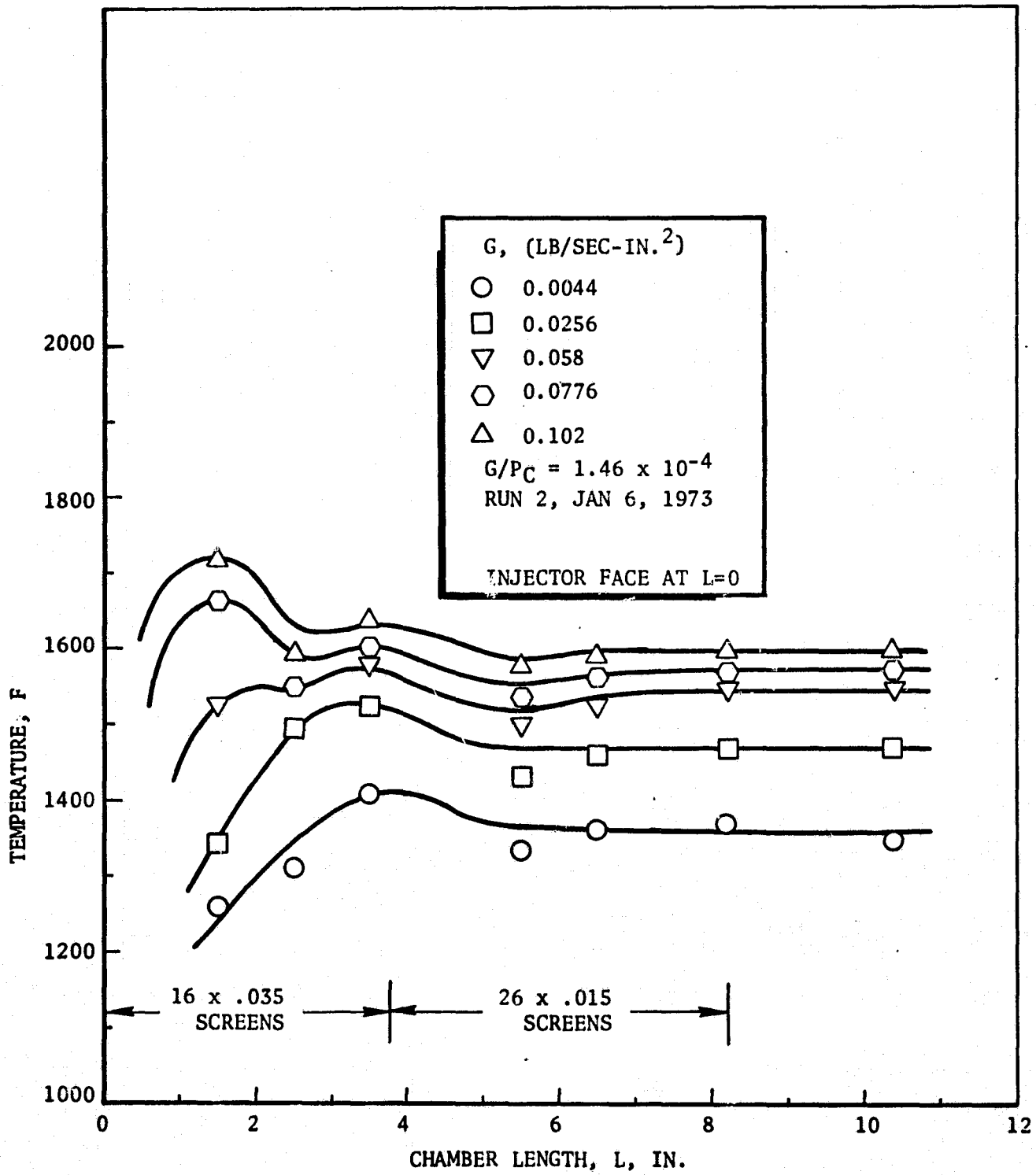

Figure 7. Bed Loading Effects on Temperature Distribution - Model GGT-268-460

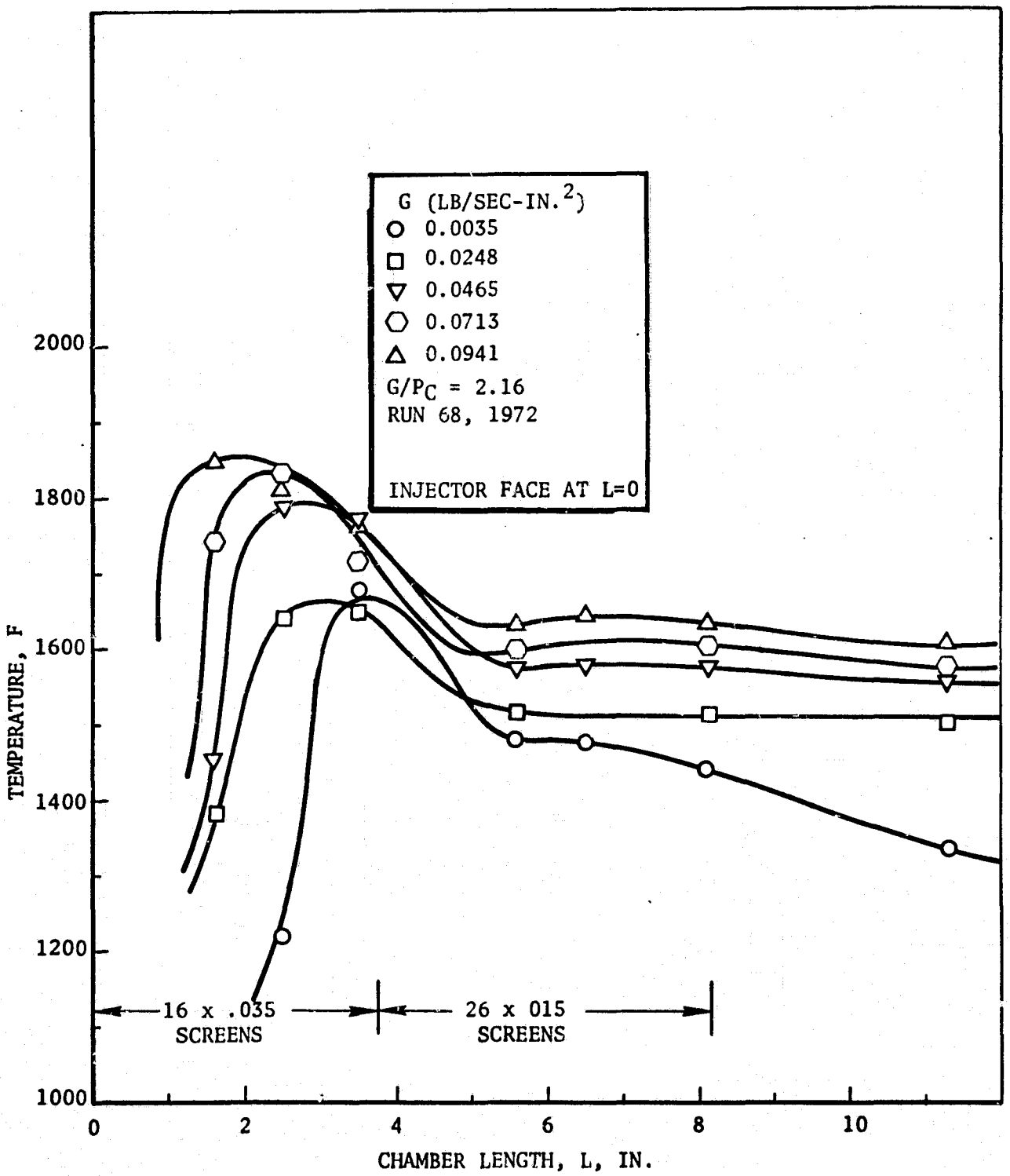

Figure 8. Bed Loading Effects on Temperature Distribution Model GGT-268-460

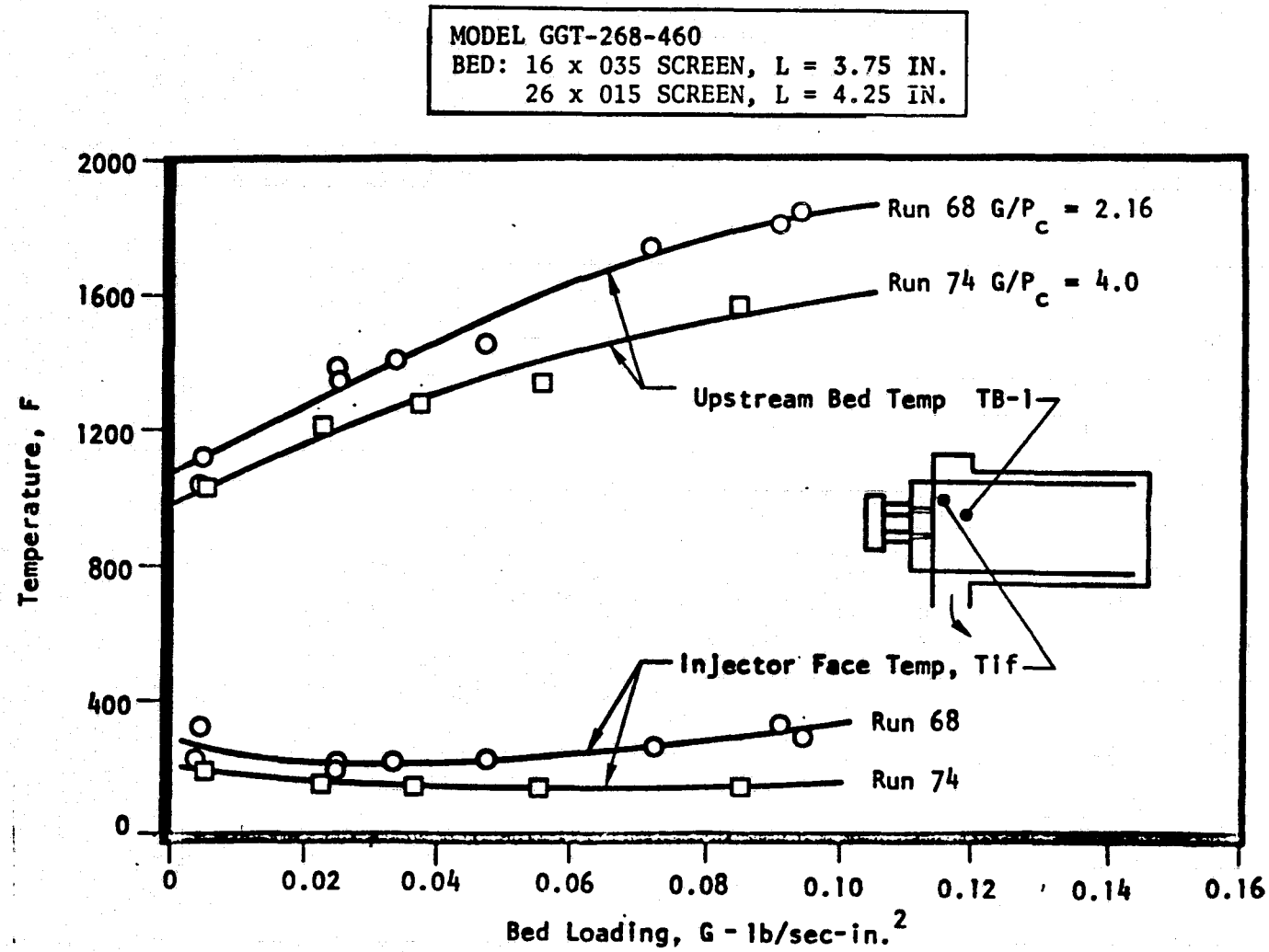

Figure 9. Effect of G/P_c on Gas Generator Operation

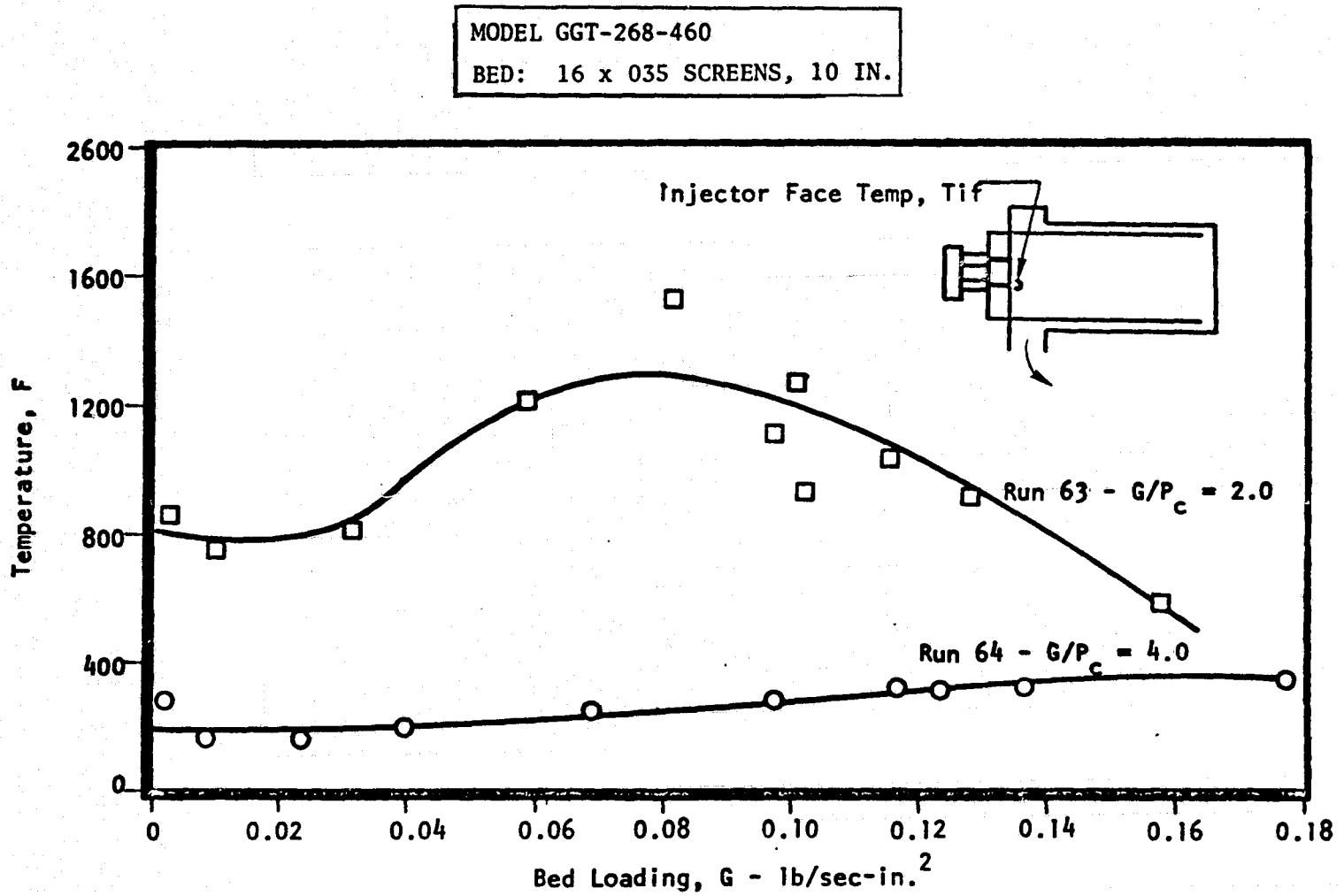

Figure 10. Effect of G/P_c on Gas Generator Operation

the major components which make up this delay is the hydrazine decomposition delay, τ_d, and the chamber capacitance time constant, τ_c. The decomposition delay represents a dead time between introduction of a step change in liquid hydrazine into the chamber and the conversion to gaseous flow. The chamber capacitance represents a lag between a change in generated gas flow and the resulting change in chamber pressure. A mathematical model of this operation is shown in Fig. 11. Based on the equations 2, 3, and 5 of Fig. 11, the chamber capacitance time constant is established by the La Place transform equation:

$$\left(\frac{P_c}{\dot{W}}\right) = \frac{(P_c/\dot{W})}{\tau_c S + 1}$$

where

$$\tau_c = \frac{1}{(\dot{W}/P_c)} \quad Z$$

$(\dot{W}/P_c)$ = nominal ratio of flowrate to chamber pressure ($in.^2/sec$)

Based upon a nominal $(\dot{W}/P_c)$ of 8.08×10^{-4} $in.^2/sec$, a volume of 47 $in.^3$, and average gas temperature of 2060 R ($Z = 8.72 \times 10^4$ $in.^{-2}$), the chamber capacitance time constant, τ_c is 0.014 secs. The 90 percent rise time can be calculated based upon the time constant as follows:

$$0.9 = 1\text{-}e^{-(t/\tau_c)}$$

where

t = 90 percent rise time

This results in a 0.032-second, 90-percent rise time. Note that the chamber capacitance is relatively independent of power level, since the gas temperature

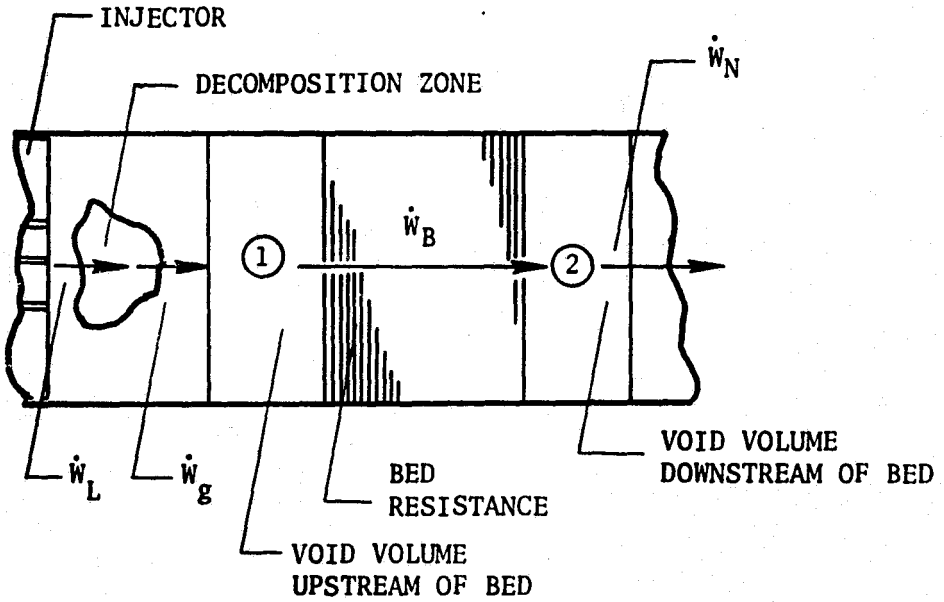

(1) $\dot{W}_g(t) = \dot{W}_L(t-a)$

(2) $\frac{dP_1}{dt} = Z_1 (\dot{W}_g - \dot{W}_B)$

(3)* $Z = \frac{\gamma RT}{V}$

(4) $\frac{dP_2}{dt} = Z_2 (\dot{W}_B - \dot{W}_N)$

(5) $\dot{W}_N = \frac{P_2 A_t g}{c^*}$

(6) $L \frac{d\dot{W}_B}{dt} = P_1 - P_2 - R \dot{W}_B^2 / \overline{P}$

* THE VOID VOLUME OF THE CHAMBER IS LUMPED AT SECTION "1"; THE TURBINE MANIFOLD VOLUME IS LUMPED AT SECTION "2"

NOMENCLATURE

P	=	PRESSURE, PSIA
$\dot{W}_g$	=	LIQUID HYDRAZINE FLOWRATE, LB/SEC
$\dot{W}_L^g$	=	GASEOUS FLOW GENERATED BY HYDRAZINE DECOMPOSITION, LB/SEC
$\dot{W}_B$	=	GASEOUS FLOW THRU BED, LB/SEC
$\dot{W}_N^B$	=	GASEOUS FLOW THRU EXIT NOZZLE, LB/SEC
γ	=	RATIO OF SPECIFIC HEAT
R	=	GAS CONSTANT, IN./F
T	=	AVERAGE BULK TEMPERATURE, F
A_t	=	EXIT THROAT AREA, IN.^{2}
g	=	ACCEL OF GRAVITY, IN./SEC^2
c^*	=	SPOUTING VELOCITY, IN./SEC^2
L	=	BED INDUCTANCE, SEC^2/IN.^{2}
$\overline{P}$	=	AVERAGE BED PRESSURE, PSIA
R	=	BED RESISTANCE, SEC^2/IN.^{4}
a	=	DECOMPOSITION DELAY, SEC

Figure 11. Mathematical Model of GG Decomposition Process

is a weak function of flowrate. Note also that decreasing the value of $(\dot{W}/P_c)$ (i.e.; decreasing the exit throat size) increase the chamber capacitance time constant. An increased chamber volume has the same effect.

Both the decomposition delay and chamber capacitance were evaluated during several gas generator tests in which "step" changes in flowrate were generated by on-off valving and orificing in the feed line upstream of the injector. Close coupled pressure transducers were located at the injector inlet manifold and at several locations in the chamber. The decomposition delay was determined by the elapsed time from initiation of injector inlet pressure change (denoting a liquid flow change into the chamber) to initiation of a change in upstream bed pressure. The chamber capacitance is measured by the 90 percent rise time in chamber pressure downstream of the bed. Figures 12 and 13 show results of a flow steps increase and decrease on the model GGT-268-560-E single wall gas generator. Decomposition delays of 10 and 12 milliseconds are indicated during the step increase and decrease, respectively. A 0.037-second, 90-percent rise time is shown in Fig. 12. The relatively long 90 percent decay time of 73 milliseconds (Fig. 13) is due to the lag associated with the injector inlet pressure, and is therefore not representative of chamber capacitance lag only.

Stability

Gas generator instability is typically in the frequency range from 5 to 30 cps with amplitudes as severe as ±30 percent in some cases. In many cases, instability is accompanied by a breakdown in the normal decomposition process as denoted by a severe decrease in decomposition zone gas temperature and/or downstream movement of the decomposotion process. Since the frequency of instability appeared to be in the range of fluid dynamic time constants, a mathematical model of the gas generator system can be made without the necessity of including complicated, high frequency combustion process equations. An analog model of the gas generator was constructed based upon test data of gas temperature distributions, fluid resistances, and both fluid and thermal response. The model included a feed system with storage tank, feed line and throttle valve.

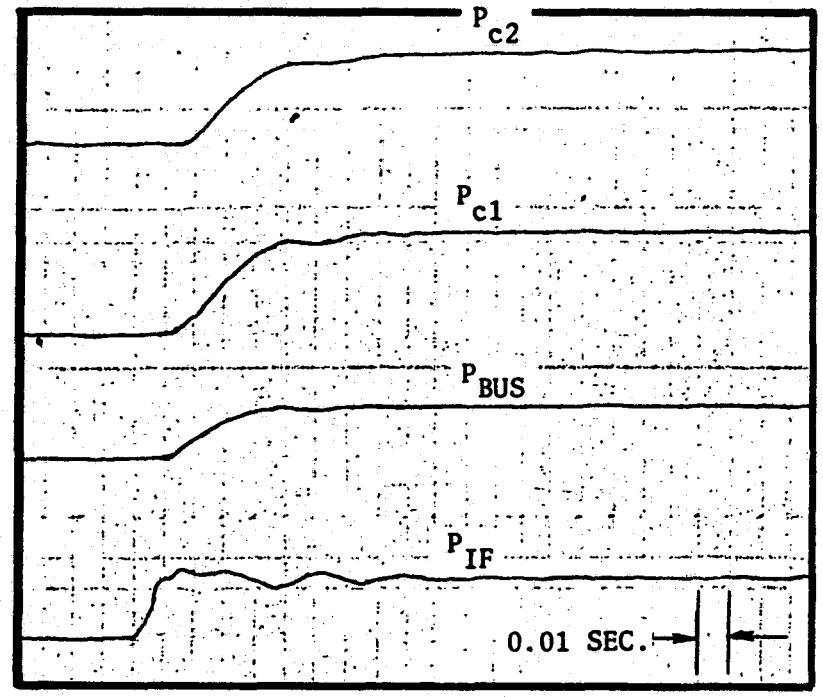

FLOWRATE STEP: 10% TO 100%

NOMENCLATURE
P_{c1}, P_{c2} - CHAMBER PRESSURE (1)
P_{BUS} - UPSTREAM BED PRESSURE
P_{IF} - INJECTOR INLET PRESSURE

CHAMBER VOID VOLUME = 44.6 IN^3

Figure 12. Model GGT-268-560-E, Test Run 10B-5, March 1973

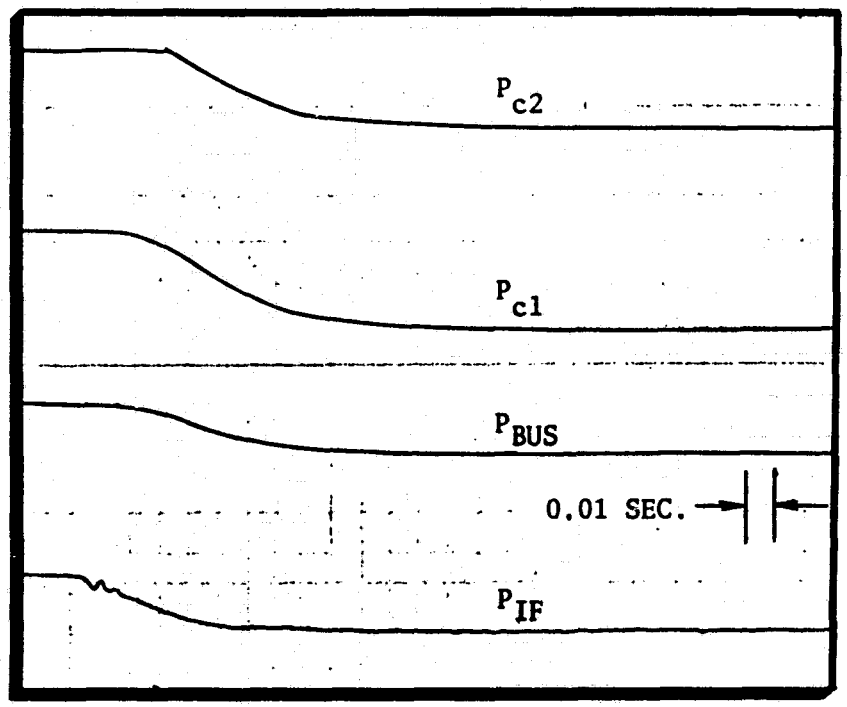

NOMENCLATURE
P_{c1}, P_{c2} - CHAMBER PRESSURE
P_{BUS} - UPSTREAM BED PRESSURE
P_{IF} - INJECTOR INLET PRESSURE

CHAMBER VOID VOLUME = 44.6 IN^3

FLOWRATE STEP: 100% TO 10%

Figure 13. Model 268-560-E, Test Run 11A-5 (d), March 1973

Results of the stability analysis identified critical design parameters which affected flow stability. These are shown in Fig. 14. A stability criterion was then established relating these parameters, the results of which are shown in Fig. 15. Each of the three curves shown in Fig. 15 represents a minimum allowable fractional feed system pressure drop as a function of fractional bed drop. For example, a gas generator with 45 $in.^3$ of void volume from the injector face to the exit throat, and operating with a 0.020-second decomposition delay would require a fractional feed system drop of at least 0.33 with a fractional feed drop of 0.2 to ensure stability. Decreasing the decomposition delay permits stable operation with a lower feed system pressure drop. Increasing the chamber void volume has the same effect.

Test data were accumulated on two GG configurations (GGT-191-460 and GGT-268-460), which permitted a correlation against the theoretically established stability criteria. The correlation was made difficult, since the decomposition delay could not be accurately measured. Only those data were used where the GG was operated at or close to 0.372 lb/sec, and the value of $\dot{W}/P_c$ was close to 8×10^{-4}. When severe instability occurred along with a drop in average gas temperature in the bed, the bed fractional pressure drop was evaluated at the highest stable flowrate. The fractional injector drop was correlated to a flowrate of 0.372 lb/sec.

Figure 16 shows test data accumulated on GGT-191-460. Although several bed configurations were used for the tests indicated, the void volume varied only between 21 and 23 $in.^3$. The decomposition delay was not determined from transient recordings, and hence a strict comparison with theory was not possible. However, the data does indicate a minimum fractional injector ΔP of 0.6 necessary for stable operation. Comparison with the theoretical stability limit would indicate that the decomposition delay for this unit may be from 0.020 to 0.025 second.

The chamber cross-sectional area was 5.67 $in.^2$; hence a bed loading of 0.0656 produced a maximum flow of 0.372 lb/sec. The pressure budget characteristics

[BASED ON MATHEMATICAL MODEL OF GAS GENERATOR AND FEED SYSTEM AND CORRELATED WITH TEST RESULTS]

CRITICAL PARAMETERS

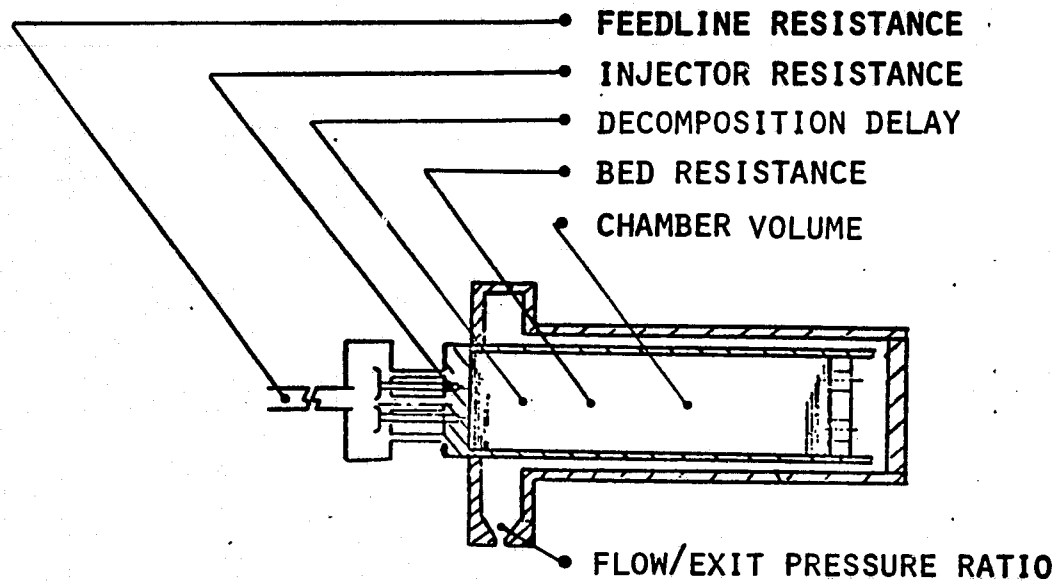

Figure 14 Stability Criteria

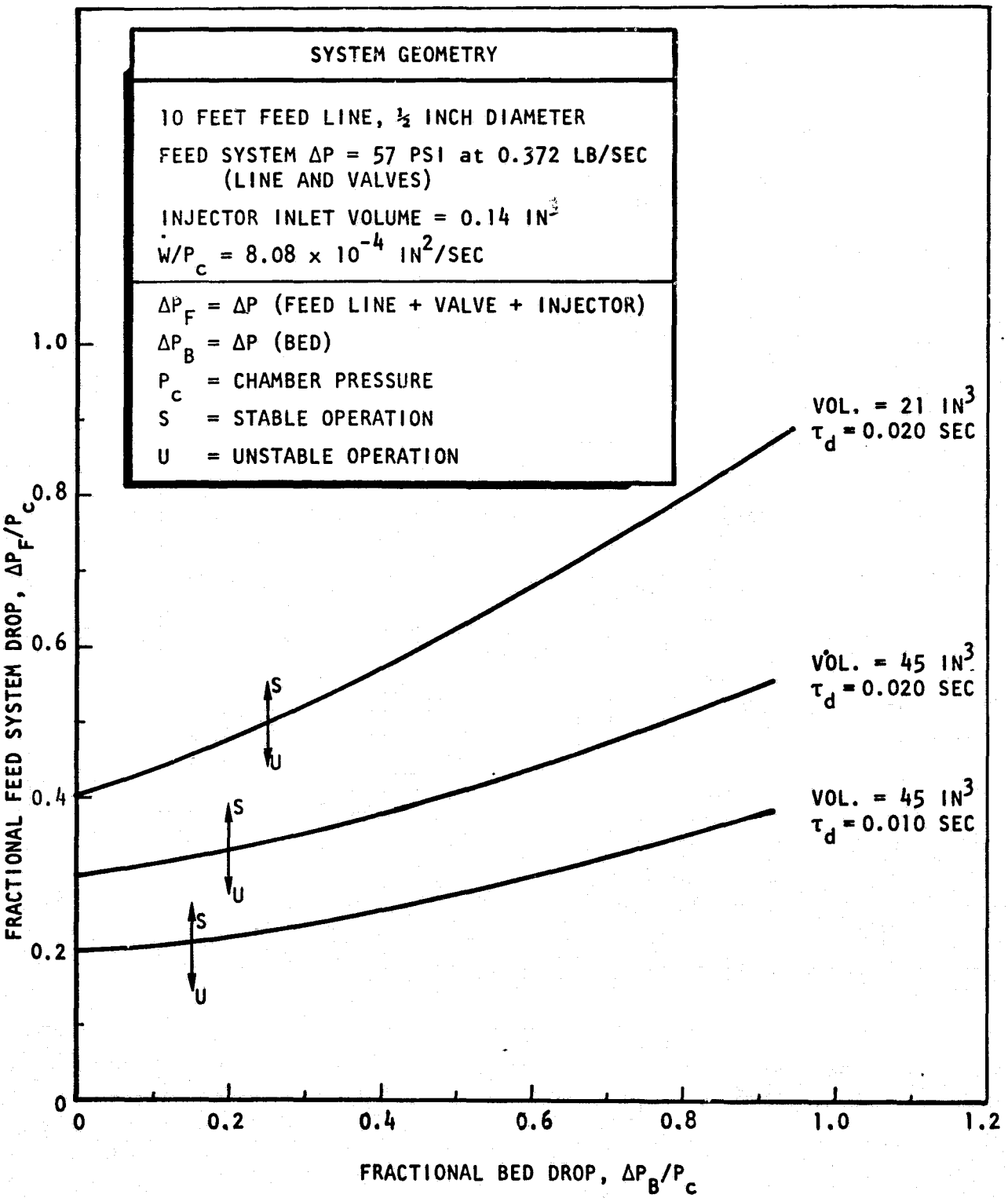

Figure 15. Gas Generator Stability Criteria Based on Analog Model Analysis (Flowrate = 0.372 lb/sec)

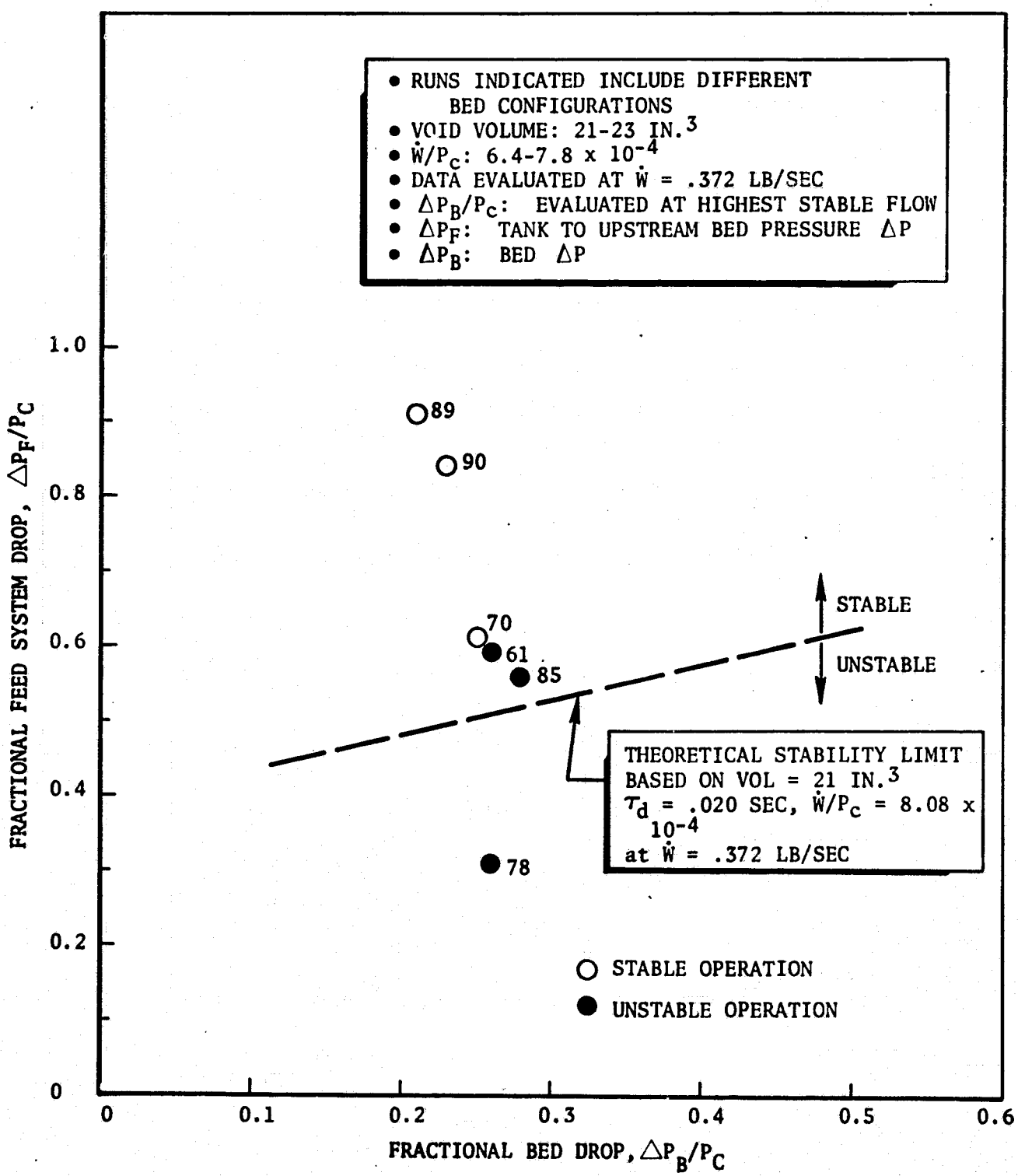

Figure 16. Stability Correlation, Test Data on GGT-191-460

are shown in Fig. 17. The fractional injector pressure drop is nearly linear with bed loading as can be seen from the relation:

$$\frac{\Delta P_i}{P_t} = R_i \left(\frac{A_t}{A_c}\right) g \frac{G}{C^*}$$

where

R_i is injector resistance,

A_t/A_c the ratio of throat to chamber area, and G is bed loading. Note that a decrease in C* at low power level offsets the linear relationship. The bed fractional pressure drop is nearly constant; a light increase at low flowrates is due to a Reynolds number effect on friction factor. The regenerative coolant passage fractional drop is relatively small, 0.028, and constant with flowrate. The total gas generator fractional pressure drop is 22.8 percent at maximum power level.

Figure 18 shows test data accumulated on GGT-268-460. The void volume for the various bed configurations varied from 40 to 45 $in.^3$. The decomposition delay was measured to be approximately 0.010 seconds. The variation in $\dot{W}/P_c$ was from 5.8 to 12.1 due to a variation in throat area for the tests indicated (the effect of $\dot{W}/P_c$ on stability has not been established). Comparison with the theoretical stability limit is fairly good. In run 7, instability existed at 80 percent flow, chamber pressure oscillation amplitude was 2.5 percent. In test 5, the chamber prssure oscillation amplitude was 2.7 percent at 87-percent flow.

PERFORMANCE CHARACTERISTICS

Performance

Performance of the model GGT-268-560 design developed under this program is described in Table 3.

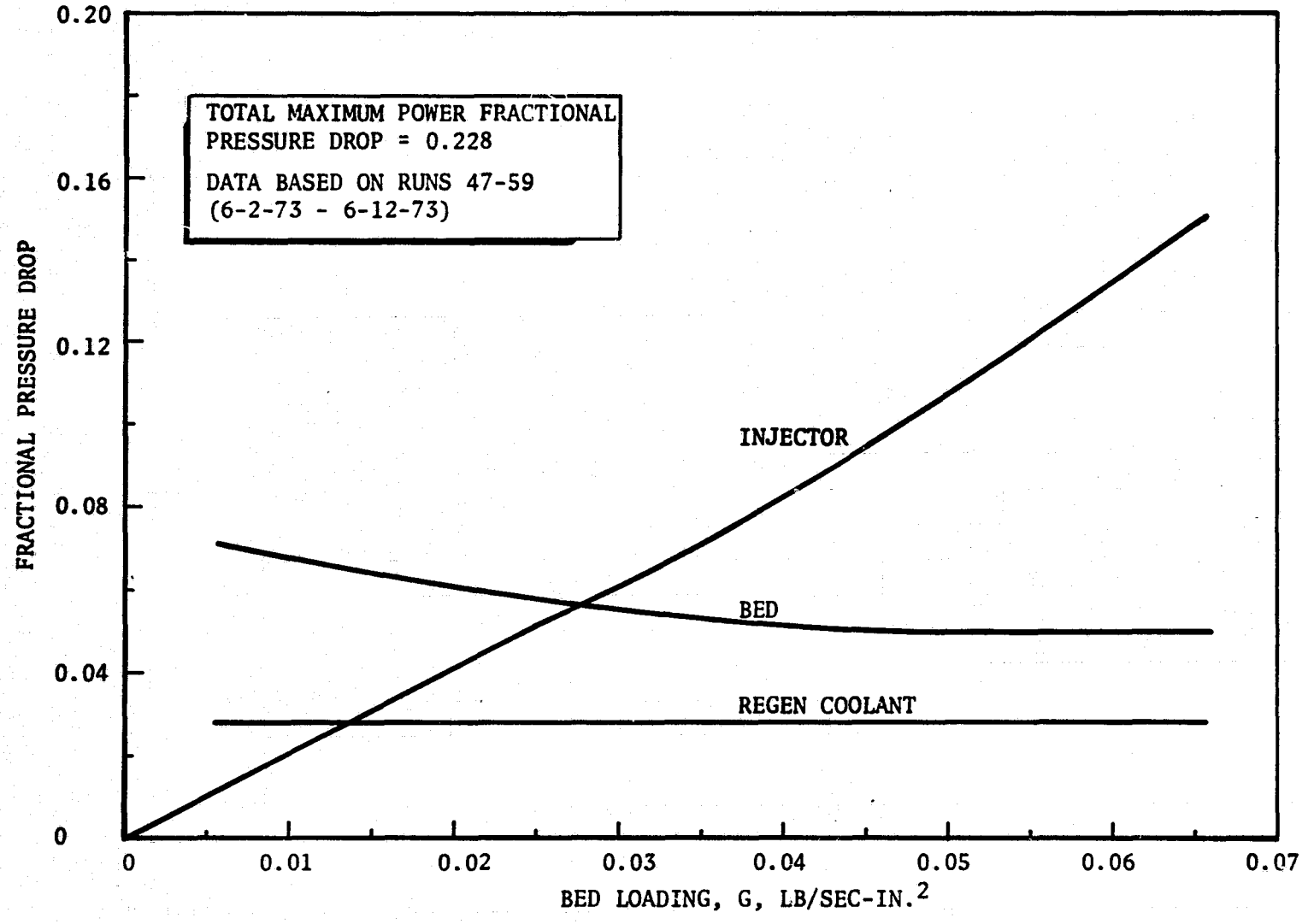

Figure 17. Pressure Budget - Model GGT-268-560

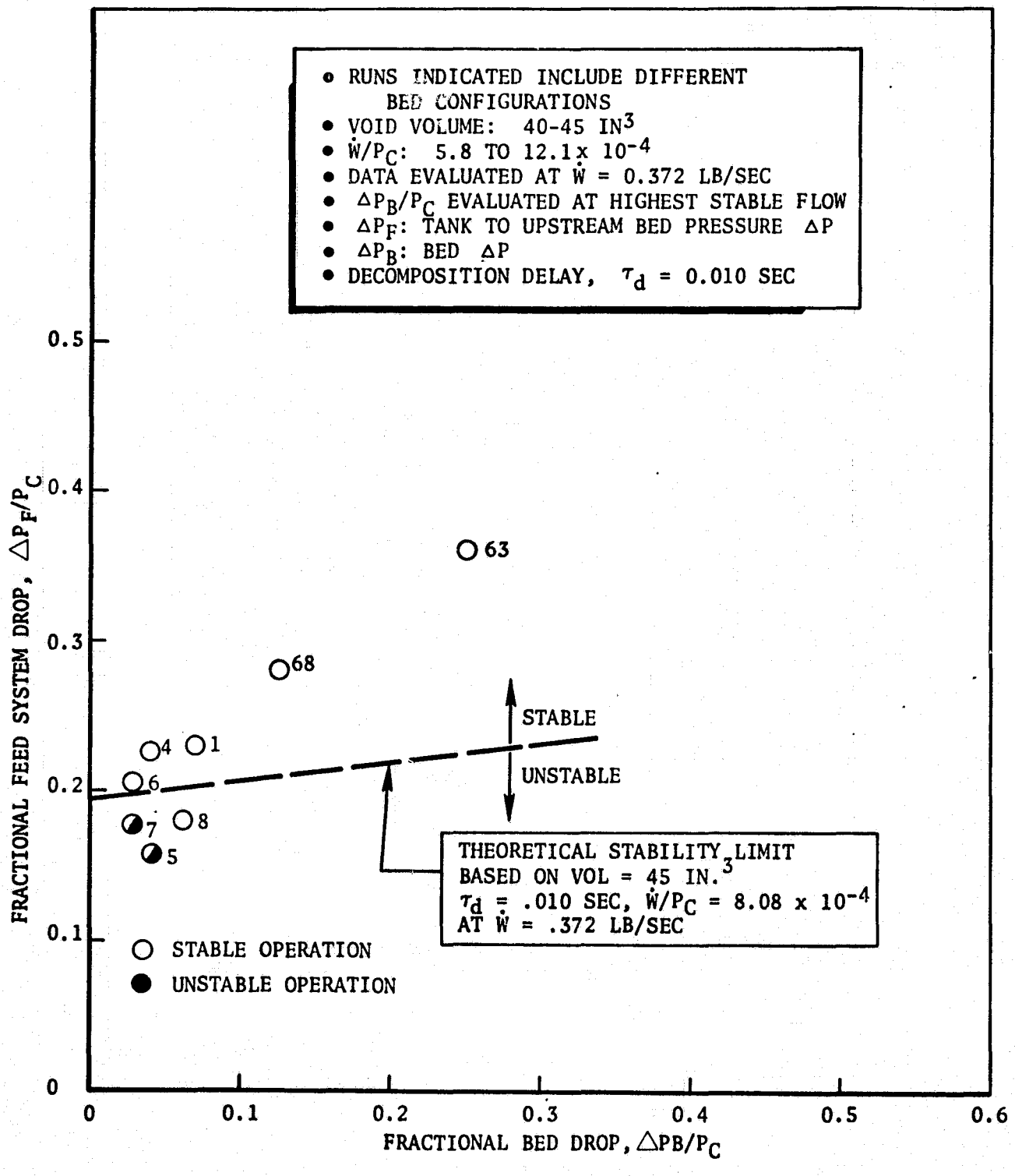

Figure 18. Stability Correlation - Test Data on GGT-268-460

TABLE 3. DELIVERED GAS CHARACTERISTICS

Power Level, percent	C* ft/sec	Bed Loading (g), lb/sec-in.^{2}	Exit Gas Temperature, F	NH_3 Dissociation Fraction	Molecular Weight, gr/gr mole	Exit Gas Pressure, psia
100	4260	0.0656	1633	0.615	12.90	565.0
50	4230	0.0328	1577	0.652	12.65	280.5
25	4207	0.0164	1512	0.697	12.40	139.5
10	4168	0.00656	1438	0.750	12.10	55.3

In Table 3, C* is defined by the relation:

$$\dot{W} = \frac{P_c A_t g}{C^*}$$

where

P_c is exit gas pressure

A_t is exit throat area

LIFE TEST

Test Set Up

The life test demonstration of the gas generator was conducted at the propellant research area (PRA) in Sugar Stand 2. PRA is located in the Santa Susana Field Laboratories (SSFL). The installation is shown by the photograph in Fig. 19 and the schematic in Fig. 20 shows both the critical flow components and related instrumentation. All numbered components are listed in Table 4 giving instrumentation ranges as well as method of recording during a test. The basic facility, Sugar Stand 2, was developed for both IR&A and other contracts and was modified as shown in Fig. 20.

Figure 19. Gas Generator Test Installation 5AA34-5/11/73/-S1A

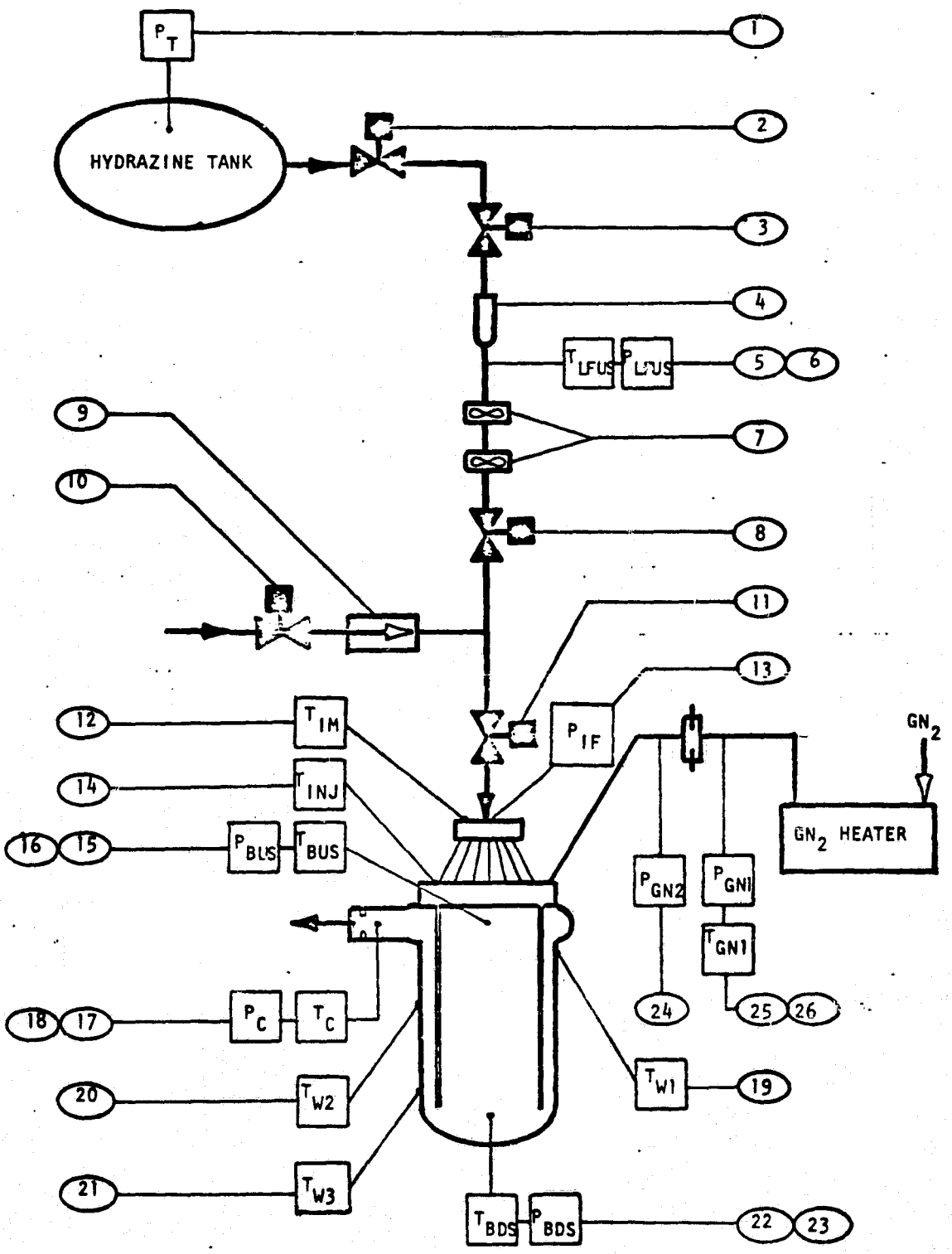

Figure 20. Gas Generator Test Installation

TABLE 4. SUGAR STAND 2 INSTRUMENTATION LIST

Schematic I.D.	Parameter		Recorder
1	Tank pressure		
2	Tank shut-off valve		
3	Pre-valve		
4	Filter - 10 microns		
5	Hydrazine line temp	T_{LFUS}	1/C 0-200 F M-H*
6	Hydrazine line pressure	P_{LFUS}	0-1000 M-H
7	Hydrazine flowmeter		0.07-0.60 lb/sec E.A. & O-graph
8	Main valve		O-graph
9	Purge check valve		
10	Purge check valve		
11	Throttle valve		
12	Manifold temperature	T_{IM}	C/A 0-1000 M-H
13	Hydrazine inlet pressure	P_{IF}	0-1000 M-H & O-graph
14	Injector temperature	T_{INJ}	C/A 0-2000 M-H
15	Bed temperature upstream	T_{BUS}	C/A 0-2000 M-H
16	Pressure upstream of bed	P_{BUS}	0-1000 M-H & O-graph
17	Discharge temperature	T_C	C/A 0-2000 M-H & O-graph
18	Discharge pressure	P_C	0-1000 M-H & O-graph
19	Wall temperature #1	T_{WI}	C/A 0-2000 M-H
20	Wall temperature #2	T_{W2}	C/A 0-2000 M-H
21	Wall temperature #3	T_{W3}	C/A 0-2000 M-H
22	Bed temperature downstream	T_{BDS}	C/A 0-2000 M-H
23	Bed pressure downstream	P_{BDS}	C/A 0-1000 M-H O-graph
24	GN_2 Pressure Orifice Discharge	P_{GN2}	0-300 M-H
25	GN_2 Pressure Orifice Inlet	P_{GN1}	0-300 M-H
26	GN_2 Temperature Orifice Inlet	T_{GN1}	C/A 0-2000 M-H

*M-H ⟶ Minneapolis-Honeywell strip chart recorder

Test Procedure

The test procedure developed for this phase of the work, consisted of conducting first the checkout test, then an acceptance test to determine typical operating characteristics of the gas generator. The initial acceptance test was then followed by ten mission duty cycles as described in Fig. 21 and Table 5. After the tenth mission duty cycle (MDC) a five hundred second full power burn was conducted followed by the final acceptance test. Comparison between the initial and final acceptance test as well as between the first and last MDC was used to determine the effect of the prescribed test series.

Data and Results

At the initiation of the first test, a pressure spike occurred. Testing was continued until excessive "chugging" indicated difficulties.

The gas generator was removed from the test facility and visually inspected. Externally there was no indication of any damage to the gas generator. X-rays of the gas generator showed that the inner liner had been deformed by the pressure spike so as to conform to the inside of the outer structural shell. This resulted in the screens being completely loose, providing a large area for hydrazine to channel, resulting in a virtual blockage of gas flow through the regenerator section, and thereby resulting in unstable operation of the gas generator.

This occurrence was caused by a facility error which resulted in a 150 psia tank pressure instead of the preset 50 psia tank pressure.

One of the beneficial conclusions which can be drawn from this pressure excursion is, that this gas generator design is probably one of the most reliable structural designs that can be incorporated into a small, compact, lightweight, flight system. This conclusion is based on the following evaluation, when an overpressure occurs in this gas generator, the extremely ductile inner sleeve (Inconel 600) deforms into the regenerative channel, thereby absorbing much of the energy release and the strong and not very ductile high temperature, high strength outer

TABLE 5. MISSION DUTY CYCLE SCHEDULE

POWER LEVEL %	DURATION ♦ SEC
0	-
10*	500
50	275
10	800
100*	2
10	100
30	800
10	100
100*	100
10	105
0	30 to 300
10*	500
50	275
10	800
100*	2
10	100
30	800
10	100
100*	100
10	105
0	30 to 300

* Power level transitions from 0% to 10% and from 10% to 100% were step changes; transitions to and from the 30% and 50% power levels took place in approximately 0.5 seconds, utilizing a preset delay circuit.

♦ Total firing time per mission duty cycle 1.546 hours

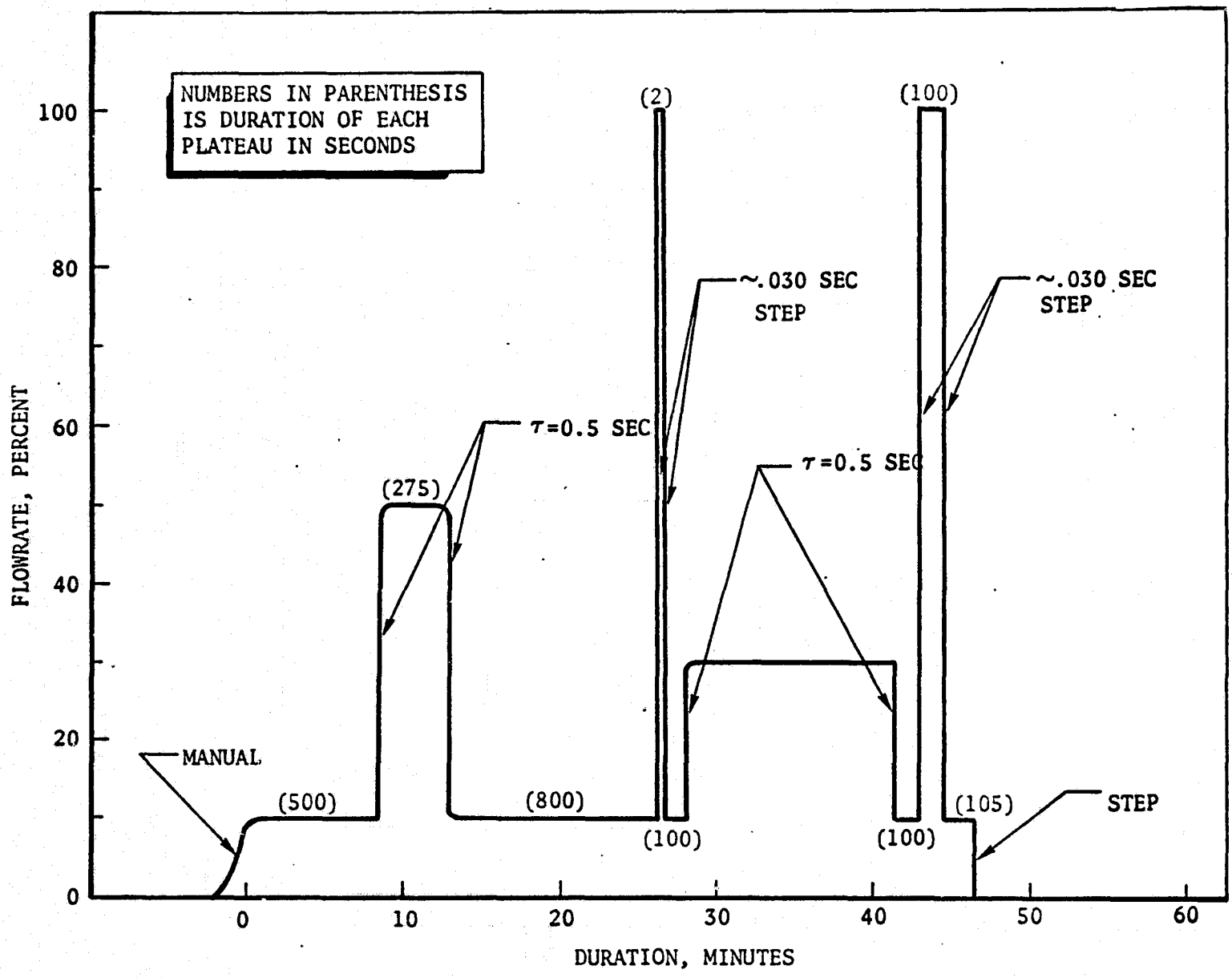

Figure 21. Approximate Flowrate Schedule (Half Mission Duty Cycle)

shell is not exposed to this sharp overpressure. Had this design consisted of solely a single high strength, high temperature outer shell, it is probable that the sudden overpressure would have resulted in shattering the gas generator. As it is, this gas generator should be able to withstand 10,000 to 20,000 psi pressure surges without causing external damage. This is a very important feature for a manrated unit.

Gas generator No. 1 was cut open and a new inner sleeve was fabricated and welded to the injector. To minimize delay in this program, the S/N 2 gas generator was packed and assembled so that it could be installed in the test facility for the mission duty cycle series.

The first checkout test was conducted successfully. This test consisted of gas generator No. 2 installed in the standard PRA facility using the facility valve instead of the throttle valve. Flow and pressure were controlled by changing tank pressurization levels. Operation of the gas generator was smooth over the entire range of flowrates. At design point condition a flowrate of 0.378 lb/sec was reached and the temperature at the discharge of the gas generator was 1674 F and chamber pressure was 559 psia. Evaluation of the data indicates that the gas generator was operating satisfactorily and performing essentially at design conditions.

Gas generator, S/N 2, was used to complete the mission duty cycle phase of this test program. This test phase, from initial acceptance test, through 10 MDCs, a 500 second full power burn, and final acceptance test was completed satisfactorily. The gas generator operated smoothly over the entire spectrum of ramp and step changes from 10 percent to 100 percent flowrates and did not show any degradation due to the 18 hours of testing.

During the step changes, consisting of operating the gas generator at 10 percent flowrate and increasing the flowrate to 100 percent at the slew rate of the throttle valve (20 to 30 milliseconds) there was no overshoot nor undershoot of any pressures. A typical set of oscillograph traces is shown in Fig. 22 which shows the data from the last two second full-power step during the 10 MDCs. It

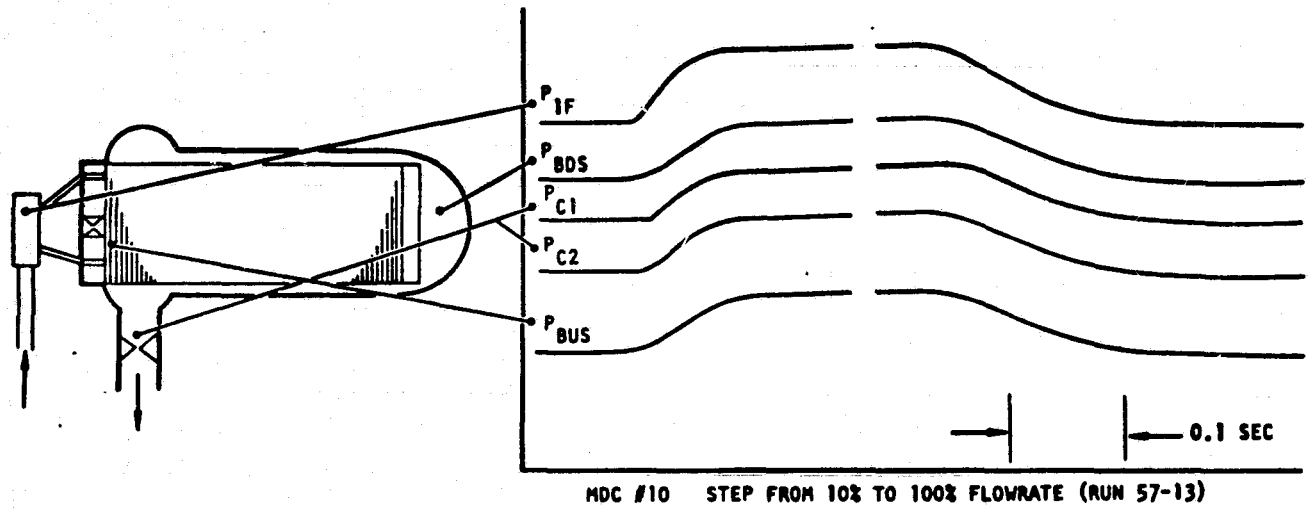

- NO DEGRADATION IN TRANSIENT PERFORMANCE (FROM 1st MDC)
- NO MEASURABLE OVERSHOOT OR UNDERSHOOT
- NO MEASURABLE ROUGHNESS/INSTABILITY

Figure 22. Life Test Results, 10 MDC's + 500 Seconds Sustained Maximum Power

can be seen that in a step change, P_{IF} (pressure upstream of injector) reaches 63 percent of full pressure in 20 milliseconds and full pressure is developed in approximately 50 to 60 milliseconds.

The total variation in exit gas temperature over the operating range (Fig. 23) is approximately 20 F. The variation in exit gas pressure (Fig. 24) with flowrate was 10 psi, or less than 2 percent of maximum pressure. There was no measurable variation in injector resistance; however, the bed pressure drop increased 14 psi, or approximately 50 percent during the tests (Fig. 25), probably due to bed compaction. With respect to transient performance degradation, Fig. 22 depicts a typical power "step" between 10 and 100 percent flowrate recorded during the last mission duty cycle. There was virtually no difference between it and a similar step recorded during the first MDC.

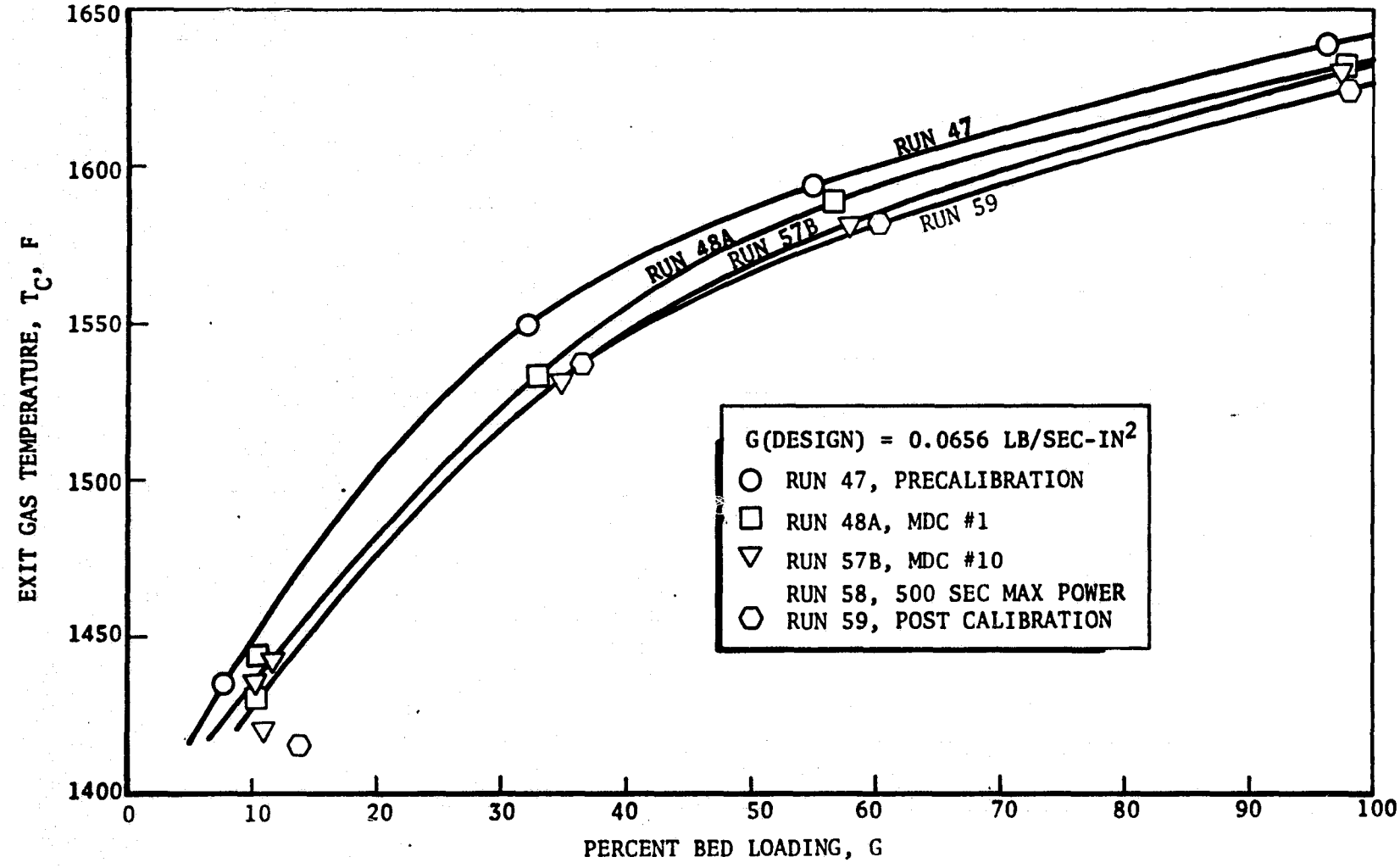

Figure 23. Life Test - Exit Gas Temperature Variation

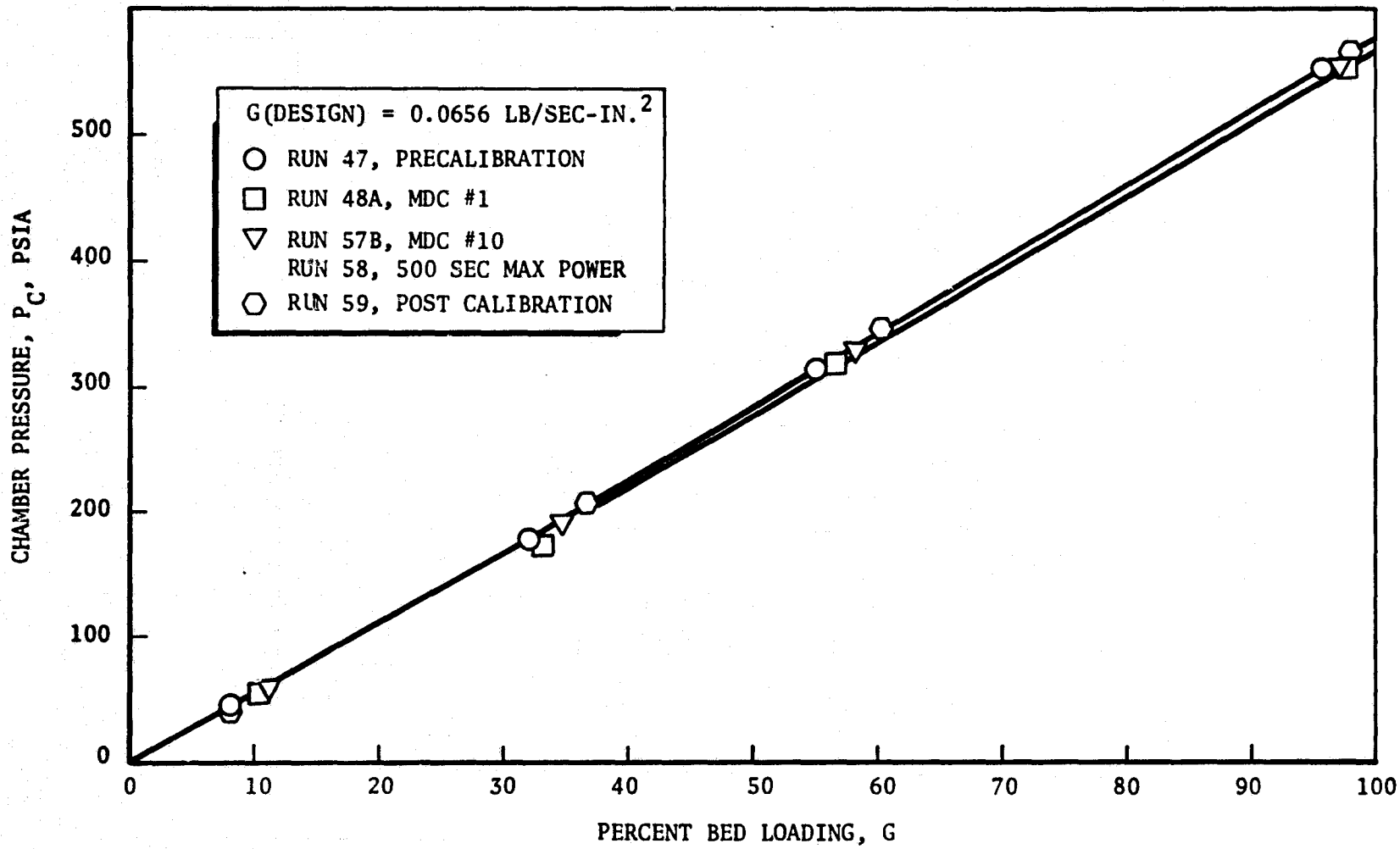

Figure 24. Life Test - Chamber Pressure Characteristics

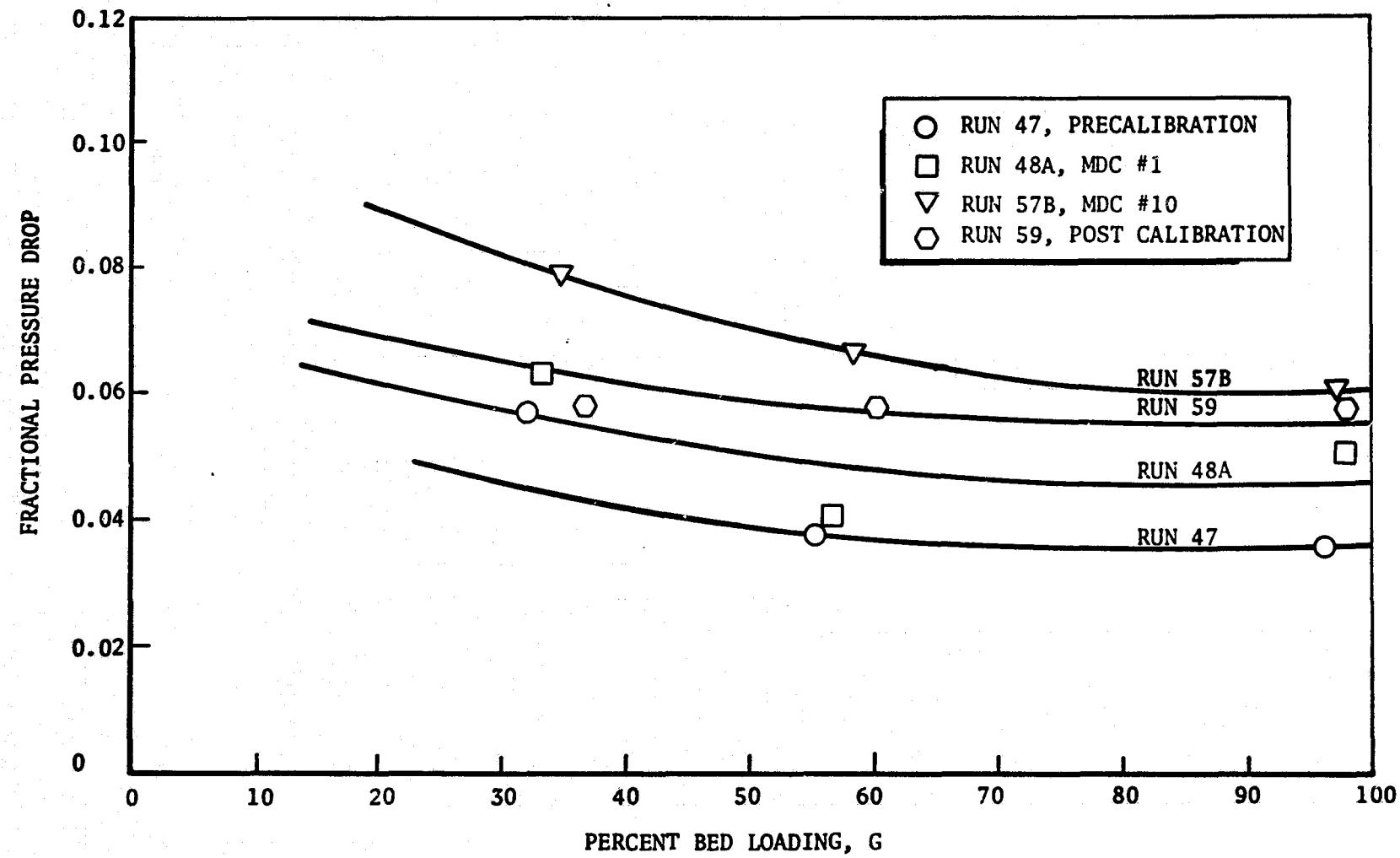

Figure 25. Life Test - Bed Characteristics

PHASE II PERFORMANCE TESTS

ACCEPTANCE TESTS

All Phase II tests were performed using the S/N 1 gas generator. The Phase I tests (S/N 2 gas generator) accumulated a total operating time of 18.3 hours, as compared to 2.48 hours total for the S/N 1 gas generator. Therefore, the changes between the initial and final acceptance tests of the Phase I program are more definitive of the small changes in operational characteristics which may occur with time.

Initial and final acceptance tests were also performed during the Phase II program. However, the primary interest was to verify the proper functioning of the gas generator, rather than to evaluate long time trends.

Experimental Setup

The acceptance tests were performed with the normal test stand installation shown in Fig. 26 and 27. The pressure, temperature, and flow measurements are shown there, and duplicate the instrumentation used in the Phase I portion of the program.

Test Procedure

Prior to performing the initial acceptance test the gas generator was operated for approximately one hour. Such preliminary operations had also been performed in Phase I. The purpose of this run (Run No. 61-Table 6) was to permit screen settling, clearance changes, screen surface changes, and other thermal cycling effects which might be expected to occur in initial operations. This corresponds, in a sense, to the break-in cycle for an internal combustion engine. Also, this test served as a checkout for the proper operation of the test stand and instrumentation. At the conclusion of this test, the acceptance test (Run No. 62) was performed. As may be seen in Table 6, this consisted of four approximate five minute periods of operation at the 10, 30, 50, and 100 percent power levels.

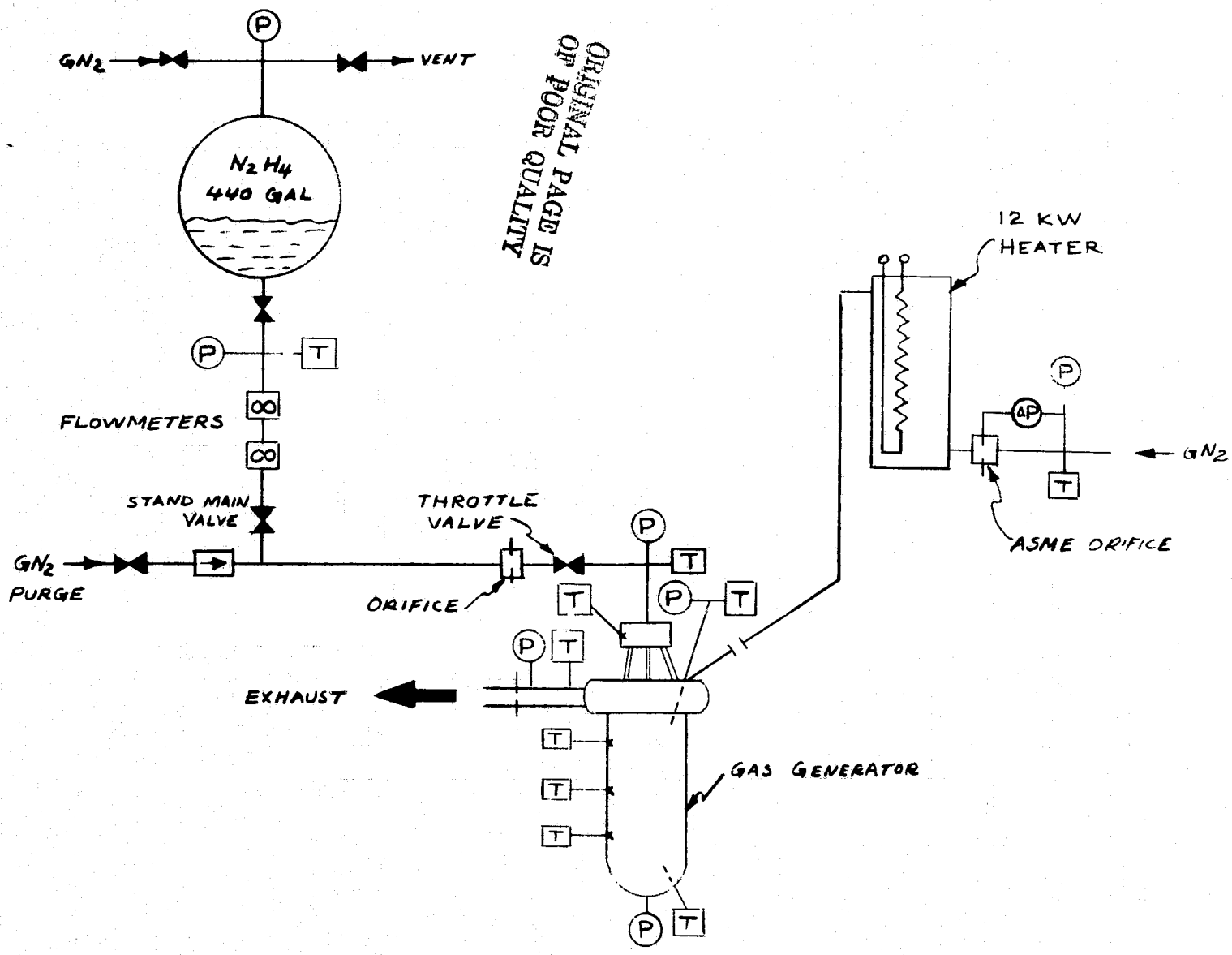

Figure 26. Test Stand Installation Used for Gas Generator Characterization Under Nominal Operating Conditions

Figure 27. Test Stand Installation Used for Gas Generator Tests Under Nominal Operating Conditions

At the conclusion of Phase II investigations, a final acceptance test was performed to demonstrate that the gas generator was properly operating and suitable for any further investigations which might be desired.

Data and Results

The data and results from the initial acceptance test (Run No. 61) and the final acceptance test (Run No. 68) are summarized in Table 6. It may be noted that the average c* efficiency for the initial acceptance test was approximately 98 percent, whereas an approximate 96 percent value was computed for the final acceptance test. It is not felt, however, that these apparent changes were real but rather due to instrumentation.

In addition to questions as to the degree of accuracy of the flow measurements, all tests after Run No. 63 were made with hydrazine having approximately 2.8 percent water. While corrections for this average water content were made, it is not certain as to the actual percent of water in the fuel for any particular tests. This results because high water content fuel was added to specification fuel, and the degree of uniform mixing attained is not known. A final consideration is that the calibrations of the pressure transducers may have been affected by the vacuum pressures they experienced.

Conclusions

The results of the initial and final acceptance tests indicate that the gas generator was initially, and is now, in good operating condition. The indicated possible decrease in performance efficiency of about 2 percent is probably the result of measurement inaccuracies.

HELIUM SATURATION STUDY

The objective of this experiment was to verify the insensitivity of the gas generator operations to the presence of dissolved helium in hydrazine. The mass of helium that can be dissolved is very small compared to the mass of the propellant (approximately 0.017 percent by weight at the conditions of this study),

	1	2	3	4	5	6	7	8	9	10	11
	RUN No.	$P_{LF\ U/S}$ PSIG	P_{IF} PSIG	$P_{B\ U/S}$ PSIG	$P_{B\ D/S}$ PSIG	P_c PSIG	P_c PSIA	$T_{B\ U/S}$ F	$T_{B\ D/S}$ F	T_c F	T_{1M-1} F
1	61-1	756	41	41	35	38	52				
2	61-2	756	220	207	195	192	206				
3	61-3	756	389	360	340	331	345				
4	61-4	755	680	598	565	551	565				
5	62-1	742	32	32	30	30	44	673	1510	1483	
6	62-2	742	179	175	165	162	176	716	1587	1576	
7	62-3	742	342	320	308	299	313	901	1632	1625	
8	62-4	742	651	575	555	540	554	1091	1679	1679	
9	63-1	752-765	+60 50-30	+70 35-20	-	+60 30-20	-	673	1453	1388	
10	63-2	755-762	+260 197-150	+235 190-150	173	+200 170-140	-	442-1116	1591	1567	
11	63-3	762	+290 350-220	+225 323-198	-	+100 304-160	-	905-1212	1658	1692	97-106
12	63-4	761	+ 60 684-130	+ 20 592-192	562	+ 20 562-190	-	1148-1510	1643	1621	
13	63-5	755	360	332	312	316	330	1000	1638	1612	
14	63-6	760-770	208	198	183	191	205	806	1603	1576	
15	63-7		58	58	51	60	74	596	1527	1492	
16	63-8		28	28	21	31	45	645	1481	1422	
17	63-9		0	0	0	9	23	894	1453	1089	
18	63-10		30	29	23	31	45	682	1459	1405	
19	63-11		197	190	173	181	195	810	1558	1545	
20	63-12		359	322	310	317	331	983	1612	1603	
21	63-13	762	683	594	563	563	577	1212	1656	1663	
22	63-14	758-770	684-24	594-25	563-20	563-30	-	1212- 669	1656-1536	1663-1527	
23	63-15	763-750	24-673	25-585	20-555	30-556	-	669-1254	1536-1665	1527-1656	
24	63-16	750	676	588	557	557	571	1229	1665	1661	
25	63-17	750-765	676-156	588-152	557-140	557-140	-	1229-756	1665-1589	1661-1567	
26	63-18	760-767	156-220	152-210	140-193	200	214	767	1589	1563	
27	63-19	760-767	220-26	26	21	31	45	626	1558	1501	
28	63-20	760	67	67	56	68	82	708-628	1547-1514	1501-1479	
29	63-21	760	202	194	179	186	200	767	1514	1527	
30	63-22	762	360	332	311	316	330	1000	1603	1585	
31	63-23	762	685	594	562	564	578	1224	1440	1654	
	63-24	760	360	333	312	318	332	1021	1634	1612	
33	63-25	754-761	204	197	181	189	203	806	1591	1565	
34	63-26	755-770	62	64	58	65	79	574	1510	1475	
35	63-27	757-752	681	589	558	560	574	1224	1665	1663	

FORM R 79-Y-3

11	12	13	14	15	16	17	18	19	20	21	22	23
T_{1M-1} F	T_{1M-2} F	T_{1F} F	T_{W-1} F	T_{W-2} F	T_{W-3} F	$\dot{W}_F$ LB/SEC	C* FT/SEC	THEOR C* FT/SEC	η_{C^*}	DURATION OF STEP SEC		GE
						0.0516	2830				PRE-ACCEPTANCE	
						0.139	4181				TO STABILIZE T	
						0.230	4232				TOTAL TIME 355	
						0.376	4239					
			1505	1507	1507	0.0292	4251	4176	-	296	INITIAL ACCEPT	
			1589	1580	1580	0.123	4037	4220	0.957	304	TOTAL TIME 118	
			1636	1625	1630	0.211	4185	4240	0.987	308		
			1683	1674	1674	0.371	4212	4260	0.989	308		
			1426	907	1470	0.0215	-	-	-	208	HELIUM SATURAT	
			1532	945	1549	0.131	-	-	-	56	TEST	
7-106			1603	979	1621	0.217	-	-	-	32	1. TOTAL TIME	
	NOT INSTALLED	NOT INSTALLED	1607	983	1598	0.392	4022	4237	0.949	36	2. INITIAL PER	
			1589	983	1589	0.220	4119	4237	0.972	36	AFFECTED BY	
			1580	971	1558	0.137	4131	4220	0.979	28	TRAPPED HEL	
			1532	901	1505	0.0501	4126	4180	0.987	44	POCKETS IN	
			1470	928	1448	-	-	-	-	92	3. TANK PRESSU	
			1448	930	1431	-	-	-	-	60	SEAT LEAKED	
			1435	937	1426	0.0251	5018	4143	-	100	A TENDENCY	
			1523	979	1519	0.131	4105	4210	0.975	76	PRESSURIZE	
			1585	1009	1580	0.220	4132	4230	0.977	88	SLIGHT VENT	
			1647	1063	1634	0.393	4019	4250	0.946	84	TANK WAS RE	
			1647-1580	1063-1038	1634-1549	-	-	-	-	60	FREQUENT IN	
			1580-1634	1038-1060	1549 1625	-	-	-	-	76	TO DESIRED	
			1647	1063	1612	-	-	-	-	36		
			1647-1603	1063-1042	1634-1565	-	-	-	-	80		
			1580	1032	1551	-	-	-	-	48		
			1558	1527	1013	-	-	-	-	32		
			1549	1013	1519	0.0595	3836	4180	0.918	8		
			1545	1017	1541	0.135	4088	4200	0.973	12		
			1580	1042	1603	0.224	4048	4225	0.958	16		
			1616	1156	1612	0.397	3987	4250	0.938	16		
			1607	1046	1598	0.223	4090	4235	0.966	44		
			1580	1038	1558	0.136	4120	4220	0.976	40		
			1510	996	1483	0.0494	4464	4175	-	96		
			1638	1055	1630	0.390	4028	4252	0.947	68		

FOLDOUT FRAME 2

TABLE 6. PERFORMANCE TESTS

FOLDOUT FRAME 2

EC	18 C* FT/SEC	19 THEOR C* FT/SEC	20 η_{C^*}	21 DURATION OF STEP SEC	22 GENERAL COMMENTS	23	24	25	26	27
16	2830				PRE-ACCEPTANCE TEST AGING					
9	4181				TO STABILIZE THERMAL BED				RUN 61	
0	4232				TOTAL TIME 3552 SECONDS					
6	4239									
92	4251	4176	-	296	INITIAL ACCEPTANCE TEST					
3	4037	4220	0.957	304	TOTAL TIME 1188 SECONDS					
1	4185	4240	0.987	308					RUN 62	
1	4212	4260	0.989	308						
15	-	-	-	208	HELIUM SATURATED N_2H_4					
1	-	-	-	56	TEST					
7	-	-	-	32	1. TOTAL TIME 1572 SECONDS					
2	4022	4237	0.949	36	2. INITIAL PERIOD OF OPERATION					
0	4119	4237	0.972	36	AFFECTED BY PASSAGE OF					
7	4131	4220	0.979	28	TRAPPED HELIUN GAS					
01	4126	4180	0.987	44	POCKETS IN PROPELLANT LINE					
	-	-	-	92	3. TANK PRESSURE REGULATOR					
	-	-	-	60	SEAT LEAKED, RESULTING IN					
51	5018	4143	-	100	A TENDENCY TO OVER-					
1	4105	4210	0.975	76	PRESSURIZE THE TANK. A					
0	4132	4230	0.977	88	SLIGHT VENTING OF THE					
3	4019	4250	0.946	84	TANK WAS REQUIRED AT					
	-	-	-	60	FREQUENT INTERVALS TO RETURN					
	-	-	-	76	TO DESIRED PRESSURE LEVELS					
	-	-	-	36					RUN 63	
	-	-	-	80						
	-	-	-	48						
	-	-	-	32						
95	3836	4180	0.918	8						
5	4088	4200	0.973	12						
	4048	4225	0.958	16						
	3987	4250	0.938	16						
3	4090	4235	0.966	44						
5	4120	4220	0.976	40						
94	4464	4175	-	96						
0	4028	4252	0.947	68						

FOLDOUT FRAME

	1 RUN No.	2 $P_{LF\ U/S}$ PSIG	3 P_{IF} PSIG	4 $P_{B\ U/S}$ PSIG	5 $P_{B\ D/S}$ PSIG	6 P_c PSIG	7 P_c PSIA	8 $T_{B\ U/S}$ F	9 $T_{B\ D/S}$ F	10 T_c F	11 T_{IM-1} F	T_{I}
1	64-1	790										
2	64-2	790										
3	64-3	990										IN
4	65-1	993										
5	65-2	993										
6	65-3	993										
7	65-4	993										
8	66-1	990	50	50	42	43	57	626	1444	1409		
9	66-2	990	134	132	119	119	133	686	1541	1541		
10	66-3	990	223	213	197	194	208	810	1585	1574		
11	66-4	990	293	277	255	252	266	852	1598	1603		
12	66-5	990	250	237	218	216	230	831	1598	1589		
13	66-6	990	188	181	163	164	178	803	1576	1558		
14	66-7	990	87	76	63	68	82	660	1527	1495		
15	67-1	766				30	44	647	1426	1349	335	
16	67-2	766				179	193	1510	1558	1538	-	1
17	67-3	766	0	0	0	0	0	-684	-1224		-	
18	67-4	766						684	1224		464	4
19	68-1	766	50	46	39	40	54	682	1442	1405		
20	68-2	766	196	181	173	171	185	852	1554	1538		
21	68-3	766	340	309	294	292	306	958	1594	1589		
22	68-4	766	538	473	452	448	462	1089	1625	1625		
23	68-5	940	622	540	513	511	525	1093	1643	1640		
24												
25												
26												
27												
28												
29												
30												
31												
33												
34												
35												

FORM R 79-Y-3

FOLDOUT FRAME 2

TABLE 6. PERFORMANCE

12 T_{1M-2} F	13 T_{1F} F	14 T_{W-1} F	15 T_{W-2} F	16 T_{W-3} F	17 $\dot{W}_F$ LB/SEC	18 C* FT/SEC	19 THEOR C* FT/SEC	20 η_{C*}	21 DURATION OF STEP SEC	22	23 GENERAL
					-					DUTY CYCLE INSENSITIV	
					-					TOTAL TIME 468 SECON	
NOT INSTALLED	~120				0.186						
					-					HOT MANIFOLD RESTART	
					-					PROPELLANT TEMPERATU	
					-					TOTAL TIME 148 SECON	
					-						
	171	1362	1388	1433	0.0587	2739*	4103	0.668	40	HEATED N_2H_4 TESTS	
	180	1448	1455	1492	0.933	4021*	4170	0.964	112	TOTAL TIME 1080 SECO	
	180	1514	1514	1545	0.148	3964*	4187	0.947	84		
	178-176	1545	1536	1574	0.190	3949*	4199	0.940	76		
	176-174	1545	1536	1567	0.163	3980*	4192	0.949	60		
	164-172	1523	1532	1556	0.125	4017*	4173	0.963	68		
	172	1470	1497	1492	0.0567	4079*	4148	0.983	112		
346	64	1250	1250	1314	1336				118	HEAT SOAKBACK AND AL	
135	64	1510	1532	1532					178	START	
98	64								796		
408	173	1216	1280	1256					-		
	63	1383	1405	1405	0.0409	3711	4103	0.904	220	FINAL ACCEPTANCE TES	
	63	1510	1532	1527	0.129	4046	4173	0.970	184	TOTAL TIME 956 SECON	
	63	1563	1572	1567	0.214	4034	4192	0.962	208	(N_2H_4 WATER CONTENT	
	63	1607	1612	1607	0.322	4048	4209	0.962	224		
	63	1616	1625	1621	0.365	4058	4214	0.963	120		

* NOTE: BASED ON MASS FLOWRATE AT FLOWMETER - A CORRE
VOLUME OF LESS DENSE, HEATED PROPELLANT WAS F
TO THE GAS GENERATOR

TABLE 6. PERFORMANCE TESTS (CONCLUDED) FOLDOUT FRAME 3

18 C* FT/SEC	19 THEOR C* FT/SEC	20 η_{C^*}	21 DURATION OF STEP SEC	22 GENERAL COMMENTS	23	24	25	26	27
				DUTY CYCLE INSENSITIVITY TESTS					
				TOTAL TIME 468 SECONDS				RUN 64	
				HOT MANIFOLD RESTART AMBIENT					
				PROPELLANT TEMPERATURE OPERATION					
				TOTAL TIME 148 SECONDS				RUN 65	
2739*	4103	0.668	40	HEATED N_2H_4 TESTS					
4021*	4170	0.964	112	TOTAL TIME 1080 SECONDS					
3964*	4187	0.947	84						
3949*	4199	0.940	76					RUN 66	
3980*	4192	0.949	60						
4017*	4173	0.963	68						
4079*	4148	0.983	112						
			118	HEAT SOAKBACK AND ALTITUDE					
			178	START				RUN 67	
			796						
			-						
3711	4103	0.904	220	FINAL ACCEPTANCE TEST					
4046	4173	0.970	184	TOTAL TIME 956 SECONDS					
4034	4192	0.962	208	(N_2H_4 WATER CONTENT 2.8%)				RUN 68	
4048	4209	0.962	224						
4058	4214	0.963	220						

* NOTE: BASED ON MASS FLOWRATE AT FLOWMETER - A CORRESPONDING VOLUME OF LESS DENSE, HEATED PROPELLANT WAS FURNISHED TO THE GAS GENERATOR

so it would not be expected that effects on c* efficiency of the gas generator would be perceptible. However, it is conceivable that the gas bubbles released from solution in the decompression resulting in passing through the throttle valve could trigger combustion instabilities.

The conclusions reached from the experimental data were that the gas generator operation was insensitive to the presence of the dissolved helium.

Experimental Setup

The major details of the test setup are shown in Fig. 28. As shown, the method used to insure complete saturation of hydrazine was to atomize it by means of a spray nozzle, and then to allow the mist to fall through the pressurized helium atmosphere. A "Spraying Systems" full cone spray nozzle (Number 1/8 GGD1) was used with an approximate 100 psi differential across it, resulting in a nominal 0.042 lb/sec injection rate.

The tanks used for these tests had the following dimensions:

Tank No. 5 (Supply Vessel): 56.5-inch ID sphere with 2.75-inch in wall thickness. Tank No. 7 (Receiver Vessel): 24-inch ID x 111-inch length, with 1.875-inch wall thickness. The temperature of the ullage space of both tanks was continually monitored with iron/constantan shielded thermocouples. Tank No. 5 thermocouple extended approximately 1 inch beyond the inner surface of the vessel, and Tank No. 7 thermocouple immersion was approximately 40 inches.

Test Procedure

The method selected to ensure complete saturation of hydrazine with helium was based on a study of various possible approaches to the problem. It was felt this method was the most compatible with time and budget considerations, while at the same time ensuring complete saturation. The procedures followed are detailed below:

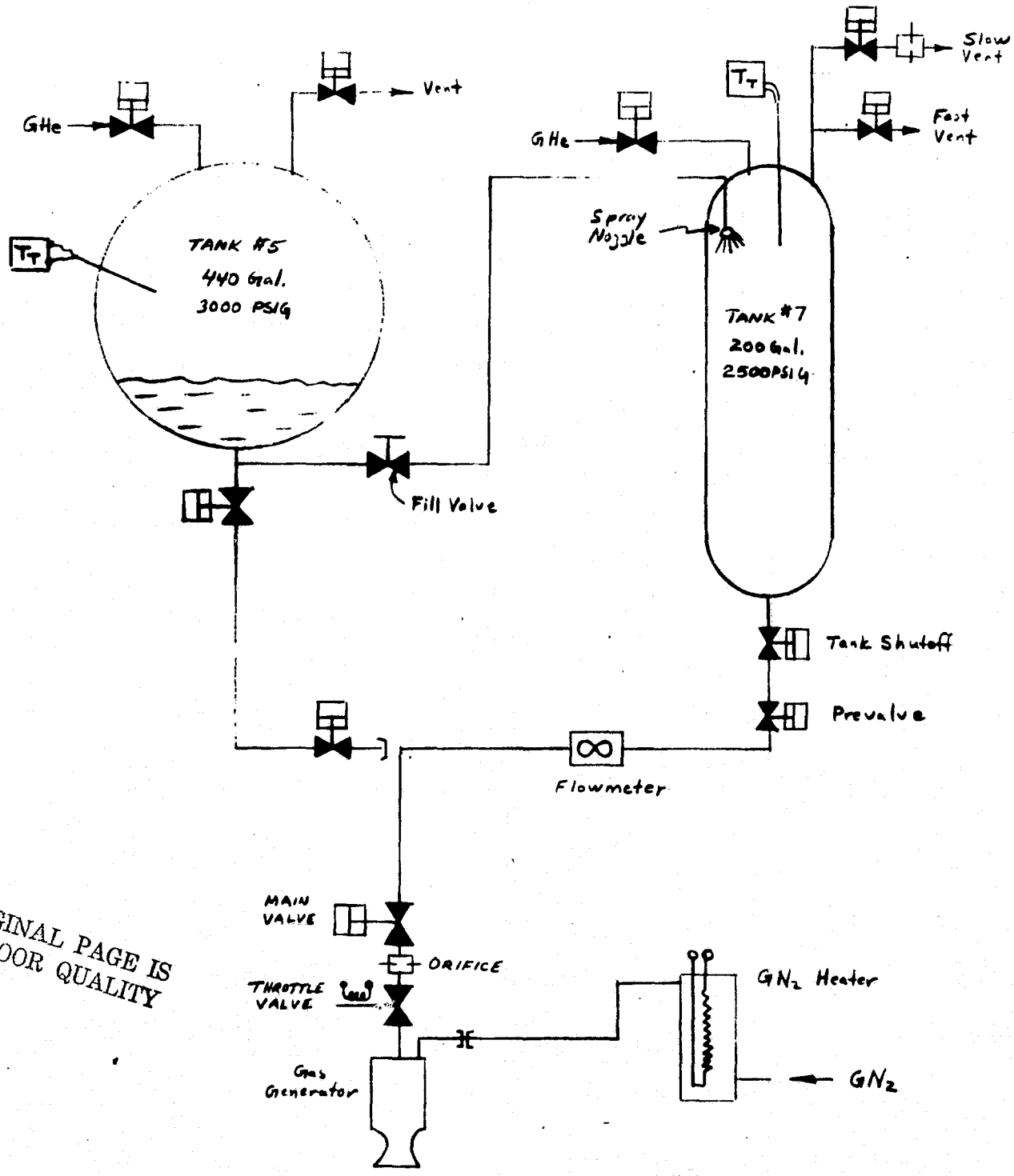

Figure 28. Test Stand Installation Used to Perform Tests With Helium Saturated Hydrazine

A. Preliminary Operations

1. Both tanks (see Fig. 28) were completely drained, including all propellant lines.
2. About 50 gallons of N_2H_4 were loaded into tank No. 5.
3. Both tanks were pressurized to approximately 150 psi with helium and then vented, three times.
4. With tank No. 7 pressurized to approximately 10 psi with helium, all valves between it and the gas generator were opened to purge that portion of the system.
5. The throttle valve and test stand main valve were then closed. It should be noted, however, that the tank (No. 7) shutoff valve and the prevalve were kept open throughout all subsequent operations.

B. Helium Saturation Operations

1. Tank No. 7 was pressurized with helium to the run pressure level (780 psig).
2. Tank No. 5 was pressurized with helium to 880 psig (to provide 100 psi pressure differential between the tanks.
3. The fill valve shown in Fig. 28 was opened.
4. Transfer of hydrazine from tank No. 5 to tank No. 7 through the atomizing spray nozzle required about 2-3/4 hours.
5. The fill valve was closed and tank No. 5 was vented. The sight gage reading made at this time indicated that approximately 40 gallons of hydrazine had been transferred into tank No. 7.

C. Gas Generator Startup and Run Operations

1. Heated GN_2 flow through the gas generator was initiated approximately one hour prior to completion of the helium saturation operation.
2. At the completion of the hydrazine transfer operation, the heated GN_2 flow was stopped and the gas generator inlet port was capped.
3. The test stand main valve was opened, with the throttle valve at its 1 percent flow setting. Note that the propellant tank was at

the run pressure level since it was not vented at the end of the saturation operations.

4. The gas generator heatup with hydrazine was completed by progresively opening the throttle valve from the one percent to the ten percent setting.
5. The throttle valve was opened to 10, 30, 50 and 100 percent step settings in increasing and decreasing sequences for steps of sufficient duration to obtain reasonably stabilized data. In addition, slow sweeps were made over the full range of throttle valve settings by means of an auxiliary potentiometer control to investigate the possibility of performance problems at intermediate flowrates.

Data and Results

The data for this study are summarized in Table 6 as run sequences 63-1 through 63-27. It should be noted that the propellant flowrates listed have a low confidence level since the flowmeter employed showed a tendency to slow down. Later calibrations were used to attempt to correct the data, but since the frictional resistance may have varied with time, this approach was not necessarily completely successful. Concomitantly, of course, the computed values of the c* efficiencies also have a similar uncertainty. As previously discussed, accurate performance evaluation was not of primary concern.

The initial operations showed sizable chamber pressure perturbations not observed in any of the previous tests. As shown in Table 6, these chamber pressure pulsations were noted at all of the power level steps (run numbers 63-1, 63-2, 63-3, and 63-4). During the course of these steps, it was noted that the magnitude and frequency of occurrence of the pulsations decreased with time. After Run. No. 63-4, further occurrences were not noted. Examination of the oscillograph data indicates that these disturbances were the result of entrapped helium gas pockets in the propellant supply line. Indicative of this was the fact that the pressure pulsations were extremely variable in nature, with no similarity to the characteristics of "chugging" disturbances occasionally observed in other thermal bed gas genenators. Most conclusive, of course, is the fact that after the first 5.5 minutes of operation, succeeding operations over a period of 20.6

minutes were free of these disturbances. It should be noted that the propellant lines were initially drained of all propellant, and that the physical configuration of the lines (i.e., horizontal orientation of most lines, with changes in line sizes) tended to encourage gas pockets.

Conclusions

1. Helium Saturation Procedure: During the time that hydrazine transfer between the two pressurized tanks was being performed, monitored temperatures in the ullage space indicated average temperatures of approximately 95 F for Tank No. 5 (supply tank) and 89 F for Tank No. 7 (receiver tank). Hydrazine line temperatures during the gas generator operations indicated that the hydrazine temperature in Tank No. 7 was also 89 F. Therefore, saturation conditions were not affected by temperature changes.

Reference 1 data indicate that at the temperature and pressure load maintained in Tank No. 7, 0.065 cc of helium (at standard temperature and pressure) would be dissolved in a gram of hydrazine. The saturation procedure followed were felt to be adequate to achieve full saturation.

2. Helium Effects on Gas Generator Operations: The gas generator operations were not affected by the presence of dissolved helium in the hydrazine. This, however, was not unexpected, since hydrazine has a greater solubility for nitrogen (approximately double-see Ref. 1); and it is likely that nitrogen saturated condition existed during some of the duty cycles performed in the gas generator S/N 2 endurance tests and no instabilities were noted during those tests.

OFF-NOMINAL TEMPERATURE TESTS

The objective of these tests was to demonstrate gas generator operation with a hydrazine supply temperature ranging between 50 to 150 F. Since propellant temperatures ranging from 46 to 52 F existed for the initial acceptance test and first three mission duty cycle tests performed during the Phase I firings, the

low temperature off-nominal condition had already been adequately investigated. The subject tests, therefore, only concerned themselves with hot hydrazine conditions.

Experimental Setup

The test stand configuration used for heated propellant investigations is shown in Fig. 29. All instrumentation remained the same as in other tests (see Fig. 26), with the addition of water bath temperature and fuel temperature measurements immediately downstream of the throttle valve. The principal system modification was the addition of the hot water bath system. This system consisted of a 40 gallon drum heated by means of a 6-kw immersed electrical heater. Approximately 230 feet of coiled 1/4-inch OD x 0.035-inch wall, stainless-steel tubing was submerged in the hot water bath to serve as a heat exchanger. The 6-kw heater was not capable of meeting heat input demands to the fuel at high flowrates; therefore, the heat storage capacity of the hot water bath was relied upon.

It should also be noted that a downstream shutoff valve was placed between the heated hydrazine and the throttle valve to allow startup of the gas generator with ambient temperature hydrazine. This use of the pilot flow system minimized demands on the heated hydrazine supply.

Data and Results

The data for the heated propellant tests are summarized as Run steps No. 66-1 through 66-7 in Table 6. These tests consisted of steady state operations for time durations of one to two minutes at various chamber pressure levels. The pressure levels ranged from a minimum of 57 psia to maximum of 266 psia. The maximum chamber pressure attainable was limited by the large flow resistance added to the system by the heat exchanger tubing coils.

Smooth operation was demonstrated at all gas generator operational levels. No anomalous behavior was observed. Fuel temperatures were always in excess of the 150 F requirements, ranging from a minimum of 164 F to a maximum of 180 F. The c* values shown in Table 6 are based on the mass flowrates through the

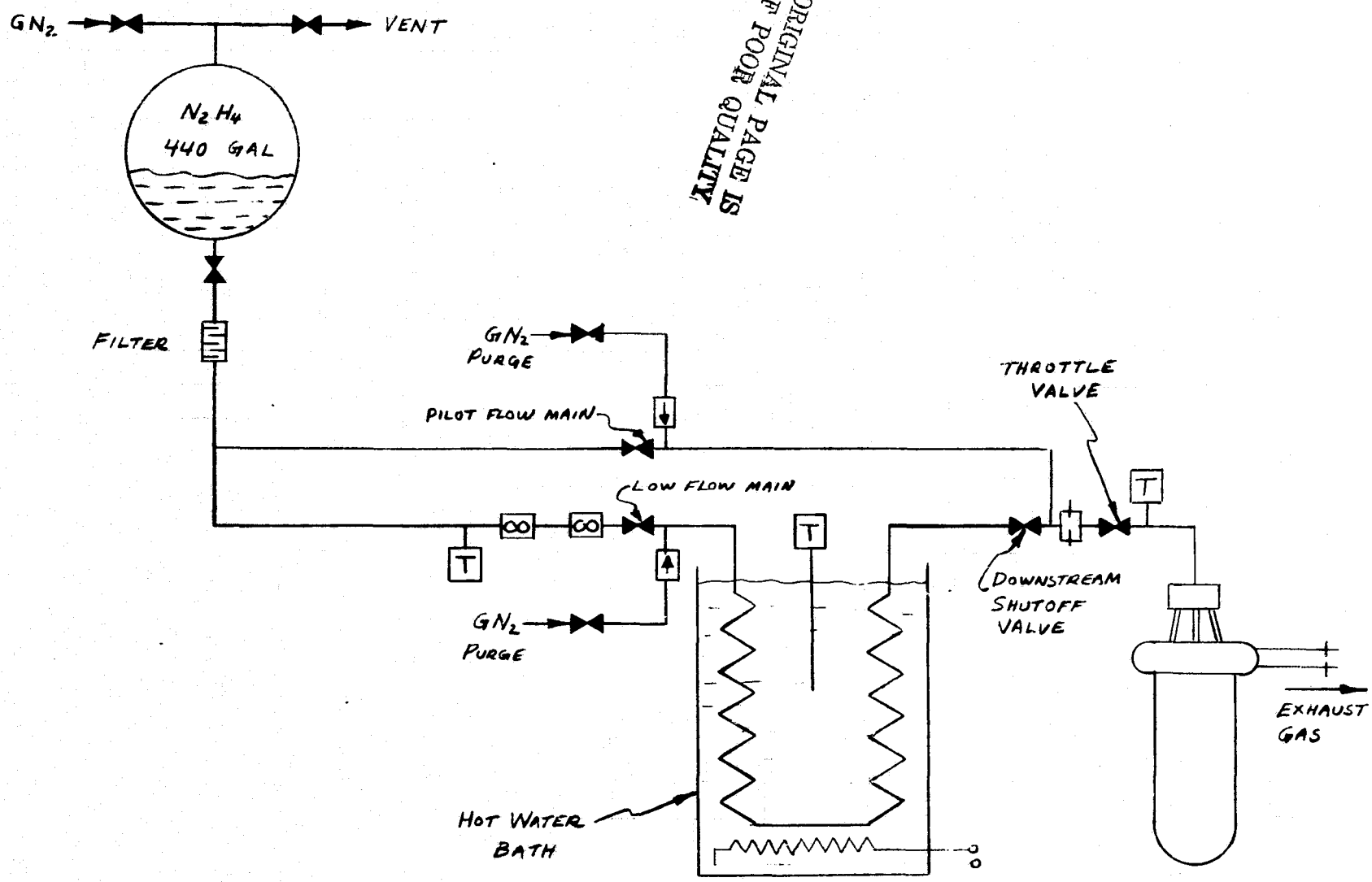

Figure 29. Test Stand Configuration Used for Heated Hydrazine Gas Generator Tests

flowmeter (which were measuring ambient temperature propellant). Obviously, a corresponding volume of heated hydrazine, of considerably lower density, was actually supplied to the gas generator.

ALTITUDE START STUDY

The objective of this experiment was to demonstrate the ability of the gas generator to restart, under altitude conditions, after allowing sufficient time for heat soakback to maximize the injector manifold temperature.

Experimental Setup

For the most part, the same test configuation as shown in Fig. 26 and 27 used, with the gas generator and its exhaust tube contained within a 3-foot diameter by 7-foot-long vacuum chamber. An additional valve was placed in the propellant line, inside the vacuum chamber, to minimize the amount of propellant between a positive shutoff valve and the gas generator.

Figure 30 is a view of the gas generator installation inside of the vacuum chamber. The added 1/4-inch solenoid valve discussed above may be seen attached to the port hole cover at the left of the photo. Microfoil insulation was used to protect the propellant and instrumentation lines against excessive heat pickup.

An external view of the vacuum chamber is shown in Fig. 31. The exhaust tube for the combustion gases was centered within the port of the tank bulkhead, and was slightly submerged to allow for temperature expansion effects. When it was desired to draw a vacuum in the chamber, an air actuated cylinder rotated a soft rubber gasketed plate over the exhaust port. The pressure differential resulting from the vacuum pump operation provided sufficient force to assure a good seal. Before attempting to open this port, the internal vacuum had to be broken by firing the gas generator, resorting to a GN_2 vacuum chamber purge, or both.

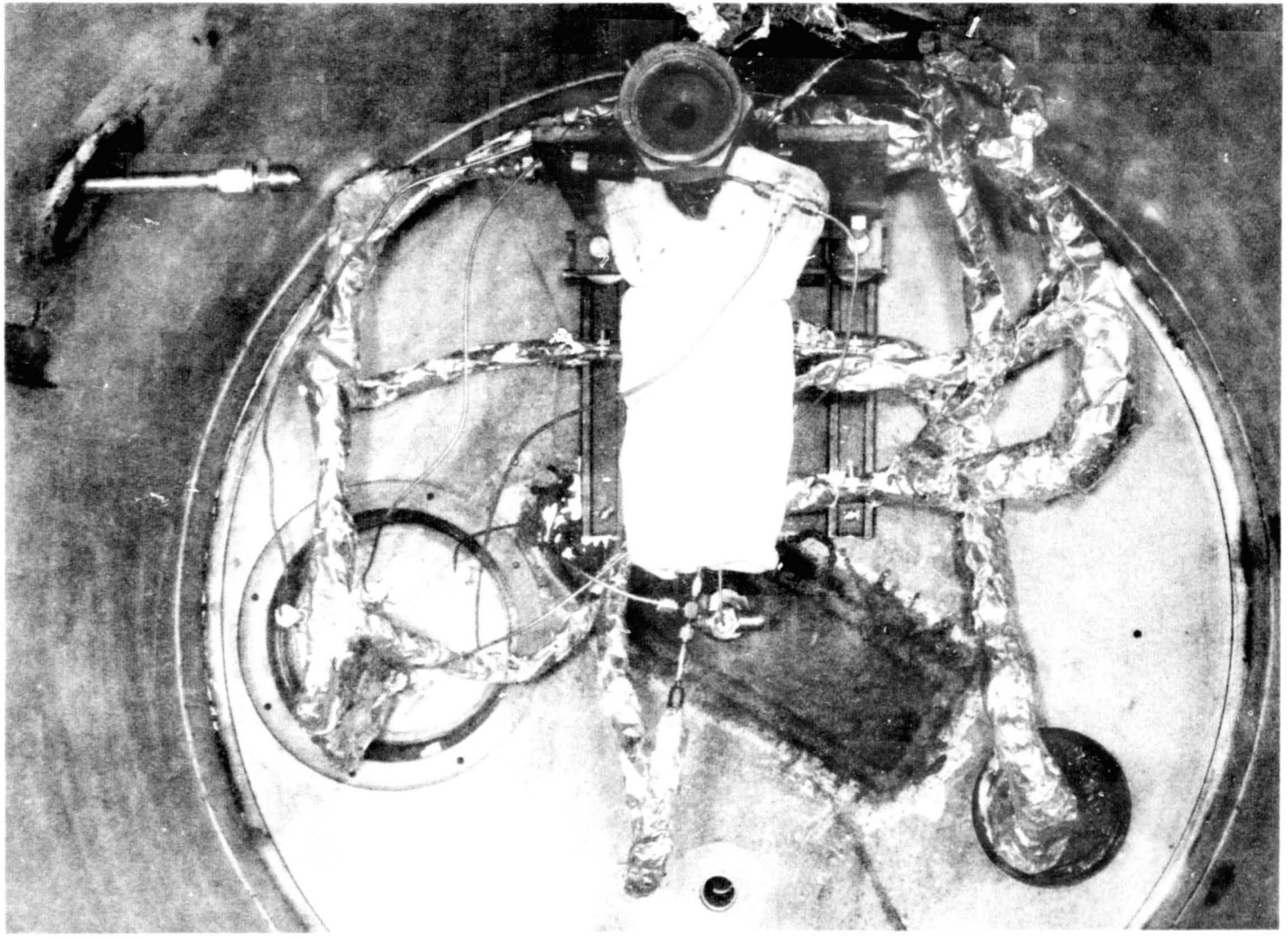

Figure 30. View of Gas Generator Installed Within Vacuum Chamber for Heat Soakback and Altitude Start Evaluation

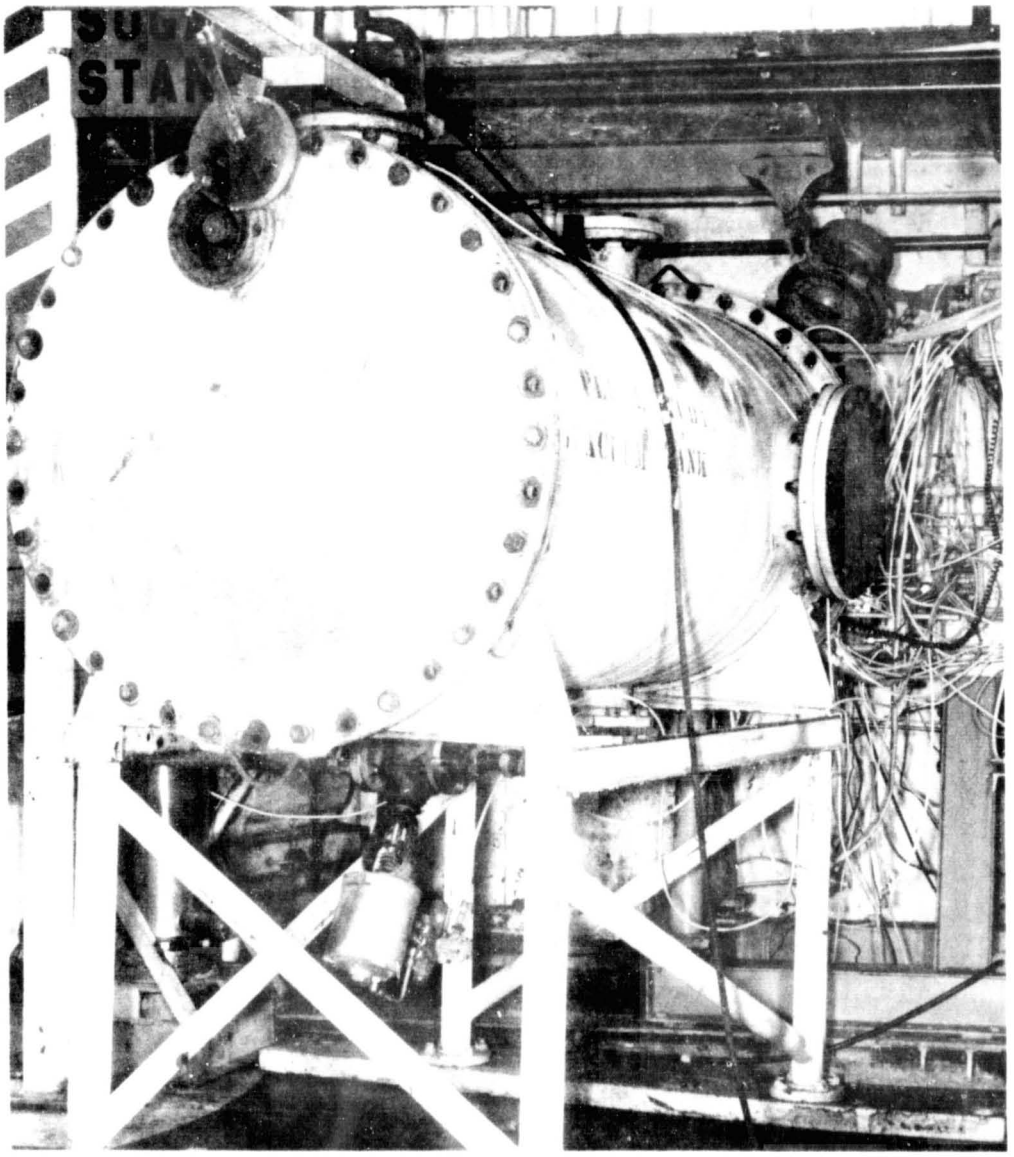

Figure 31. View of Altitude Chamber Showing Exhaust Port Closure Plate in the Open Position

Test Procedure

Operations were begun with the exhaust port of the vacuum chamber open. The vacuum pump employed was in operation, but a vacuum valve isolated it from the vacuum chamber.

Initial preheating of the gas generator was performed in the normal fashion, using heated GN_2. During this time, and at all other times except when a vacuum was being drawn, a low level GN_2 purge of the vacuum chamber was maintained. At the conclusion of the preheat cycle, the heated GN_2 system was disconnected at the vacuum chamber port and the line was capped.

At this time, a low flowrate of hydrazine to the gas generator was initiated to complete the heatup cycle. This was followed by approximately 2 minutes of operation at a 44-psia chamber pressure and three minutes at a 193 psia chamber pressure. The firing was then terminated by closing the propellant shutoff valve inside of the vacuum chamber. The vacuum chamber purge flow was stopped, the exhaust port closure plate was rotated into the closed position, and the vacuum valve was opened. Internal and external gas generator temperatures at this time were all in excess of 1500 F, with a 135 F injector manifold temperature (Table 6 - Run No. 67).

The maximum obtainable vacuum was drawn and maintained for approximately 13.3 minutes. The vacuum chamber ambient pressure during this time was 5.60 inches of mercury, corresponding to a 40,000-foot altitude condition. Post-run inspection showed that the inability to attain a higher vacuum resulted because of the complete collapse of a section of plastic hose joining the vacuum pump to the vacuum valve. The hose was reinforced with a nylon coil, rather than a steel coil, and temperatures encountered were high enough to soften the plastics.

The injector manifold temperatures were monitored during this heat soakback period, and the hydrazine flow to the gas generator was initiated when the T_{IM-1} temperature reached 464 F. This did not represent a full stabilization temperature, since some increasing trend was still noticeable, but the decision was made to restart below 500 F temperature.

The gas generator operation was resumed by opening the propellant shutoff valve located immediately upstream of the throttle valve. This reinitiated operation at a 54 psia chamber pressure condition (10 percent throttle valve setting).

At restart the gas generator wall temperatures ranged from 1216 to 1280 F, the upstream bed temperature was 682 F, and the downstream bed temperature was 1224 F. Restart was smooth and rapid, not discernably different from step changes performed from one operating level to another in normal steady-state test sequences. It was observed, however, that some temperature spiking did occur in the injector manifold. The basic injector manifold temperature measurement used in all tests, T_{IM-1}, increased from 464 F to a momentary peak of 482 F. A supplementary manifold temperature added for this test, designated T_{IM-2} in Table 6, increased from 408 F to 525 F.

Shortly after restart the vacuum valve was closed, the vacuum chamber low purge was activated, and the air cylinder was pressurized to unseal the firing port. As soon as the combination of the gas generator combustion gases and the purge flow decreased the vacuum sufficiently, the port closure plate rotated out of the way. At this point, the first run step for the final acceptance test was underway.

Conclusions

Previous Rocketdyne work in heated tube flow experiments (liquid side heat transfer characterizations) with hydrazine indicates a desirability to limit injector manifold temperatures to a 500 F ceiling. Results of this test indicate that some momentary decomposition activity did occur in the manifold. While this does not mean that higher temperatures cannot be satisfactorily accomodated, it would be recommended that a systematic study be conducted (preferably using only the injector-manifold assembly) to investigate the higher temperature ranges.

DUTY CYCLE INSENSITIVITY TESTS

The objective of this experiment was to demonstrate the ability of the gas generator to respond to rapid changes in operational level, without incurring instabilities or other anomalous behavior. Since the mission duty cycle tests employed two step changes per cycle, going from the 10 percent level to the 100 percent power level, such perturbations had already been demonstrated many times without encountering any problems. A somewhat different procedure was used for these tests. The power level was varied continuously over the entire power level spectrum from zero to 100 percent.

Experimental Setup

The test installation used during this demonstration is shown in Fig. 29. For the subject tests, the hot water bath was preheated to approximately 120 F (in order to reduce the time to attain 170 to 180 F temperatures desired for subsequent heated propellant tests).

The throttle valve setting variations were obtained by rapidly twisting a potentiometer knob, which permitted traversing the full range of valve positions.

Data and Results

The duty cycle insensitivity tests are entered in Table 6 as Run No. 64. The additional system pressure drop associated with the approximate 230 feet of immersed tubing in the water bath (see Fig. 29) limited the maximum chamber pressure to approximately 260 psia. Approximately 40 perturbations were performed, including full sweeps commanding 0 to 100 percent throttle valve positions, and intermediate sweeps of 25 to 30 percent of full range at various levels. These operations were entirely smooth in nature, and demonstrated that the gas generator was always at essentially the steady state operating condition corresponding to the throttle valve setting. It should be noted that the manual variations of the potentiometer setting were accomplished in 1 second or less.

Conclusions

Within the limitations of instrument response, the gas generation was able to perform smoothly over the entire spectrum of power level changes. Because the power level changes were "sweeps" rather than step changes, as in the MDC tests, complete confidence in this gas generator has been established for all intermediate power level changes.

START SEQUENCE VARIFICATION

The procedure for initiating gas generator operations was basically the same throughout all Phase I and Phase II tests. However, during the Phase I tests, heated GN_2 flowrates were not measured, since the system was simply run at maximum capacity. The purpose of the start verification demonstration was to completely define the typical gas generator heatup sequence details.

Experimental Setup

The test stand installation shown in Fig. 26 was typical for these tests. A commercial 12 kw heater was used to heat GN_2 to approximately 1250 F. The heated GN_2 line consisted of 1/2 by 0.042-inch wall stainless-steel tubing. A 0.170-inch diameter ASME sharp-edge orifice was used to measure flowrates.

Test Procedure

Run No. 66 (Table 6) was selected as representative of a typical start procedure. For this run it may be noted that ambient temperature hydrazine (with an approximate 2.8 percent water content) was employed and the tank was pressurized to the normal 780-psig level.

Heated GN_2 flow was maintained for 30 minutes at an average flowrate of 0.012 lb/sec, with a 130-psig pressure at the gas generator inlet fitting. The hot GN_2 supply temperature was manually regulated to 1200 $\pm$50 F.

After 30 minutes of heating, the temperature distribution in the gas generator is as shown in the table below:

Time	Condition	Bed Temperatures, F		Temperature, F			
		Upstream	Downstream	Chamber Gas	Wall		
		$T_{B\ U/S}$	$T_{B\ D/S}$	T_C	TW-1	TW-2	TW-3
0	Start GN_2 Flow	67	67	67	67	67	67
30 min	Stop GN_2 Flow	712	937	844	742	776	835
30 min	Start Propellant Flow	660	878	486	784	776	831
34 min	Valve Command @ 10%	578	1362	1284	1009	1194	1263

During the time required to shutdown the GN_2 system and to cap the gas generator inlet fitting, the temperatures decayed somewhat to the values shown at the "start propellant flow" time. Propellant flow was initiated with approximate 1.8-percent valve opening, which was maintained for 80 seconds. During the course of the next 110 seconds, the throttle valve was stepped to the 2.5-percent open, 4.0-percent open, and finally to the 77-percent open position. At this time, the gas generator was considered to be started, and continued to run at this flow step until steady state conditions were reached.

Conclusions

With the system employed, the typical time for preheating the gas generator was in the order of 30 minutes. However, no attempt was made to further minimize this time. Obviously if a more elevated GN_2 temperature, a higher GN_2 flowrate, or both would be provided, the startup cycle time could be reduced considerably.

PHASE III PROGRAM

INTRODUCTION

The previously completed Phase I and II programs investigated the efficiency and stability of the Rocketdyne SS APU candidate gas generator over a wide range of conditions. These studies were all based upon the type of operations and conditions for which the gas generator was originally designed. The nominal design operating conditions (full power) for the gas generator are:

Chamber pressure, psia	560 p
Exhaust Gas Temperature, F	1650
Flowrate, lb/sec	0.37 lb/sec

A proportional flow (throttle valve) control system was used to vary the gas generator operating power level.

This Phase of the program investigated the applicability of the Rocketdyne gas generator to the operating conditions of the present Space Shuttle system. For this program, the gas generator chamber pressure was increased to 1000 psia, and a pulse rate modulated control system type of operating was adopted.

The objectives of the program were:

1. To obtain experimental data for the gas generator under pulse mode operating conditions.
2. To determine from this data the efficiency of the gas generator under such operating conditions, i.e., to ascertain the pulse degradation factor for each type of duty cycle.
3. To obtain corresponding operating/efficiency data for the gas generator operating in the pressure modulated (throttled) mode of steady state operation.

4. To compare the relative efficiencies of pulse mode operations with the pressure modulated regime.

5. To further investigate the ability to shutdown the gas generator (without performing system purging) and to safely restart after allowing time for heat soakback to elevate the injector and propellant manifold temperatures.

EXPERIMENTAL PROGRAM

The experimental program was conducted at the Thermodynamics Laboratory test facilities of the B-1 Division. Initial tests were performed with the S/N 1 gas generator. However, in the course of the firings some pinhole leaks developed in braze-joints sealing the injector standoff tubes to the injector body. At this point, the S/N 2 gas generator was installed, and used throughout the remainder of the program.

TEST SETUP

The major features of the test installation are shown in Figure 32. Two propellant supply systems were provided for the gas generator. For normal operations in the throttle mode, which usually had long durations, the main hydrazine tank was used. This tank had a capacity of 98 gallons. For such operations, both the isolation and the main valve were opened, and the gas generator was operated from a very low idle level (<15 psia) to full power at the maximum flowrate by remotely controlling the throttle valve pintle position. In this system the flowrate was measured with a turbine flowmeter.

A second propellant supply system was provided for the pulse mode test operations. The tank storage capacity was approximately two gallons. This capacity was sufficient to allow 13 of the longest duration pulses with a single filling, and hundreds of pulses for most of the other, shorter, durations.

The auxiliary fuel tank was filled from the main tank. The fuel transfer took place by first opening the auxiliary tank vent, and then opening the isolation

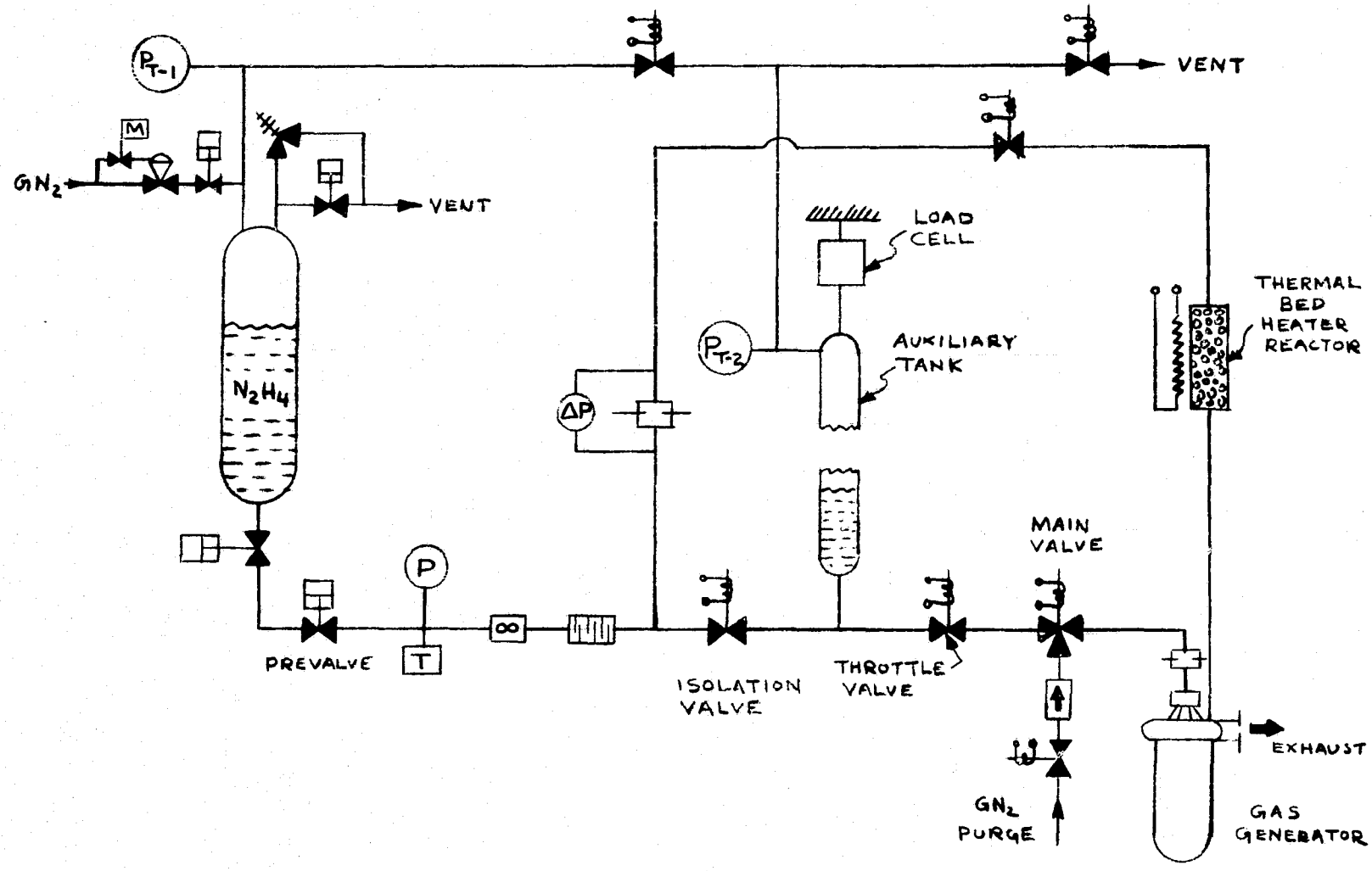

Figure 32. Details of Test Stand Installation With Thermal Bed Heater Reactor for Preheating Main Gas Generator

valve, while keeping the downstream main valve closed. For use, the isolation valve was closed, the auxiliary tank vent was closed, and the valve in the line joining the ullage spaces of the two tanks was opened.

The auxiliary tank was suspended from a load cell to allow the measurement of the propellant consumed during a given set of pulses. In order to accommodate this weighing system, flexible metal tubing was used between the tank and the rigid line systems. The load cell itself was attached to its support channel beam and to the auxiliary tank by means of flexures in order to minimize potential load measurement errors. These flexures consisted of 1/16 diameter sections of drill rod, approximately two inches long, brazed into drilled bolt heads. Details of this tank installation can be seen in Figures 33 and 34.

Gas Generator Preheat System

The thermal bed heater reactor system shown in Figure 32 was used during the first eight tests. In use, it was designed to operate at full tank pressure, with fuel flow controlled by means of a solenoid valve.

The heater reactor itself is shown in Figure 35. This was a ball packed thermal bed hydrazine gas generator, which was electrically preheated to reach hydrazine decomposition initiation temperatures.

The thermal bed consisted of 1/16-diameter, type 400C stainless-steel balls in a 0.5-inch ID chamber approximately 4 inches long. The injector consisted of two 2.5-inch-long hypodermic tubes (0.042-by 0.012-inch wall) welded to the injector face of the chamber and to an orifice fitting. In order to provide some mechanical strength, while maintaining a high degree of thermal isolation between the gas generator and fuel supply line, a section of 0.25- by 0.042-inch wall stainless steel tubing was perforated with drilled holes and welded to these components (see Figure 35).

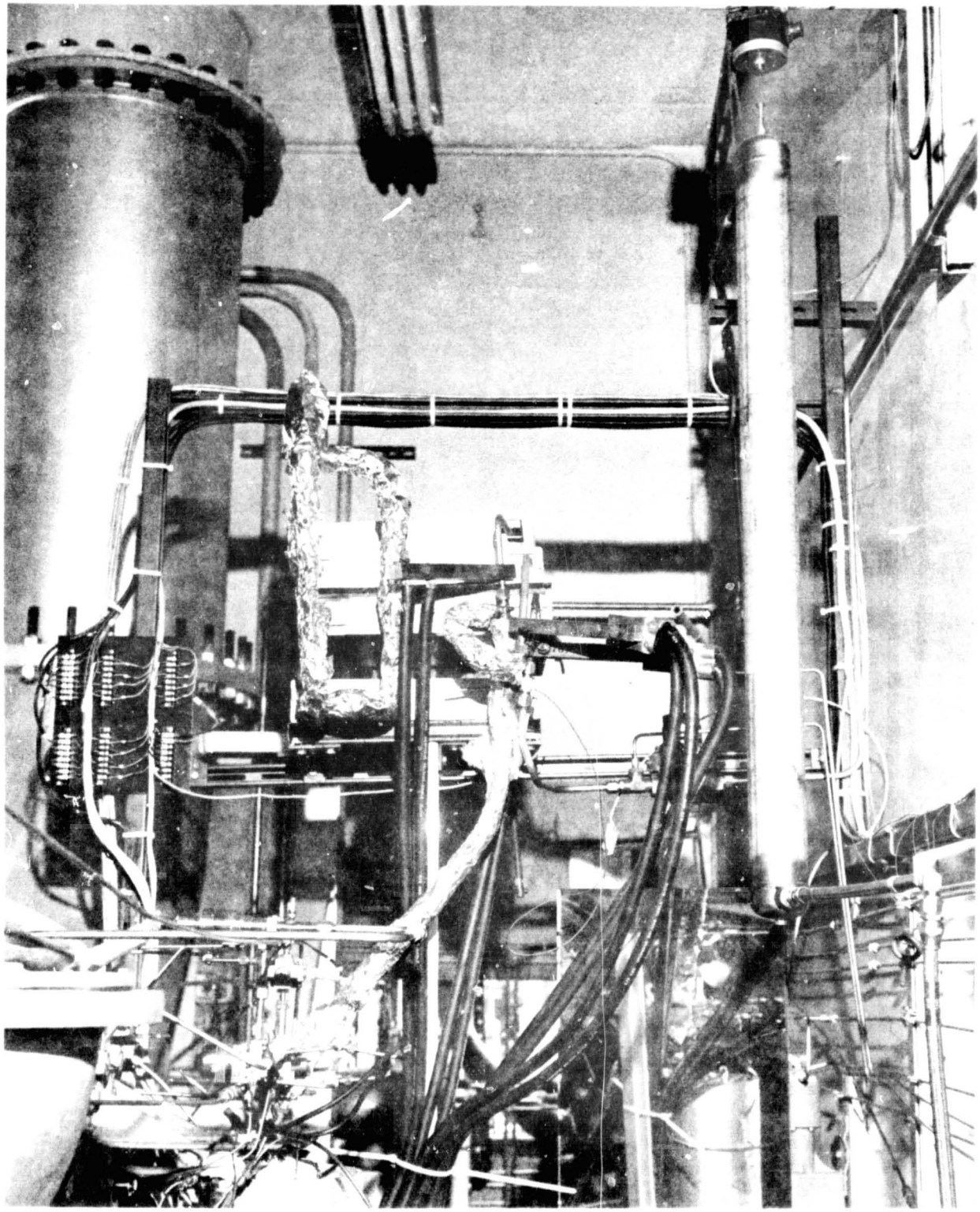

Figure 33. Overall View of Test Installation Showing Auxiliary Fuel Tank and Electrically Powered GN_2 Heaters

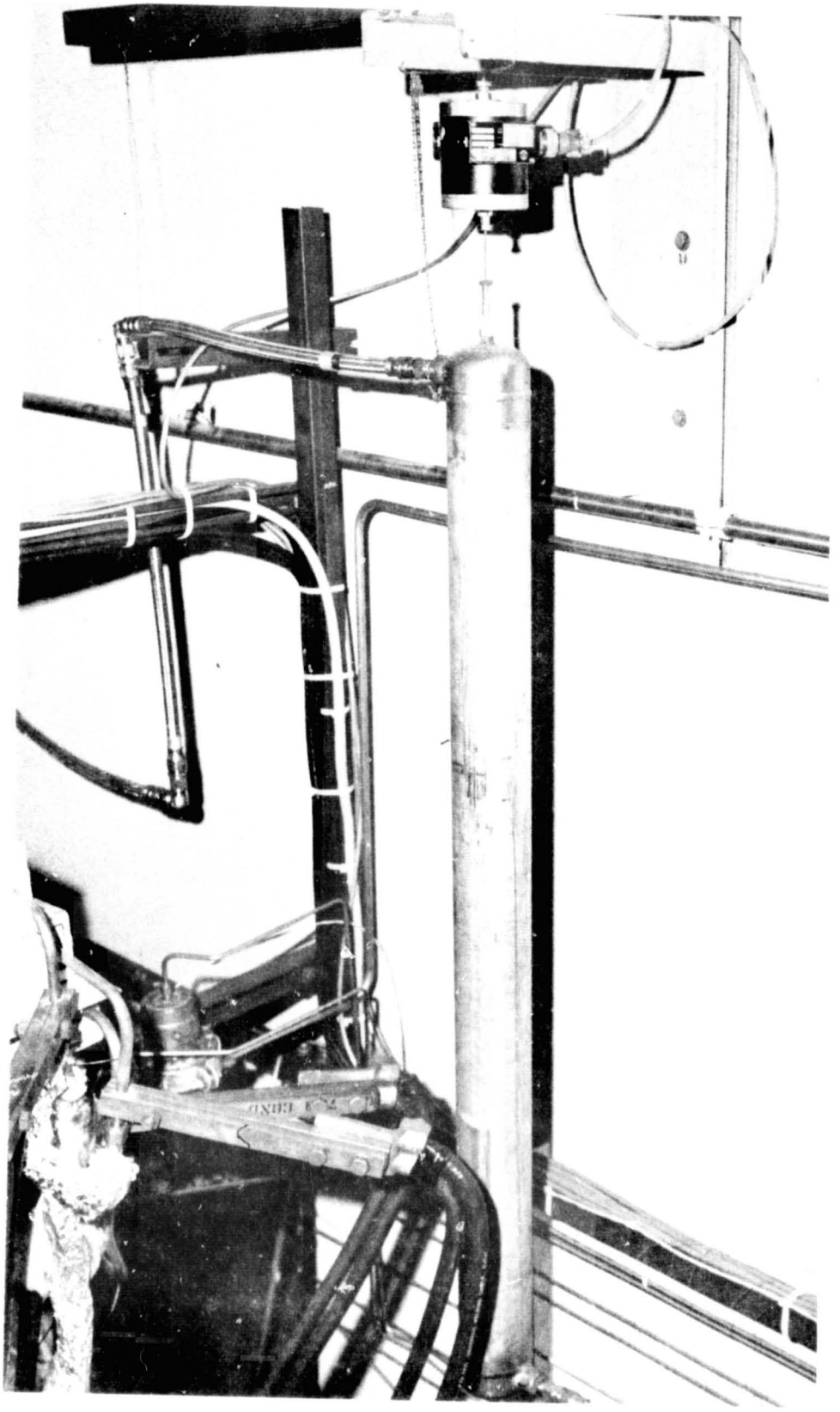

Figure 34. Auxiliary Fuel Tank Installation

Figure 35. Thermal Bed Heater Reactor

The hot gas outlet line was a section of 0.25-inch OD by 0.065-inch wall, type 321 stainless-steel tubing. The heater reactor nozzle throat was sized to provide a chamber pressure of 1000 psia. This 0.052-inch-diameter throat was incorporated into the connector fitting used to couple the heater reactor assembly to the hot gas inlet part of the main gas generator.

The above described pilot gas generator preheat system encountered a number of problems during the course of the initial tests. Once it was recognized that a significant problem did exist, the decision was made to switch back to a hot GN_2 preheat system, as used in all of the previous testing at the Propulsion Research Area test site at Rocketdyne.

The GN_2 electrical heaters employed can be seen in Figure 33. They consisted of a 10-foot length of coiled, 3/4-inch OD stainless-steel tubing enclosed in an asbestos board box. Low voltage current, at high amperage level, was conducted through the tubing to maintain it at a high temperature level. A number of these units were paralleled, to result in a capability of absorbing 50 kw of electrical power. The actual power level attained was regulated by adjusting the output voltage of a variable transformer. The power level used during the gas generator preheat was estimated to be approximately 25 kw. The GN_2 flowrate was adjusted to result in a 1200 F output temperature.

Gas Generator Test Configuration

The gas generators used were developed and tested during the preceding phases of this program. The only modifications performed were to remove the original outlet tube throat section and to replace it with a revised section. This new section provided a capability for flush mounting a Photocon transducer, to permit high response rate chamber pressure measurements. In addition, the new throat diameter was reduced from a nominal 0.333 inch diameter to a 0.243 inch diameter in order to increase the operating chamber pressure to 1000 psia, while maintaining the design 0.365 lb/sec flowrate. Figure 36 shows the design details of the modified throat section.

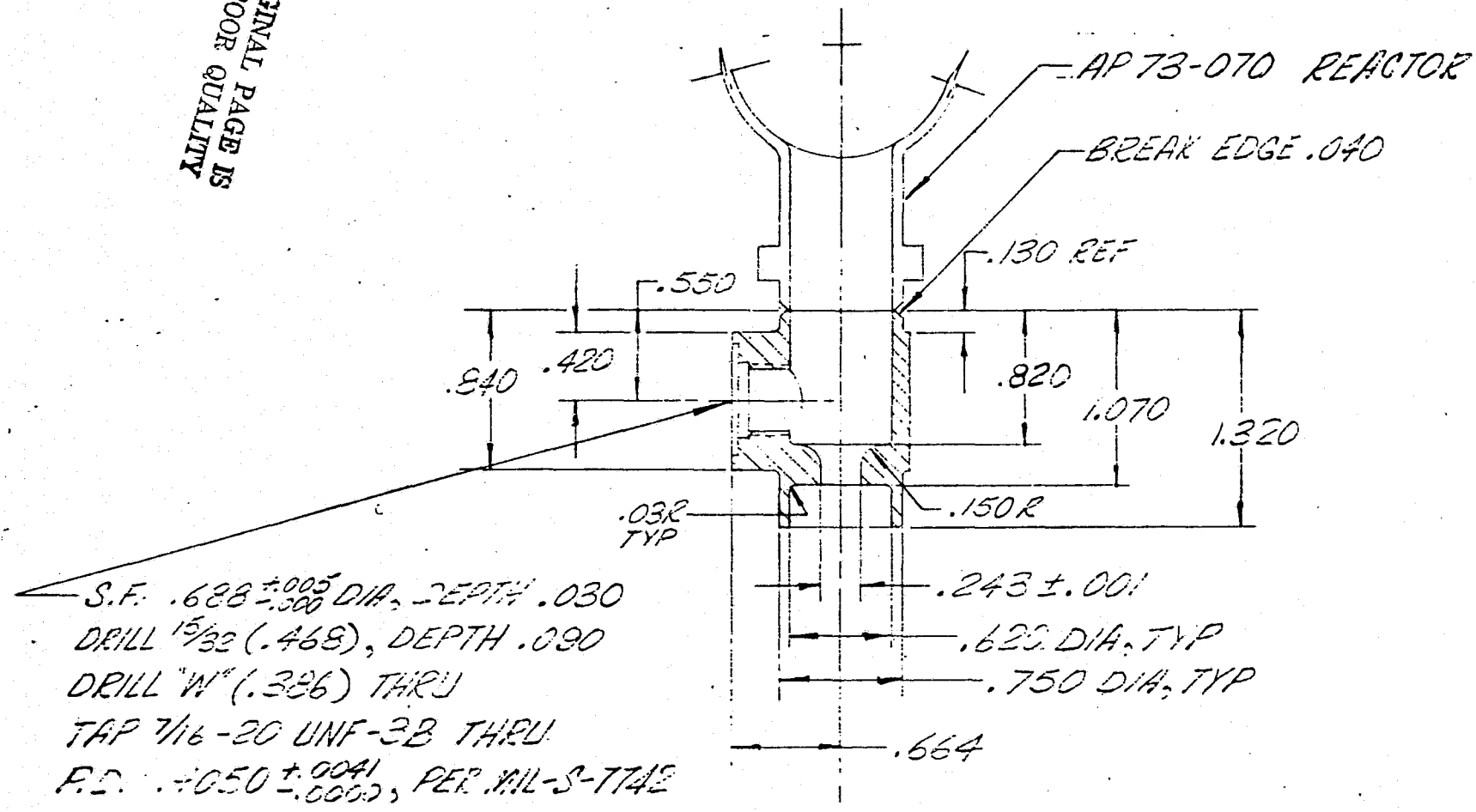

Figure 36. Modified Throat Section

The gas generator assembly was completed by welding a 3/4 by 0.065 wall stainless-steel tube to the end of the gas generator outlet fitting. This tube was approximately 1-foot long. The exhaust gas outlet tube ducted the gas generator decomposition products into a continuously evacuated 30-inch diameter pipe. The exhaust gas outlet tube penetrated a flange cover through a close fitting hole, to allow free thermal elongation of the outlet tube without permitting significant inflows of air into the exhausting system. This outlet tube and other installation details can be seen in Figure 37.

The most straightforward method of using a heated GN_2 thermal bed preheating system was to physically disconnect the GN_2 line at the gas generator hot gas inlet port, and then capping the inlet port, at the completion of the preheating cycle. This was desirable in order not to increase the gas generator connected void space which would have to be pressurized by the gas generator decomposition products. Obviously, such accumulator effects would significantly affect the response characteristics of the gas generator to step changes.

To minimize all possible personnel hazards, the gas generator was enclosed within a length of heavy-walled steel pipe. This pipe was welded to the top of a steel table, effectively enclosing the bottom end of the gas generator. The upper end of the steel pipe of course had to be open, but the gas generator support structure tended to block much of the area.

Heat losses from the gas generator were minimized by use of an insulation blanket fabricated from "MIN-K, HT 1301" material.

Valves and Controls

The valving systems and pressure regulating systems employed are shown in the Figure 32 schematic diagram. The direct control of the gas generator operating conditions was effected by means of the throttle valve and main valve shown in Figure 32. These valves are visible in Figure 37, with the throttle valve being the uppermost valve and the main valve being the closest to the gas generator.

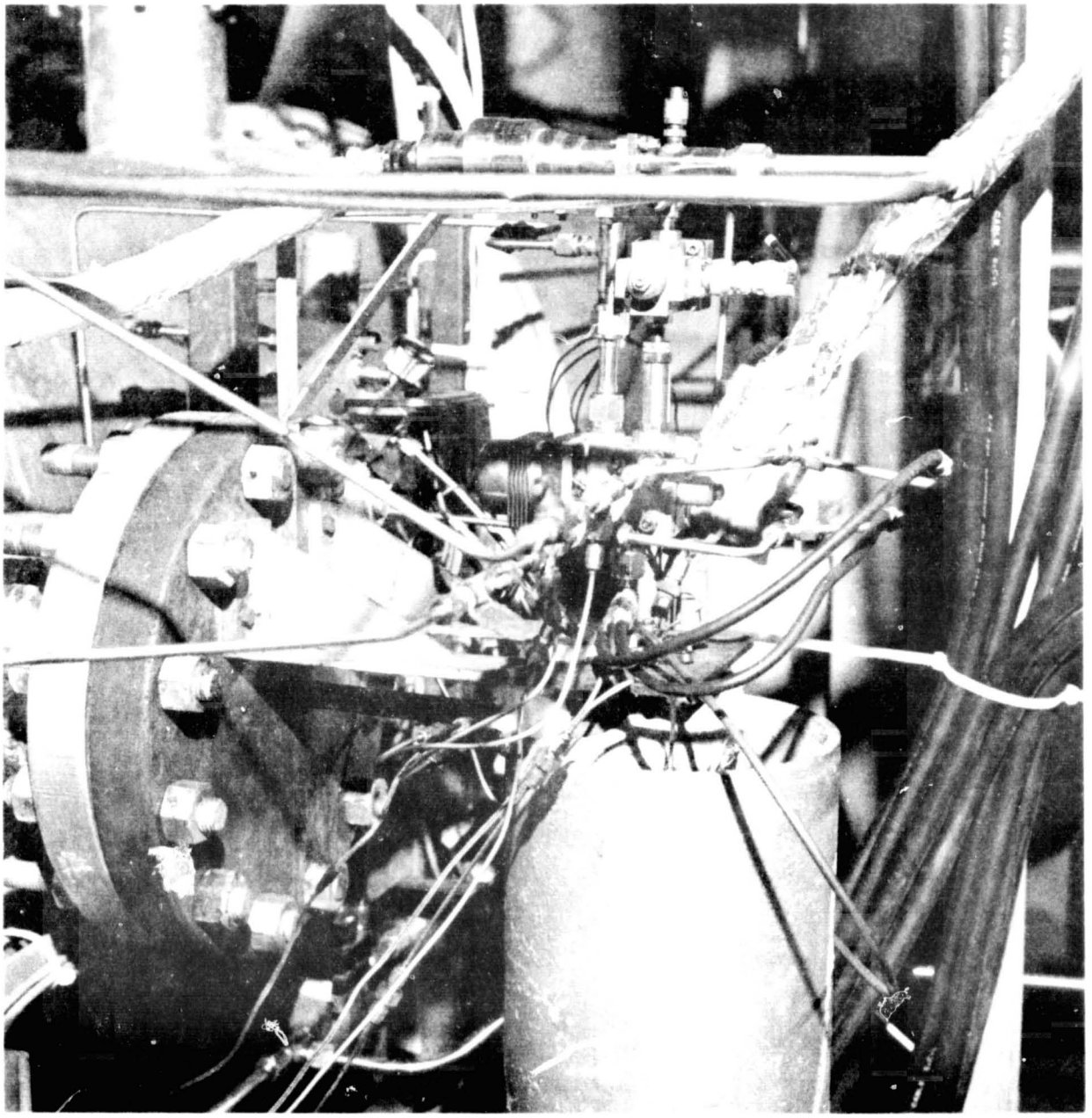

Figure 37. Gas Generator Installation

The throttle valve pintle position could be remotely controlled over the range of approximately 1 percent open to 100 percent open. Varying the level of the signal voltage to the control system resulted in corresponding variations in the valve position. A pintle position meter indicated the percentage of full flow that the valve position would allow.

The throttle valve was used to control all steady state operations, with the main valve remaining open throughout the test. However, for pulsing tests the throttle valve was commanded into its full open position and the main valve was pulsed. The reasons for using the main valve (in addition to the throttle valve) were that the throttle valve was not guaranteed to be a tight shutoff valve and was not as adaptable for the incorporation of a water cooled jacket.

To minimize system volumes in general and propellant holdup volume between the valve and injector in particular, the main valve was located as close to the gas generator as possible. The distance between the main valve and the injector manifold was approximately 2.5 inches. In order to prevent the valve from attaining temperatures which might be high enough to damage its components, aluminum plates incorporating milled passages for water coolant flow were bolted to both sides of the valve body. This water cooling was required particularly during the gas generator preheat cycle since during this time temperatures in the order of 1000 F were maintained at the injector for durations of 30 to 40 minutes. During this operation no propellant was flowing through the valve to take away heat, and activating the GN_2 purge through the valve body would have dumped cold GN_2 gas into the gas generator.

The pulsing rate of the main valve was controlled by means of two solid state digital timers. One timer was set for the time representing the cycle period. As it started its period it would also start a second timer which was set for the valve "ON" time. This "ON" time controller supplied the 24 volt D.C. electrical signal to the valve.

A "Vacco" 1/2-inch solenoid valve, with a nominal 10-millisecond opening and closing time, was used as the main valve.

Exhaust Evacuation System

Since tests in the Thermodynamics Laboratory facilities at the B-1 Division are conducted in essentially closed bays, all exhaust gases are contained and exhausted through a 30-inch piping system. The exhaust ducting is continuously evacuated by means of a 25 lb/sec air-driven ejector system or by a high-capacity vacuum pump system. This also enables the simulation of altitude conditions, if required. To case operation at this facility all firings were conducted with an exhaust duct pressure of 1 psia (60,000 feet altitude).

Instrumentation

A list of the parameters monitored during the tests, the transducer types and ranges, and the recording system employed are shown in Table 7. Figure 38 shows the locations and the nomenclature for the measurements pertaining directly to the gas generator.

Transducers

Pressure measurements were in most cases made with Transducers Inc., pressure transducers. These transducers were not close coupled to the measurement location because of the necessity to isolate them from the high local temperatures associated with the gas generator. In addition, the use of a protective shield around the gas generator resulted in some further increase in the lengths of the connecting tubing. These pressure lines (1/8 OD by 0.032 wall thickness) had the following approximate lengths:

Chamber Pressure, P_{c_1}, 30 inches

Upstream Bed Pressure, P_{BUS}, 33 inches

Downstream Bed Pressure, P_{BDS}, 40 inches

The high response rate pressure transducers used were Model 307-2560 water cooled Photocons. These transducers were flush mounted to maximize the response characteristics. The transducers themselves had a diaphragm resonant frequency

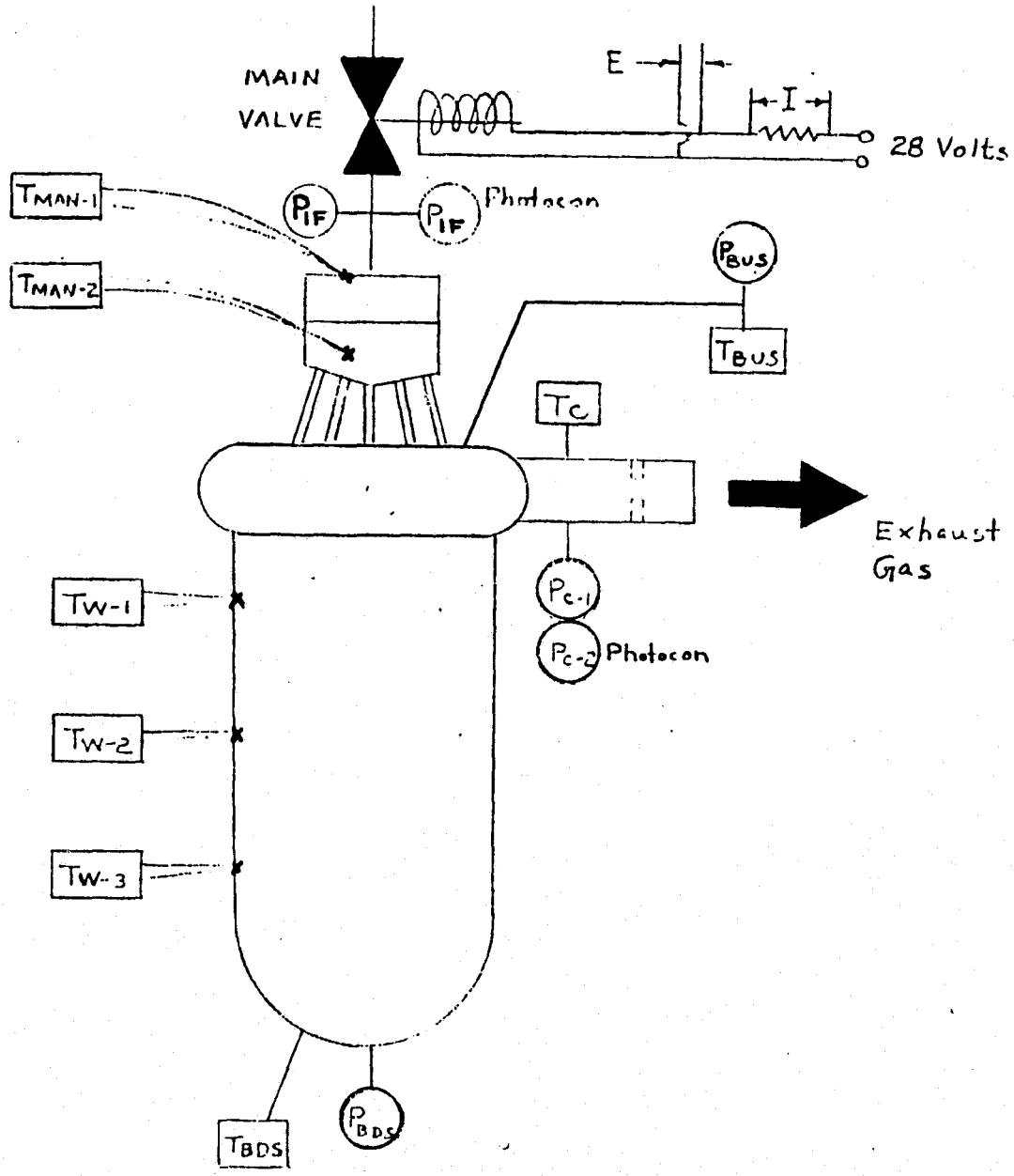

Figure 38. Gas Generator Instrumentation

TABLE 7. INSTRUMENTATION

PARAMETER	TRANSDUCERS	RANGE	BRUSH	ASTRO DATA	OSCILLO-GRAPH	VISUAL GAUGE
P_{LINE}	TRANSDUCERS, INC.	0-2000 PSIG	-	x	-	-
T_{LINE}	C/A THERMOCOUPLE	0-150F	-	x	-	-
W	F&P 1/2-4	0-0.5 LB/SEC	-	x	-	-
PINTLE PISTON	-	0-100%	-	-	-	x
E	-	0-30 VOLTS	-	-	x	-
I	-	+2 TO -2 AMPS	-	-	x	-
P_{IF}	TRANSDUCERS, INC.	0-1500 PSIG	-	x	x	-
P_{IF}	PHOTOCON	0-2000 PSIG	-	-	x	-
$T_{B\ U/S}$	C/A THERMOCOUPLE	0-2000F	x	x	x	-
T_{W-1}	C/A THERMOCOUPLE	0-2000F	-	x	-	-
T_{W-2}	C/A THERMOCOUPLE	0-2000F	-	x	-	-
T_{W-3}	C/A THERMOCOUPLE	0-2000F	-	x	-	-
T_{B} D/S	C/A THERMOCOUPLE	0-2000F	x	x	x	-
P_{B} D/S	TRANSDUCERS, INCL	0-1000 PSIG	-	x	-	-
P_{c-2}	PHOTOCON	0-2000 PSIG	-	-	x	-
P_{c-1}	TRANSDUCERS, INC.	0-1000 PSIG	x	x	x	-
P_{DELTA}	CEC	0-50 PSI	x	-	-	-
T_{c}	C/A THERMOCOUPLE	0-2000F	x	x	x	-
T_{IM-1}	C/A THERMOCOUPLE	0-1000F	-	x	-	-
T_{IM-2}	C/A THERMOCOUPLE	0-1000F	x	x	-	-
P_{T-1}	TABOR	0-2000 PSIG	-	x	-	x
P_{T}-2	TRANSDUCERS, INC.	0-2000 PSIG	-	x	x	x
T_{H}	C/A THERMOCOUPLE	0-2000F	-	-	-	x
$P_{BU/S}$	TRANSDUCERS, INC.	0-1000 PSIG	-	x	-	x
F	BLH	0-50 LB	-	x	-	x

of 46,000 Hz. Figure 36 shows the geometry of the Photocon port for the chamber pressure measurement (P_{c-2}). The P_{IF} Photocon installation was made by welding a 1/4 inch AN boss to the 1/2 inch propellant line joining the propellant main valve outlet port to the gas generator injector manifold. The Photocon port centerline was approximately two inches downstream of the main valve, and 7/8 inches upstream of the injector manifold.

All temperature measurements were made using chromel/alumel thermocouples with a 150 F reference junction. Gas temperatures were measured with either 0.040 or 0.0625 OD, stainless-steel sheathed (0.010 wall thickness), closed end, and grounded junction thermocouples. The thermocouple wires had a 0.005-inch diameter.

Surface temperature measurement thermocouples similarily used 5-mil CR/AL wire and had their junction spot welded directly to the surface (in the case of the manifold temperature T_{m-1} and T_{m-2}) or held against the surface in the case of the gas generator exterior wall temperatures (T_{w-1}, T_{w-2}, and T_{w-3}). These wall temperature thermocouple junctions were clamped against the wall, with a layer of high-temperature insulation between the clamping agent and the thermocouple. Spot welding of the thermocouples to the Haynes 188 alloy gas generator walls is proscribed because of the local changes in the alloy that could result. This could compromise the high strength-long service life characteristics of the gas generator.

A Baldwin-Lima-Hamilton, 50-pound (single precision, Model U3G2) load cell was used as the basis for the auxiliary fuel tank weighing system.

A Fischer-Porter 1/2-4 turbine flowmeter was used to monitor flowrates when the main fuel tank was supplying the hydrazine.

The remaining measurements were electrical in nature, and consisted of the main valve current and voltage signals and the throttle valve pintle position. The main valve electrical signals provided a valve signature which could be interpreted to define the opening and closing time characteristics. The pintle position was a meter which allowed visual indication of the relative flowrate

which the degree of valve opening would allow. This pintle position was not recorded on any of the data acquisition systems.

Recording Systems

As shown in Table 7, three data recording systems were used. The primary data acquisition system was the digital "Astrodata" system. This system recorded all data other than the extremely high response rate data. A complete data survey sweep was performed at intervals of 4 milliseconds. Data printouts obtained consisted of a complete data dump (i.e., all data at 4-millisecond time intervals) and an arithmetic average of these data readings for 0.113-second intervals.

A Minneapolis-Honeywell "Visicorder" oscillograph was the primary recording method for high frequency response measurements. Paper speeds of approximately 100 in/sec were used to secure data for detailed time response analyses.

The Brush recorder was used for those parameters of special interest in monitoring the gas generator startup procedure and for adjusting pressure operating level. These records constituted "quick look" data and normally were not used for the determination of accurate values of the parameters measured. A paper speed of one millimeter per second was normally used.

Due to the extreme time durations of many of the tests, the intervals of operation which were not of real value for data purposes, only the Brush recording furnished a full and continuous recording of the runs. The Astrodata and oscillograph recorders were activated intermittently to sample appropriate data.

Calibration Procedures

All calibrations were performed using secondary or tertiary standards traceable to the U.S. Bureau of Standards. Pressure transducer calibrations were performed using an appropriate Heise gauge. The flowmeter was calibrated using water and a "catch and weigh" system. The tank weighing load cell was calibrated in place, pressurized to normal run pressure levels, by applying weights to a

pan attached to the bottom of the tank. The calibrating weights were of the "Class C" type with a weight tolerance accuracy of ±0.01 percent.

TEST PROCEDURES

As previously indicated, all tests were conducted with a continuously evacuated duct system used to remove the exhaust products.

The operation of the duct vacuum was initiated prior to the start of any other test procedures. An internal water spray system, inside of the 30-inch duct, was aimed at the general wall area upon which the gas generator exhaust gases impinged. This water spray system was activated intermittently to cool the duct walls.

Gas Generator Preheat Operations

The initial series of tests employed the heater reactor assembly shown in Figure 35. With this test configuration, the pilot gas generator was first preheated to a nominal 1400 F temperature. Three 200-watt tubular electrical heaters, with their current supply regulated by means of a variable output voltage transformer, were used for this purpose. Normally, the voltage was regulated to 80 percent of full voltage to increase the life expectancy of the heating elements.

When the heater reactor reached the appropriate temperature level, the electrical heating was stopped, the main propellant tank was pressurized to the level required by the main gas generator, and the valve in the heater reactor propellant supply line was opened. The pilot gas generator operation was permitted to continue until the upper bed temperature reading (T_{BUS}) reached the 1400 F. At this point, the hydrazine supply valve for the heater was closed, and the propellant main valve was given short pulses (with the throttle valve in the approximate one percent flow position). If gas generator bed temperatures showed an increase response, the main valve was then opened permanently. When bed temperatures reached approximate stabilization, the pintle valve was opened to the desired setting for the test operation.

During most of the tests, no attempt was made to minimize the heatup time cycle. However, the fuel consumed during the approximately 24 minute duration heatup cycle of Run. No. 7 was computed. This heatup cycle consumed approximately 7.6 pounds of hydrazine.

After the first heater reactor failure was encountered, the startup procedure was revised. Subsequent heater reactor operations were initiated with a supply tank pressure in the order of 100 psig, and the tank pressure was slowly increased to a maximum of 800 psig. The main gas generator chamber pressure and bed temperature parameters were continuously monitored, and the behavior of these parameters was used as a guide as to the suitability of increasing the heater reactor supply pressure.

A second failure of the pilot gas generator was encountered and at this point a heated GN_2 preheat system was adopted in order to eliminate further potential program delays.

The heated GN_2 system used 120-psig nitrogen supply pressure. The voltage to the electrically heated stainless steel tubes was slowly adjusted to the level required to maintain the gas temperature at about 1200 F. When the gas generator appeared to stabilize, in the general vicinity of 1100 F, hydrazine flows were initiated in exactly the same manner as described for the heater reactor startup discussed above. The hot GN_2 preheating required time intervals in the order of 30 to 40 minutes, but here again the heatup time was not minimized.

Pressure Modulated Tests

The pressure modulated test series was performed with the auxiliary tank hydrazine system (see Figure 34) disconnected from the main propellant supply system. This was done to ensure proper flow measurements. The pintle valve was progressively opened, using approximate 10, 30, 50, 75, and 100 percent flow settings. Each condition was maintained for three minutes, to ensure maximum data stabilization, with full data recordings made near the end of each period. Data stabilization did not actually require 3 minutes, but such a procedure was conservative.

Pulse Mode Tests

The pulse mode tests utilized both of the propellant supply systems. The first operations involved transfer of hydrazine from the main tank to the auxiliary tank. The load cell millivolt output reading was monitored to determine when the auxiliary tank was filled to the desired level. To transfer fuel, the auxiliary tank pressurization valve was closed, the auxiliary tank vent valve was opened, and the isolation valve (Figure 32) was opened. At the completion of the transfer, the auxiliary tank vent valve was closed, and its pressurization valve was opened.

At this point, with the throttle valve in its full open position, the main valve was opened for a full power firing of 10 to 30 seconds duration. Fuel for this operation was supplied from the main fuel tank. This 100-percent firing served as a claibration to indicate possible gradual changes in instrumentation and to secure gas generator bed temperatures that would be essentially the same for every group of pulse tests.

When the 100-percent firing interval was completed, the isolation and main valves were closed. This terminated the firing and ensured that the auxiliary tank would furnish the fuel during the pulsing portion of the run. Just prior to the initiation of the pulsing operations, an Astrodata recording was taken of this pre-run zero condition. The primary data of interest here was the initial (loaded) auxiliary tank weight.

The pulse sequencer was activated at this time. It opened and closed the main valve with a preset "ON" time and pulsing frequency. Oscillograph and Astrodata recordings were made of the initial group of cycles (in most runs approximately 10 pulses), a middle cycle group, and then a final group of cycles at the end of the run. The total number of cycles performed was selected to exhaust the major portion of the tanked propellant. This was usually in the range of 10 to 11 pounds of hydrazine.

At the completion of the pulsing test the main valve was closed, and the data recording systems again were activated to secure a postrun zero. The auxiliary

propellant tank and all lines remained pressurized, and no venting was performed prior to the recording this zero. This data were used to determine the total propellant consumption during the run, and by dividing the total weight change by the number of pulse cycles, the average propellant consumption per pulse.

The same sequence of events detailed above was performed for each pulsing sequence performed.

Restart Tests and Shutdowns

At the termination of test activities, the normal shutdown sequence followed was to close the main valve, activate the GN_2 purge of the gas generator, vent the propellant tanks, and finally to close all system valves. GN_2 purging of the gas generator was the most rapid way of reducing bed temperatures below the level at which rapid hydrazine decomposition would occur. Purging was stopped at bed temperatures in the order of 300 to 400 F. Stopping at this point minimized possibility of condensing moisture out of the GN_2 purge, which would tend to rust the service nitrided Inconel 600 screens. At this time the test bay was cleared for entry by personnel.

The final portion of the experimental program investigated the shutdown practices currently envisaged for the Space Shuttle APU system. Operations were always stopped without performing any system purging, and after allowing a sufficient length of time for heat soakback to raise the injector manifold to the temperature level desired, the gas generator was restarted.

Initially, the gas generator was operated at the 100-percent flow level for about 150 seconds to get the bed temperatures to the maximum obtainable level. At that point, the throttle valve setting was decreased to the 20-percent power level, resulting in a 120-psia chamber pressure level. All restarts then were at this reduced power level condition, in order to conform to the actual vehicle system conditions.

After the main valve was reopened, it was maintained open for approximately one second. All recordings were examined for signs of pressure spikes, and in the absence of any significant perturbations, the manifold temperature was allowed to increase to a higher level for the next restart experiment.

DATA AND RESULTS

Pressure Modulated Tests

The summary of the data obtained during the pressure modulated tests (Run 7) is presented in Table 8. The S/N 1 gas generator was used in this test, with an 0.243-inch-diameter throat in the exhaust tube. This resulted in a 1000 psia chamber pressure condition at the design 0.365 lb/sec flowrate.

The chamber pressure versus hydrazine flowrate and exhaust gas temperature versus flowrate profiles are shown in Figure 39. These curves exhibit expected characteristics and are comparable to similar data obtained in preceding phases of this program. Agreement between these data and previously obtained data is well within limits of experimental accuracy.

Examination of the 10-percent power condition data shows that the turbine flowmeter exhibited significant drag at this flowrate. Consequently the computed flowrate is too low, resulting in indicated c* efficiencies in excess of 100 percent, and shifting the associated chamber pressure data point slightly off the Figure 39 curve. It may be noted that the flowrate was below the range for which this flowmeter would be recommended.

Pulse Mode Tests

The data for the pulse mode tests are summarized in Table 8. These tests are listed as Run Numbers 10-A through 10-R. These 18 runs were divided into 10 runs performed following a furnished pulse schedule for the high inertia machine, and 8 runs following the low inertia machine schedule. The last two power levels for the low inertia machine (20 and 10 percent) were not performed because the

	1	2	3	4	5	6	7	8	9	10	11
	RUN NO.	$P_{LF\ U/S}$ PSIA	P_{1F} PSIA	$P_{B\ U/S}$ PSIA	$P_{B\ D/S}$ PSIA	P_c PSIA	$T_{B\ U/S}$ F	$T_{B\ D/S}$ F	T_c F	T_{1M-1} F	T_{1M-2} F
1	1	1250	-	-	-	-	1400	-	-	-	-
2	2	1250	-	-	-	950	~1600	-	-	-	-
3	3	1250	-	-	-	-	-	-	-	-	-
4	4	1250	-	-	-	-	-	-	-	-	-
5	5	1250	-	-	- -	-	-	-	-	-	-
6	6	1250	-	-	-	-	-	-	-	-	-
7	7-A	1255	83.2	90.6	92.3	91.4	510.0	1433.4	1373.7	45.8	107.7
8	7-B	1256	281.4	277.1	276.0	274.2	641.0	1525.2	1496.2	24.1	107.9
9	7-C	1255	490.5	475.5	471.5	468.0	744.8	1571.3	1552.9	61.2	111.0
10	7-D	1254	780.7	745.9	737.9	732.8	715.5	1611.0	1599.3	55.5	115.4
11	7-E	1254	1080.3	1009.2	996.5	991.8	753.6	1638.3	1628.8	57.9	112.3
12	8	650	-	-	-	-	-	-	-	-	-
13	9	1250	-	-	-	-	-	-	-	-	-
14	10-A	778	655.8	558.7	520.0	508.9	1565.8	1587.5	1553.4	105.0	99.5
	10-B	779	657.0	564.5	527.5	515.6	1576.4	1581.4	1579.8	104.7	98.3
16	10-C	778	663.8	563.8	527.0	514.5	1588.8	1581.7	1586.4	105.0	90.9
17	10-D	778	654.2	564.1	528.3	515.2	1585.8	1594.2	1595.6	106.6	91.9
18	10-E	779	658.6	562.2	527.2	514.0	1577.8	1595.3	1596.1	103.6	89.3
19	10-F	779	662.1	563.4	528.2	515.2	1601.1	1595.6	1596.2	106.1	90.8
20	10-G	778	660.2	565.0	528.0	515.2	1566.8	1591.8	1595.0	110.6	90.6
21	10-H	779	660.3	562.0	527.7	515.0	1553.6	1596.5	1596.2	110.5	90.9
22	10-I	780	662.6	561.3	527.8	515.2	1568.0	1596.4	1595.1	108.0	96.9
23	10-J	780	662.8	562.2	527.7	515.5	1504.2	1603.5	1599.3	106.5	94.6
24	10-K	782	659.1	560.2	528.0	514.6	1588.3	1585.5	1590.8	109.9	98.3
25	10-L	784	660.0	566.6	529.8	515.8	1627.0	1577.8	1589.1	112.8	90.2
26	10-M	788	659.4	558.9	521.7	509.2	1585.0	1570.0	1569.4	106.6	99.4
27	10-N	789	639.7	547.6	496.6	497.7	1556.7	1561.4	1559.2	109.6	102.6
28	10-O	789	654.2	548.7	493.2	498.4	1563.9	1567.2	1561.7	115.3	104.7
29	10-P	787	425.6	498.2	323.3	464.6	1464.6	1542.6	1542.9	103.9	99.0
30	10-Q	790	307.2	511.0	341.7	467.0	1464.8	1550.9	1545.6	109.9	96.6
31	10-R	790	750.6	335.0	183.7	379.7	1355.2	1534.0	1521.6	111.2	105.3
	11	790	-	-	-	~120	~1200	~1140	-	565 (MAX)	-
33											
34											
35											

FOLDOUT FRAME /

11	12	13	14	15	16	17	18	19	20	21	22	
M-2 F	T_{W-1} F	T_{W-2} F	T_{W-3} F	$\dot{W}_F$ LB/SEC	C* FT/SEC	THEOR. C* FT/SEC	η_{C*}	DURATION OF STEP	NO. OF PULSES	PULSE "ON" TIME SEC	PULSE "OFF" TIME SEC	
-	-	-	-	-	-	-	-	-	-	-	-	TE
-	-	-	-	-	-	-	-	-	-	-	-	TE
-	-	-	-	-	-	-	-	-	-	-	-	TE
-	-	-	-	-	-	-	-	-	-	-	-	TE
-	-	-	-	-	-	-	-	-	-	-	-	TE
-	-	-	-	-	-	-	-	-	-	-	-	TE
7.7	1386.9	1392.5	1389.8	0.020	6830	4140		180	-	-	-	
7.9	1491.5	1493.8	1491.6	0.097	4225	4220	100.1	180	-	-	-	
1.0	1542.3	1543.7	1540.2	0.170	4109	4250	0.967	180	-	-	-	
5.4	1584.6	1586.4	1581.8	0.266	4114	4270	0.963	180	-	-	-	
2.3	1613.4	1614.7	1610.6	0.355	4173	4290	0.973	180	-	-	-	
-	-	-	-	-	-	-	-	-	-	-	-	TE
-	-	-	-	-	-	-	-	-	-	-	-	TE
9.5	1539.7	1536.8	1536.6	-	-	-	-	-	156	0.140	1.121	
8.3	1546.2	1544.7	1545.9	-	-	-	-	-	171	0.143	0.657	
0.9	1550.7	1551.8	1553.3	-	-	-	-	-	132	0.183	0.507	
1.9	1559.3	1561.2	1561.6	-	-	-	-	-	114	0.223	0.383	
9.3	1550.5	1558.0	1560.7	-	-	-	-	-	102	0.273	0.315	
0.8	1552.9	1558.6	1560.0	-	-	-	-	-	86	0.333	0.255	
0.6	1551.2	1557.9	1559.5	-	-	-	-	-	71	0.408	0.180	
0.9	1554.2	1556.4	1559.3	-	-	-	-	-	53	0.558	0.242	
6.9	1530.3	1544.6	1550.8	-	-	-	-	-	33	0.983	**0.267**	
4.6	1536.9	1551.8	1555.9	-	-	-	-	-	13	3.033	0.300	
8.3	1535.1	1549.0	1546.2	-	-	-	-	-	164	0.171	0.115	
0.2	1544.2	1554.5	1547.8	-	-	-	-	-	221	0.132	0.121	
9.4	1541.2	1547.8	1545.1	-	-	-	-	-	311	0.083	0.147	
2.6	1539.6	1547.0	1535.5	-	-	-	-	-	425	0.058	0.157	
4.7	1544.8	1547.0	1544.5	-	-	-	-	-	491	0.053	0.151	
9.0	1524.7	1530.1	1523.5	-	-	-	-	-	595	0.033	0.167	
6.6	1533.2	1541.2	1526.0	-	-	-	-	-	566	0.034	0.176	
5.3	1501.8	1510.1	1510.6	-	-	-	-	-	1086	0.028	0.202	
-	-	-	-	-	-	-	-	-	-	-	-	H

FOLDOUT FRAME 2

TABLE 8. PULSE MODE TESTS

18	19 DURATION OF STEP	20 NO. OF PULSES	21 PULSE "ON" TIME SEC	22 PULSE "OFF" TIME SEC	23	24	25	26	27	28	29
					GENERAL COMMENTS						
	-	-	-	-	TEST ABORTED - HOT GAS LEAK AT FITTING						
	-	-	-	-	TEST ABORTED - EXCESSIVE SMOKING OF DUCT PAINT						
	-	-	-	-	TEST ABORTED - HEATER REACTOR FAILURE						
	-	-	-	-	TEST ABORTED - HEATER REACTION NOZZLE PLUGGING						
	-	-	-	-	TEST ABORTED - HEATER REACTOR P_c TRANSUDCER FAILURE						
	-	-	-	-	TEST ABORTED - HEATER REACTOR OUTLET TUBE FAILURE						
	180	-	-	-	S/N 1 GAS GENERATOR ASSEMBLY - 0.243 IN. D_t						
.1	180	-	-	-	STEADY STATE (THROTTLED OPERATION) TESTS						
67	180	-	-	-							
63	180	-	-	-							
73	180	-	-	-							
	-	-	-	-	TEST ABORTED - HEATER REACTOR FAILURE						
	-	-	-	-	TEST ABORTED - PROPELLANT LEAKAGE @ INJECTOR						
	-	156	0.140	1.121	S/N 2 GAS GENERATOR ASSEMBLY - 0.332 IN. D_t						
	-	171	0.143	0.657							
	-	132	0.183	0.507							
	-	114	0.223	0.383							
	-	102	0.273	0.315							
	-	86	0.333	0.255							
	-	71	0.408	0.180							
	-	53	0.558	0.242							
	-	33	0.983	0.267							
	-	13	3.033	0.300							
	-	164	0.171	0.115							
	-	221	0.132	0.121							
	-	311	0.083	0.147							
	-	425	0.058	0.157							
	-	491	0.053	0.151							
	-	595	0.033	0.167							
	-	566	0.034	0.176							
	-	1086	0.028	0.202							
	-	-	-	-	HOT MANIFOLD RESTART TESTS						

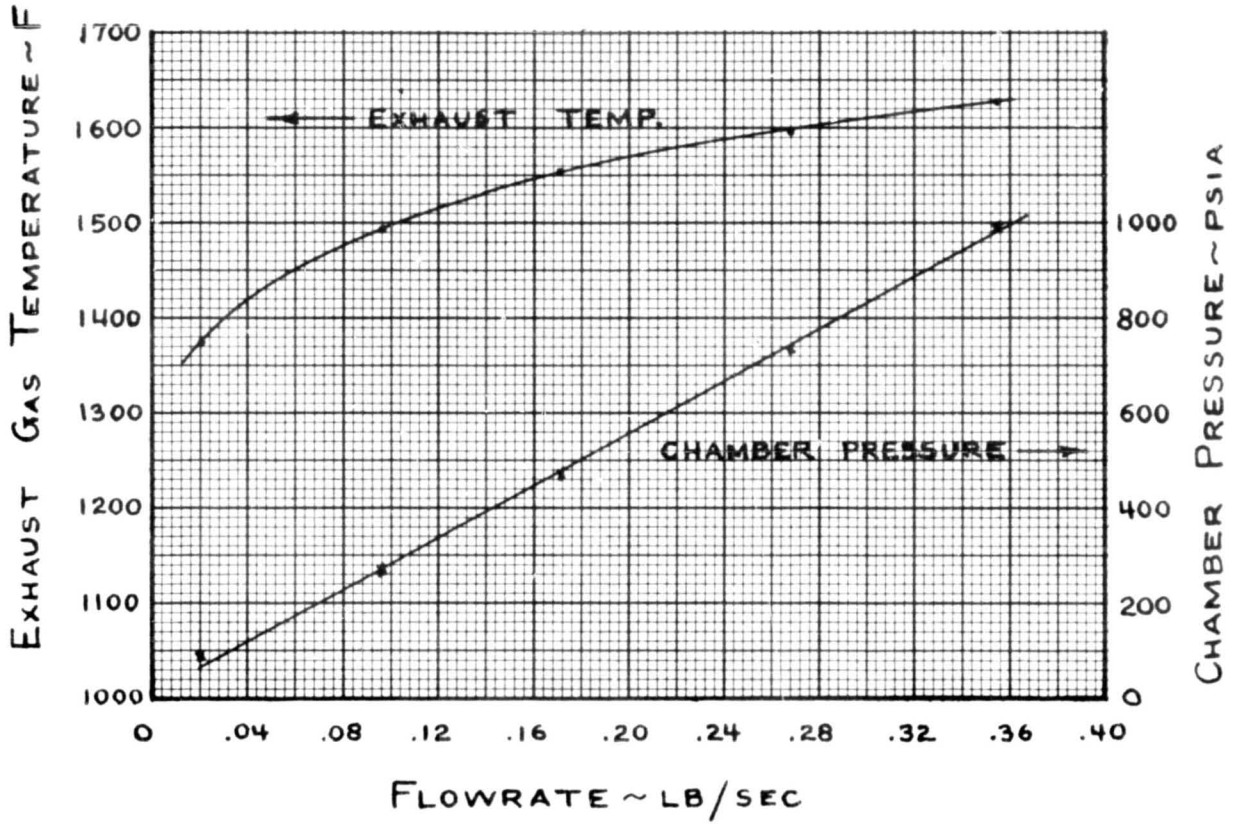

Figure 39. Chamber Pressure and Temperature as a Function of Flowrate

propellant main valve did not open when the sequencer was programmed for those particular "ON" times. The relative "ON" times and pulse frequencies for the various power levels are shown in Tables 9 and 10 under the "PROGRAMMED" headings. These power level schedules are also shown in Figures 40 and 41, with the fractional "ON" times plotted as a function of the pulse frequency.

Tables 9 and 10 show that the power level schedules actually accomplished during the tests deviated from the requested schedules. This resulted because a spring loading adjustment in the "Vacco" main valve apparently changed. Initial tests indicated valve opening and closing times in the order of 10 milliseconds. However, the valve adjustment changed in such a manner that a long induction period prior to start of valve opening motion resulted. Valve closing times apparently were not affected. This induction period delay in the valve opening cycle (approximately 67 milliseconds) is shown in the Figure 42 oscillograph traces. The change in the valve operating characteristics was not noted during the course of the 3.5-hour continuous series of tests which produced all of the Table 9 and 10 data. As a result, all of the valve "ON" periods were effectively shortened by approximately 67 milliseconds, as compared to the times that were actually programmed by the sequencer.

Figure 43 is similar to Figures 40 and 41 and may be compared to them. It shows the actual pulse test schedules performed. It should be noted that here, and in Tables 9 and 10, the valve "ON" time has been taken as the total time interval from the start of valve opening to the end of the valve closing cycle (as deduced from high response rate measurements recorded on the oscillograph).

The power level that each of the test pulse series would produce cannot be computed without knowledge of the performance characteristics of the "high inertia machine" and "low inertia machine". Since such information was not available, a somewhat idealized machine power-valve fractional "ON" time relationship was assumed for discussion purposes. This was done by adopting the fractional "ON" time for the 100 percent power level (as listed in the NASA provided schedules) and assuming a direct proportionality between "ON" time and the power level. This results in the curves shown as Figure 44. These proportionalities were

TABLE 9. HIGH INERTIA MACHINE SCHEDULE TESTS

PROGRAMMED			*TEST DATA AND RESULTS					
POWER LEVEL PERCENT	PULSE WIDTH SEC	PULSE FREQ Hz	POWER LEVEL PERCENT	PULSE WIDTH SEC	PULSE FREQ Hz	PULSE EFF P	SPC LB/HP-HR	NO OF TEST PULS ES
10	0.200	1.0	12	0.140	1.0	.903	2.47	156
20	0.210	1.25	19	0.143	1.25	.935	2.38	171
30	0.250	1.45	28	0.183	1.45	.953	2.33	132
40	0.290	1.65	40	0.223	1.65	.967	2.31	114
50	0.340	1.7	50	0.273	1.7	.974	2.29	102
60	0.400	1.7	61	0.333	1.7	.979	2.28	86
70	0.475	1.7	74	0.408	1.7	.984	2.27	71
80	0.625	1.25	75	0.558	1.25	.996	2.24	53
90	1.050	0.8	84	0.983	0.8	.987	2.26	33
100	3.100	0.3	98	3.033	0.3	.997	2.24	13

* CHANGES IN THE OPERATIONAL CHARACTERISTICS OF THE VALVE BEING PULSED REDUCED THE EFFECTIVE PULSE WIDTH AS SHOWN. THE TEST POWER LEVEL SHOWN IS THE RATIO OF THE FRACTIONAL "ON" TIME OF THE TEST PULSE COMPARED TO THE FRACTIONAL "ON" TIME GIVEN FOR THE 100 PERCENT POWER LEVEL SCHEDULE.

TABLE 10. LOW INERTIA MACHINE SCHEDULE TESTS

PROGRAMMED			*TEST DATA AND RESULTS					
POWER LEVEL PERCENT	PULSE WIDTH SEC	PULSE FREQ Hz	POWER LEVEL PERCENT	PULSE WIDTH SEC	PULSE FREQ Hz	PULSE EFF P	SPC LB/HP-HR	NO OF TEST PULS ES
10	0.075	2.9	-	-	-	-	-	-
20	0.075	3.8	-	-	-	-	-	-
30	0.080	4.35	.123	0.028	4.35	.849	2.63	1086
40	0.100	4.75	.161	0.034	4.75	.903	2.47	566
50	0.100	5.0	.166	0.033	5.0	.900	2.48	595
60	0.120	4.9	.261	0.53	4.9	.933	2.39	455
70	0.125	4.65	.270	0.058	4.65	.932	2.39	425
80	0.150	4.35	.361	0.083	4.35	.950	2.35	311
90	0.200	3.95	.522	0.132	3.95	.969	2.30	221
100	0.250	3.5	.598	0.171	3.5	.974	2.29	165

* CHANGES IN THE OPERATIONAL CHARACTERISTICS OF THE VALVE BEING PULSED REDUCED THE EFFECTIVE PULSE WIDTH AS SHOWN. THE TEST POWER LEVEL SHOWN IS THE RATIO OF THE FRACTIONAL "ON" TIME OF THE TEST PULSE COMPARED TO THE FRACTIONAL "ON" TIME GIVEN FOR THE 100 PERCENT POWER LEVEL.

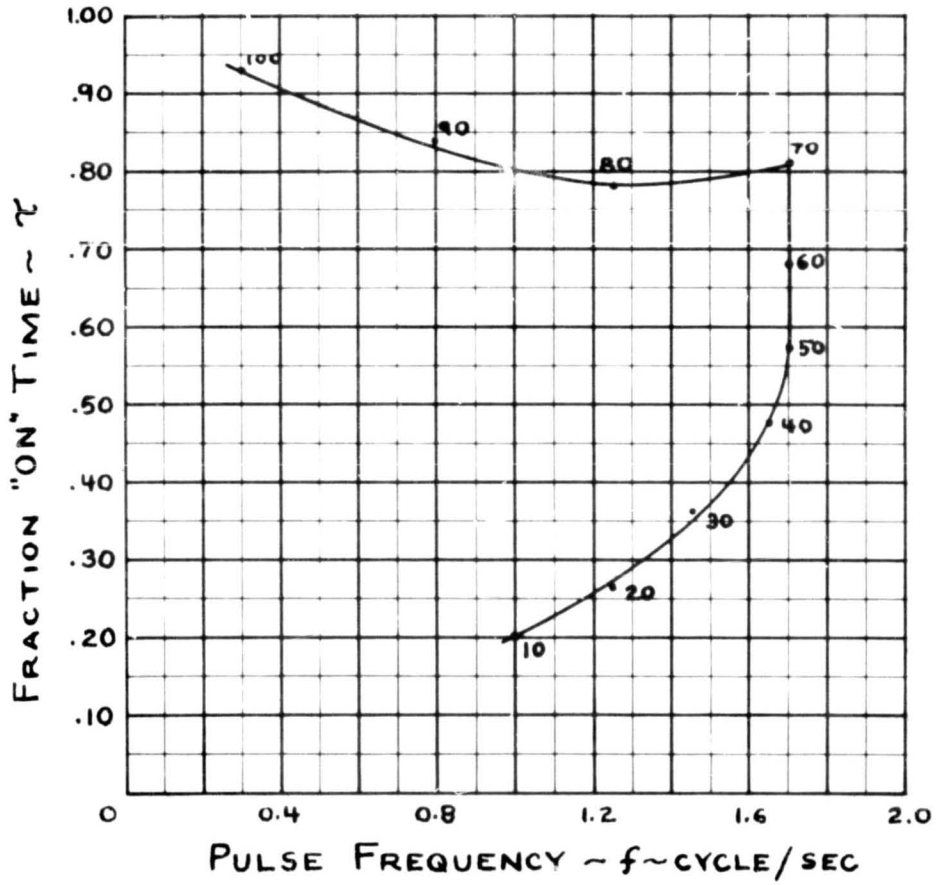

Figure 40. Fraction "On" Time for Low Inertia Machine

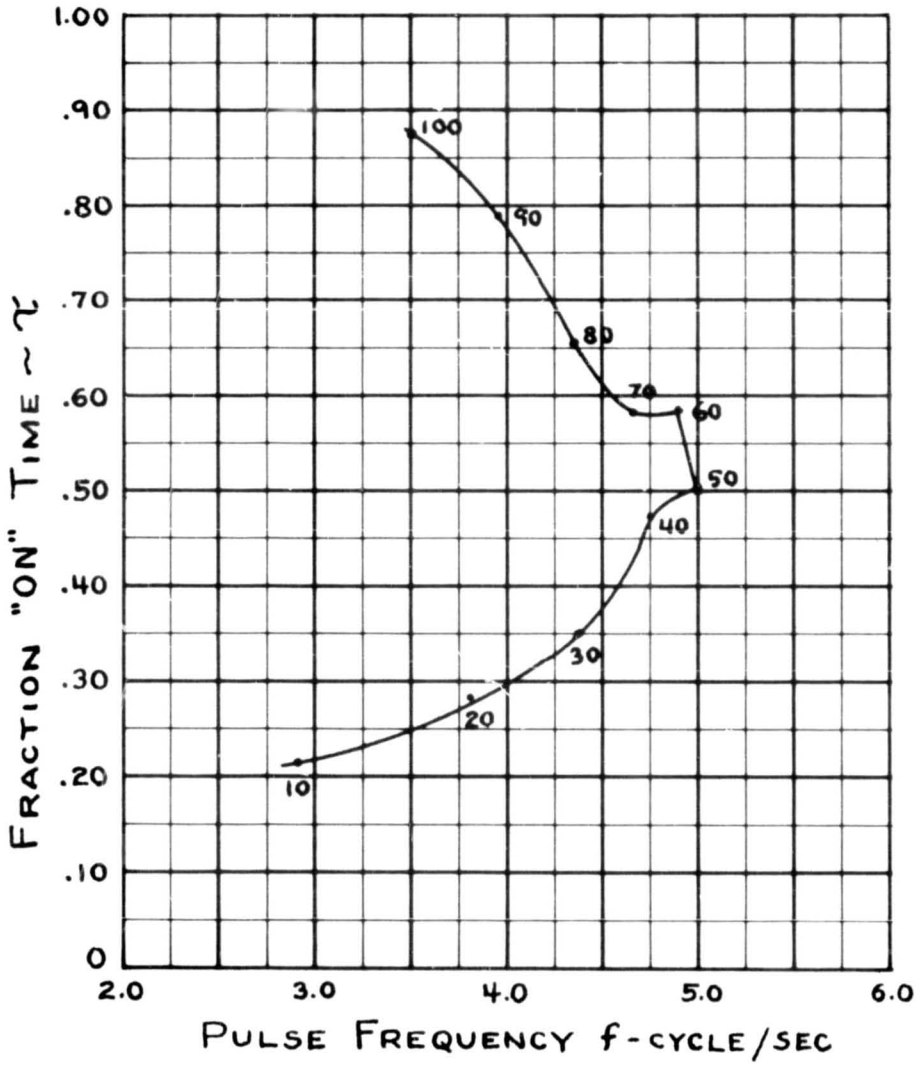

Figure 41. Fraction "On" Time for High Inertia Machine

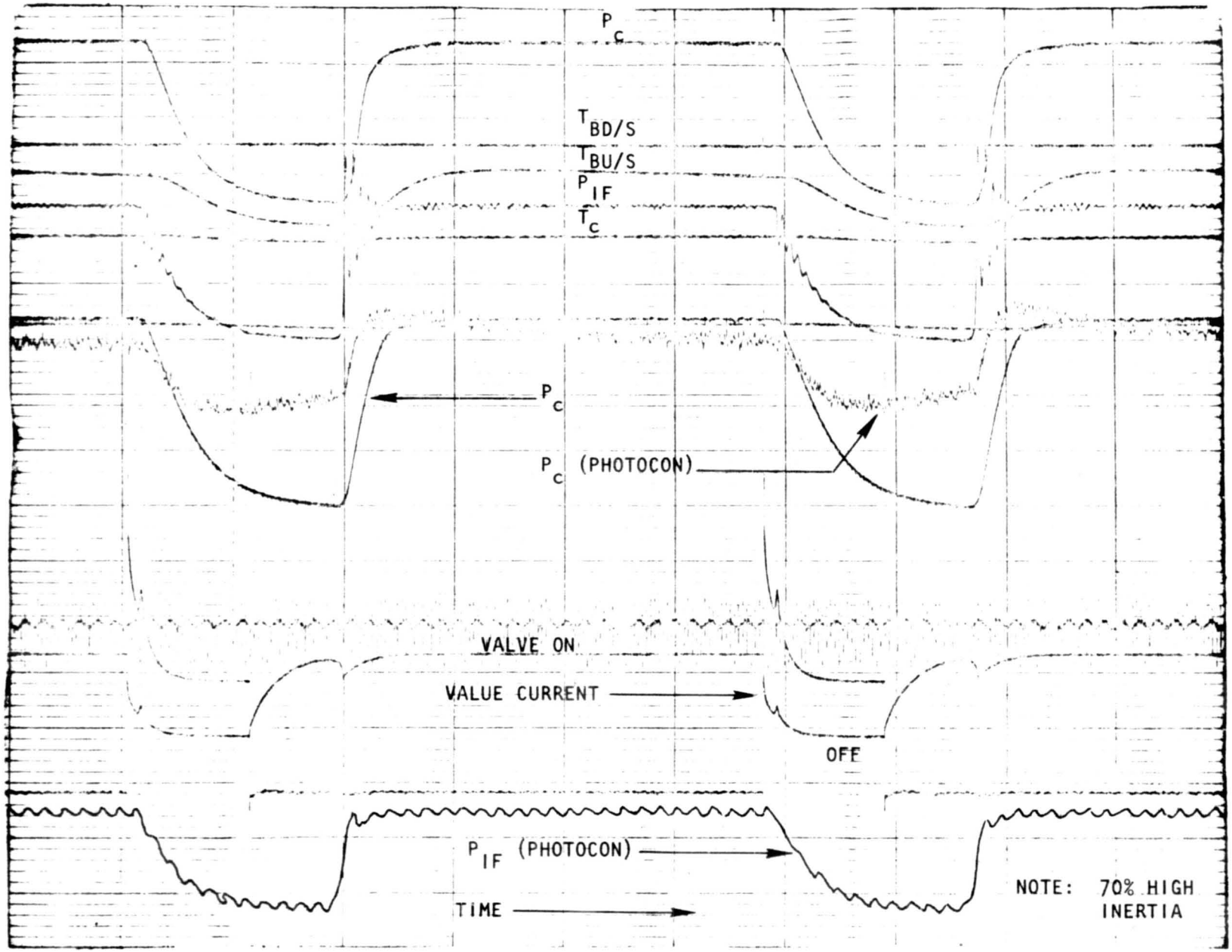

Figure 42. Typical Oscillograph Trace for Pulse Operation

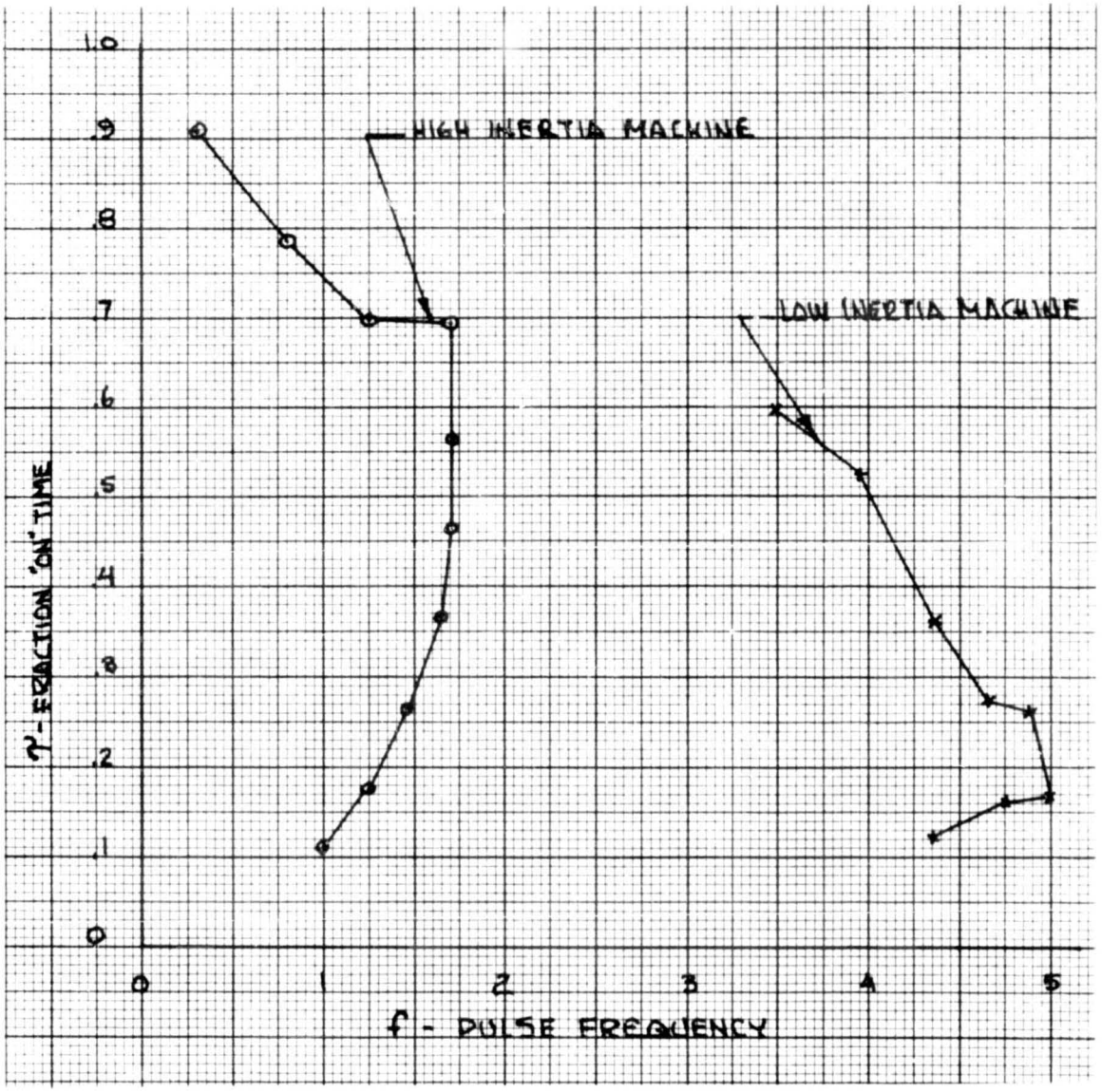

Figure 43. Test Conditions of τ and f for High and Low Inertia Machines

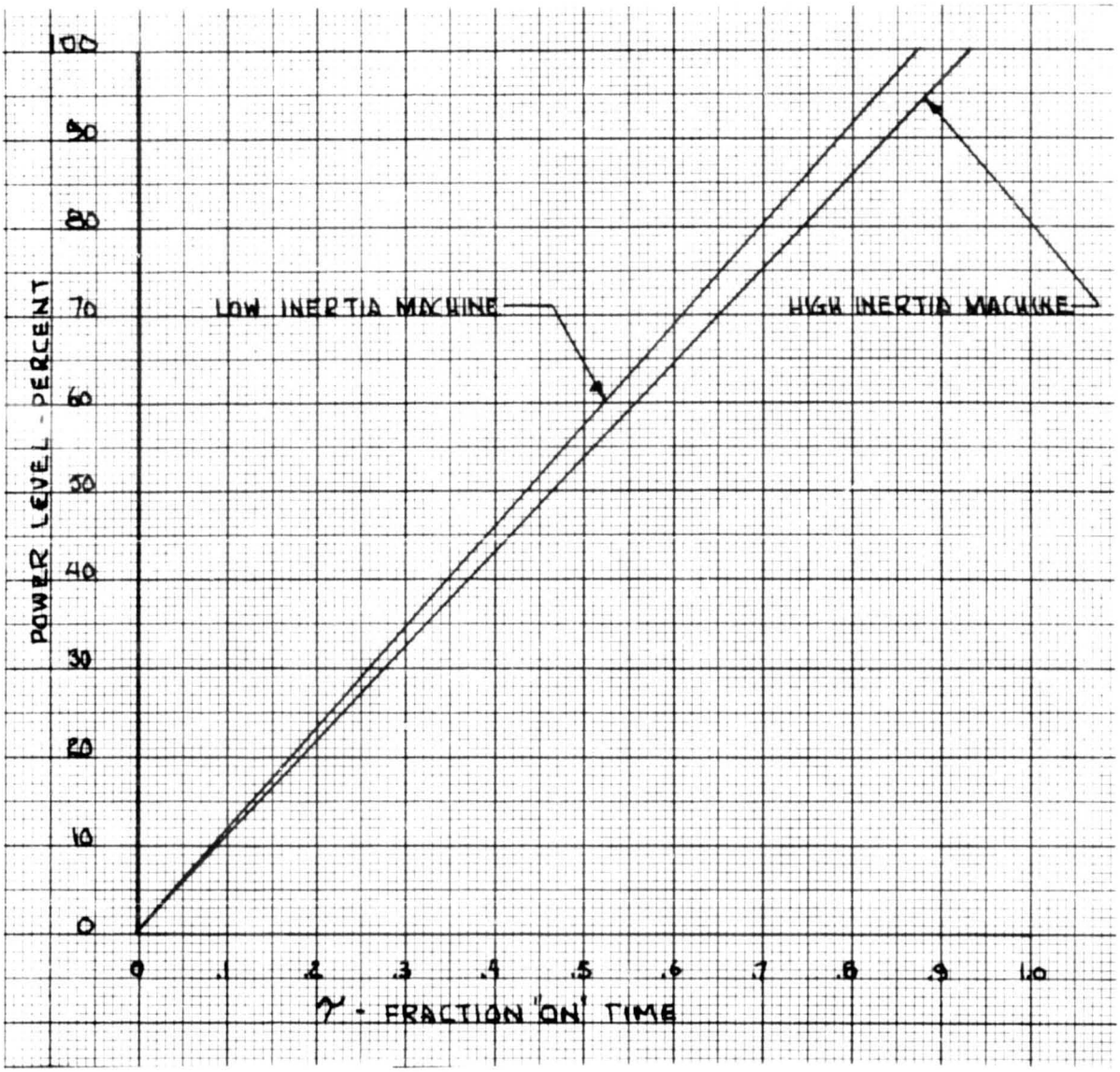

Figure 44. Power Level as a Function of Machine Inertia and τ

also used to arrive at the Tables 9 and 10 listings of "Power Level Percent" under the "Test Data and Results" headings.

Data Analyses and Results

Representative data from each of the various pulse cycles performed with the S/N 2 gas generator operating at approximately 515 psia chamber pressure, and a 10 percent power level cycling test previously performed with the S/N 1 gas generator at a 992-psia chamber pressure, were used to compute pulse cycle efficiencies. The derivation of the equations used in the pulse efficiency computation and a listing of the G.E. Timeshare program that was written to perform these computations are given in Appendix A. These analyses consider the energy available for use by the turbine and then compute the relative power that an ideal turbine could derive from it as compared to the energy content available with the gas generator operating in a steady state condition.

The reference steady state gas generator output conditions used by the computer program were obtained from the 100 percent power level high inertia pulse tests. Well stabilized data from the last pulse in these series was averaged to obtain these reference chamber pressure and temperature valves. The tabulated valves presented in Table 11 were used to compute these average values. It should be noted that each value listed in the columns is already the result of a previous averaging of 30 data points by the Astrodata data reduction performed.

The results of these computations are listed in the pulse cycle efficiency columns of Tables 9 and 10. These results are also incorporated in Figure 45 with the pulse efficiencies plotted as a function of valve "ON" time. These results follow the trends to be expected, showing decreases in the pulse efficiency as pulse on times are reduced.

Not included in Table 11 is the single set of pulse data obtained with the S/N 1 gas generator operating at a 992-psia chamber pressure. This "high inertia machine" schedule point had a 0.180 second "ON" time and a pulse frequency of 0.99 Hz. The computed pulse efficiency for this pulse cycle was 0.930. This point falls very closely to the curve plotted for the "high inertia machine" in

TABLE 11. 100 PERCENT POWER LEVEL (HIGH INERTIA MACHINE)
STABILIZED TEST DATA

TIME SLICE SEC	AVERAGED CHAMBER PRESSURE PSIA	AVERAGED EXHAUST GAS TEMPERATURE F
29.230 - 29.343	515.165	1601.65
29.347 - 29.460	515.782	1600.93
29.464 - 29.577	515.970	1600.00
29.581 - 29.714	515.458	1599.29
29.718 - 29.831	515.316	1599.32
29.835 - 29.947	514.947	1599.50
29.952 - 30.065	514.442	1599.52
30.069 - 30.201	514.337	1599.60
30.206 - 30.318	514.262	1599.68
30.323 - 30.435	513.991	1599.50
30.440 - 30.552	514.488	1599.73
30.557 - 30.689	514.442	1599.62
30.693 - 30.806	514.586	1599.70
30.811 - 30.923	514.028	1599.73
30.927 - 31.040	513.796	1599.86
31.044 - 31.157	513.939	1599.68
31.161 - 31.294	513.999	1599.99
31.298 - 31.411	514.450	1600.22
31.415 - 31.528	514.209	1600.12
31.532 - 31.645	514.254	1600.03
31.649 - 31.782	514.074	1600.24

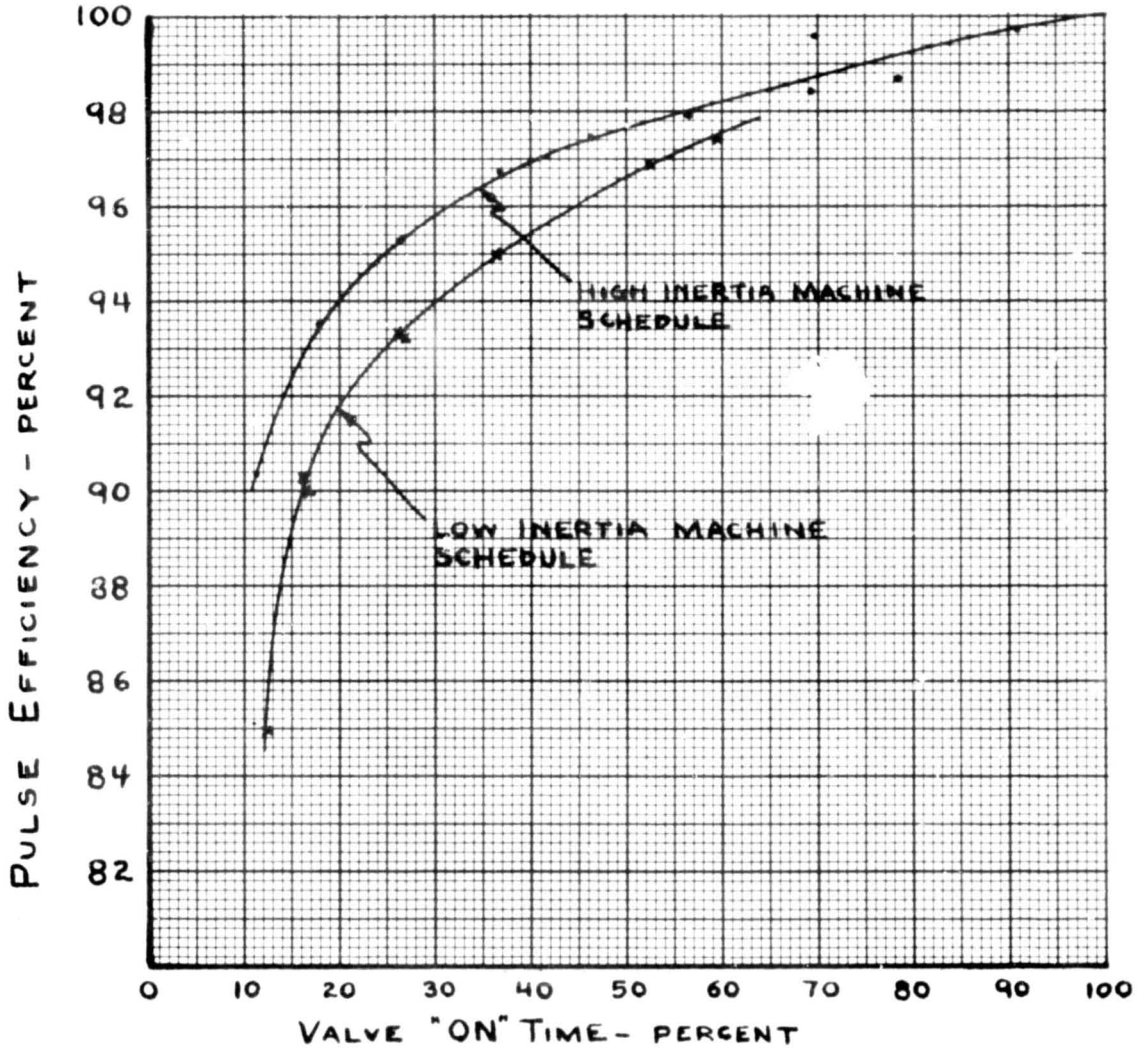

Figure 45. Pulse Efficiency

Figure 43. This result is of great interest since it demonstrates the applicability of the results obtained with the S/N 2 gas generator at 515 psia to the 1000 psia operating conditions initially planned for this program.

Gas Generator Response Characteristics

The high response rate instrumentation, recorded on the oscillograph, Figure 42, permit measurement of the response characteristics of the gas generator in the test configuration. The results of analysis of a typical start transient during the pulse tests is given below:

Injection Pressure Buildup (Photocon P_{1F})	Start	Rise	0
	90%	Rise	15 milliseconds
	100%	Rise	17 milliseconds
Chamber Pressure Buildup (Photocon P_c)	Start	Rise	10 milliseconds
	90%	Rise	30 milliseconds
	100%	Rise	36 milliseconds
Chamber Pressure Buildup (Bonded Strain Gage Transducer)	90%	Rise	43 milliseconds
Valve Opening Time			11.5 milliseconds

The reference zero time for all tabulated items above was the start of rise for the P_{1F} measurement. Necessarily, with the start of opening of the fuel valve, the gases in the propellant line between the valve and the injector manifold would start to be compressed. It should also be noted that the valve opening time is a very significant portion of the time required for the injection pressure (P_{1F}) to attain its 90 percent level.

The chamber pressure buildup to the 90-percent level required an additional 15 milliseconds after the injection pressure had reached that level. This time lag is a result of the sizeable void volume which must be pressurized, and the time required to reattain temperature equilibrium. During such times when more

heat is being abstracted from the chamber gases than normally is required to satisfy heat losses, the chamber pressure will be lower due to this cooling.

The chamber void volume was derived by measuring the amount of fluid required to fill the assembly. This indicated volume is 52.5 cu in. The additional volumes associated with pressure transducer lines and the fuel line between the main valve and the gas generator increase the total void volume to 53.1 cu in.

Heater-Reactor Performance

The pilot thermal bed hydrazine gas generator shown in Fig. 35 was used for tests No. 1 through 8. Preheat times for the main gas generator in the order of 24 minutes were noted, but a higher temperature level was attained than with the heated GN_2 system. No attempt was made to minimize the preheat period.

The first heater reactor assembly was used successfully during tests No. 1 and 2, and then failed during the third test. This chamber explosion occurred immediately after hydrazine flow to the chamber was initiated. A photograph of the gas generator after this explosion is presented as Fig. 46. It should be noted that no other significant damage to the test installation components resulted because of this failure.

The pilot gas generator was repaired by replacing the body section, and repacking with fresh 1/16-inch-diameter, stainless-steel balls. A chamber pressure measurement for this pilot gas generator was added to the instrumentation complement in order to shed some light on the problem area encountered. However, the transducer experienced a pressure excursion during Run No. 5, resulting in a diaphragm failure and hot gas leakage out of the transducer housing.

Additionally, after encounter of the initial pilot gas generator system failure, the startup technique was modified. Instead of instituting an abrupt propellant full flow start, the fuel tank pressure was reduced from 1200 to 100 psig.

For Run No. 6, the pressure transducer was disconnected and the pressure pickup line was capped. This run was aborted by another failure; this time a rupture

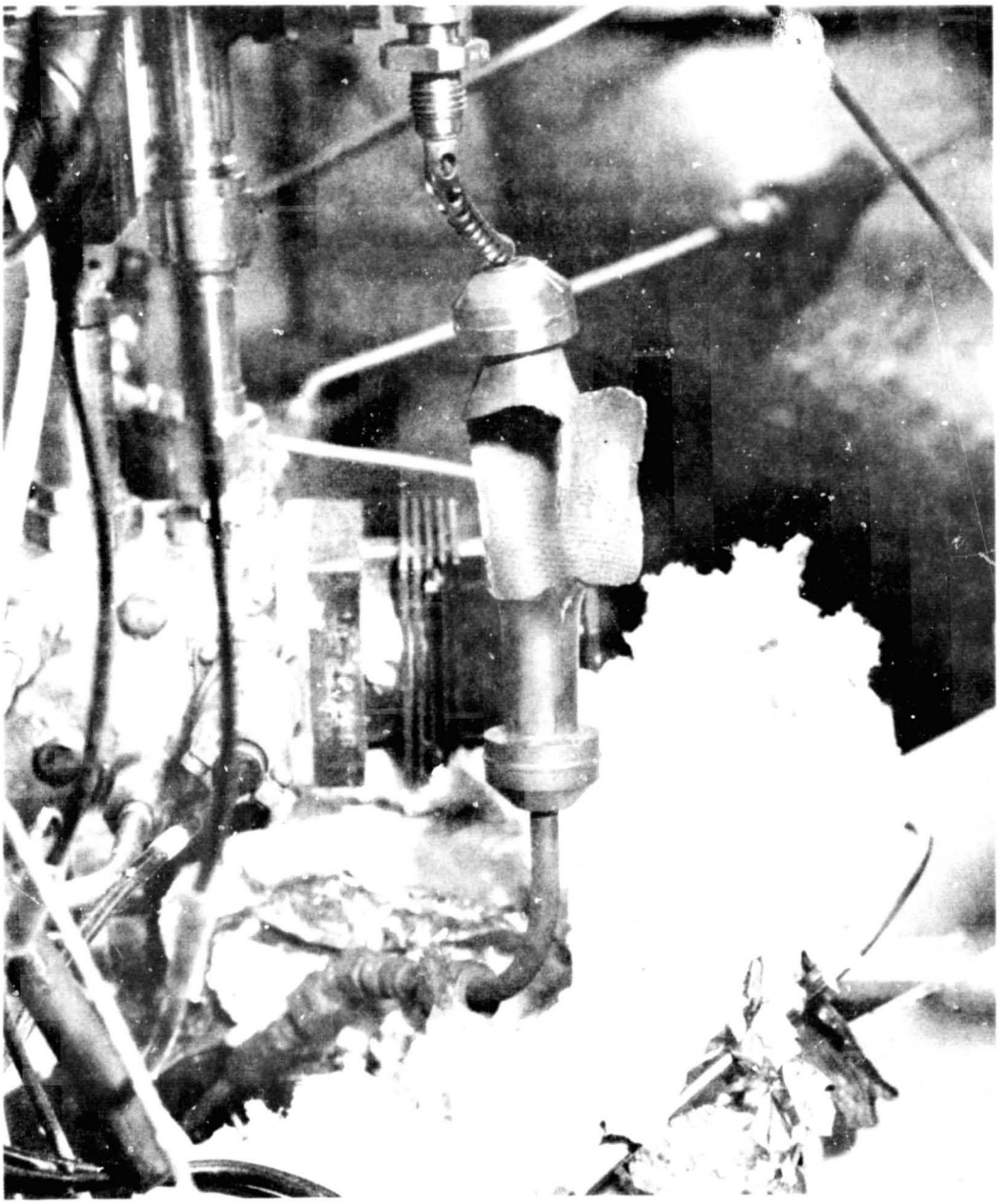

Figure 46. Pilot Heater Gas Generator After Explosion

occurred in the 1/4-inch OD tube ducting the hot gases out of the generator. This tubing was replaced by a heavier walled tube (0.065-inch wall instead of 0.042). Subsequently, the heatup cycle for Run No. 7 was performed without incidence.

The final heater reactor failure occurred during the course of Run No. 8. This failure resulted in reverting to the hot GN_2 heatup technique used in previous phases of the program. In this instance, a failure of the heater gas generator body occurred, resembling the initial chamber failure (Fig. 46) very closely. The pilot gas generator had been operating for several minutes, and the propellant tank pressure had been gradually elevated from 90 to 650 psig (800 psig would have been the maximum use level), when the explosion occurred. These failures were interpreted to be the result of pressure spiking encountered at certain chamber pressure levels. Since it was impractical to embark upon a development effort to eliminate these problems, further use of the heater reactor was abandoned.

Restart Tests

A series of 11 hot restart tests was performed. Each time the gas generator operation was shutdown, heat soakback was allowed to elevate the injector manifold temperature to the point desired for that particular restart attempt. At no time were any system purges performed.

The successive temperature levels (T_{MAN-2} in Fig. 38) which existed at the propellant manifold for this series of tests were as follows: 115, 115, 167, 298, 335, 389, 469, 495, 508, 548, and 565 F.

The gas generator was always restarted at the 20-percent flowrate, and the flow was maintained for about 1 second prior to shutdown. Longer operating durations would cool down the propellant manifold excessively (insofar as progressively higher temperatures were required for the investigation) and also would not be representative of pulse mode type operations.

Prior to the last restart test, no significant spiking was discernible in either the Photocon pressure measurements or in any of the temperature measurements. During the last test, a small overshoot in the manifold temperature occurred, immediately following the initiation of fuel flow. This temperature increase was from 565 to 591 F. Shutdown occurred after approximately 800 milliseconds. At that time, the indicated manifold temperature was 513 F. This shutdown resulted in a manifold explosion. The results of this explosion were to stretch the threaded sections of the two 10-32 NF bolts used to fasten the propellant inlet line fixture to the manifold (see Fig. 38), and thus relieve the excess pressure condition. No damage was incurred by the gas generator or the facility.

GAS GENERATOR OPERATIONAL MODE EFFICIENCIES

The primary objective of the Phase III program was to evaluate the efficiency of the gas generator under steady state and pulsing modes. These basic results are embodied in Tables 10 and 11 and in Fig. 45.

In order to compare the relative efficiencies of the two modes of operation, further calculations were performed. These calculations were based on the standard thermodynamic relationships relating enthalpy changes to output power for ideal turbomachinery. Accordingly, specific fuel consumption (SPC) was computed using the formula below:

$$SPC = \frac{1.98 \times 10^6}{(778)(C_p)(T_1)\left[1-(P_2/P_1)^{\gamma-1/\gamma}\right]} \quad (lb_m/HP\text{-}HR)$$

The specific fuel consumption computed using this relationship were increased, by dividing by the pulse efficiency (η_p) previously determined, for each type of pulse mode operation. In the case of the steady state runs (pressure modulated operation) no such adjustment was required.

As may be seen in Fig. 47, the pulse mode operations reflect a higher operational efficiency at most power levels. At the 100-percent power level, of course, the pressure modulated type of operation has a slight margin of better performance. It should be re-emphasized at this point, that the power level percentages shown as the Fig. 47 abscissa refer back to the Fig. 44 relationship which assumes an ideal turbine. The specific fuel consumption for an actual machine would have to be increased by its nonideality factor for each range of power level operation.

The relationship between the specific fuel consumption for the pulse modulated operations and pressure modulated operating modes are shown in Fig. 48, in which all points above the line of equal performance represent lower SPC for pulse modulated units.

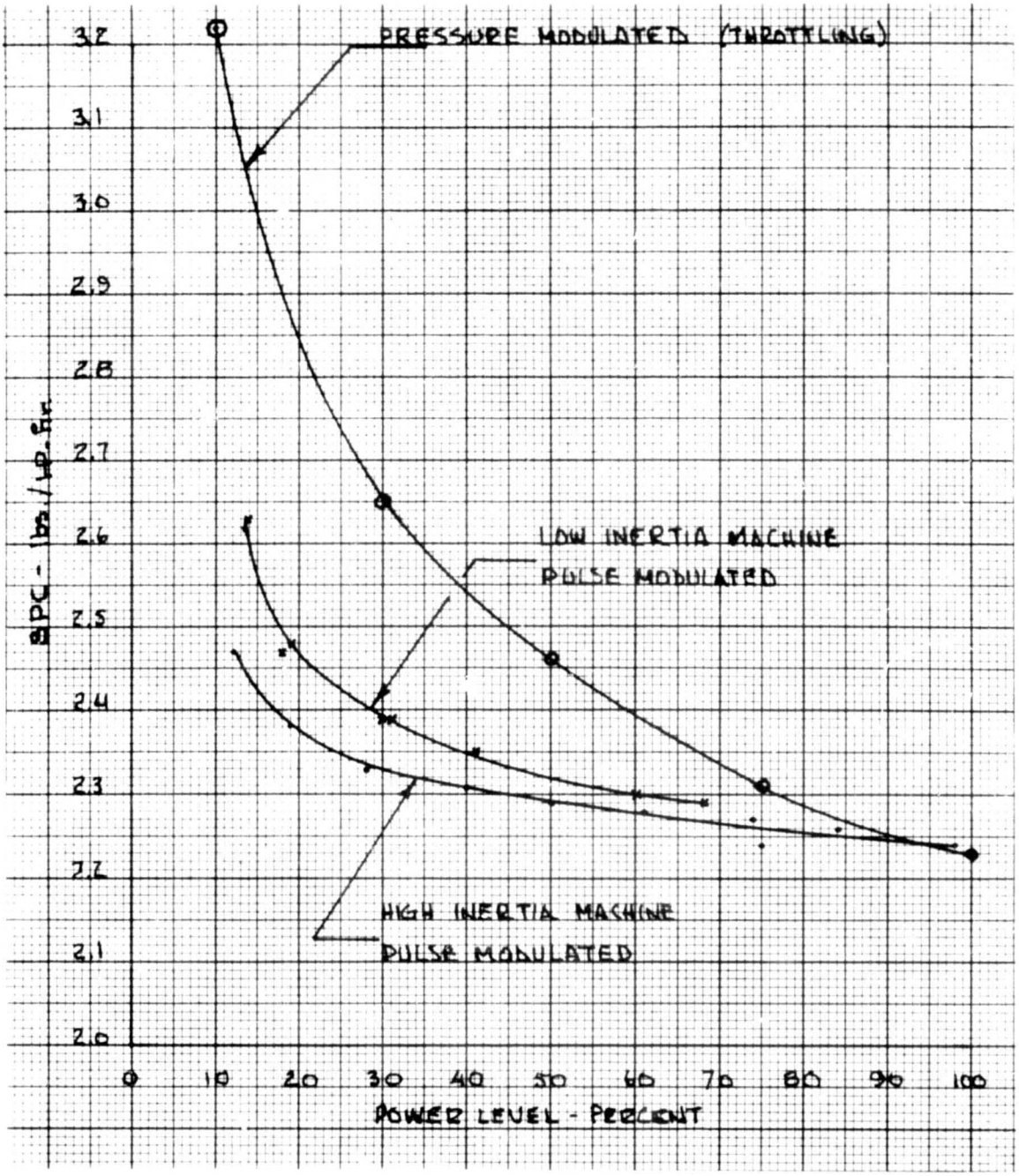

Figure 47. SPC as a Function of Power Control-Pulse vs Throttling and Machine Inertia

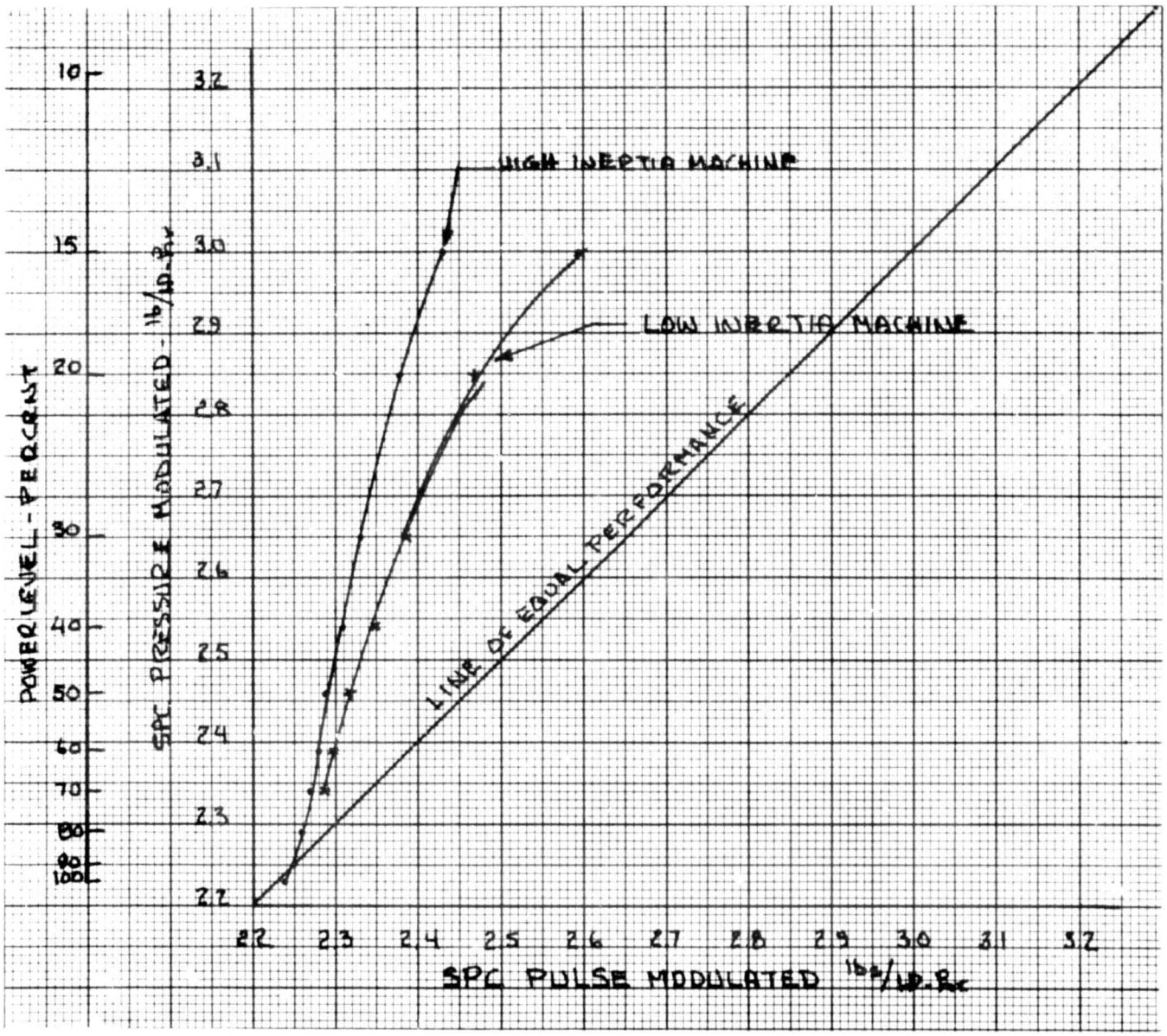

Figure 48. Pressure vs Pulse Modulated Relationship at Varying Power Levels

The penalty for operating the gas generator in the pressure-modulated mode, as compared to the two pulse-modulated schedules experimentally evaluated, is presented in Fig. 49. The power level variable is again based on the supposition of an "ideal" turbine. This, of course, has no effect on the relative efficiencies of the two operating modes evaluated, since the same assumption holds in all cases.

The explanation for these relative differences in operating efficiencies is, of course, the energy degradation associated with operating at lower pressures and temperatures. Pulse mode operations essentially are at full chamber pressure, except for a relatively short period of time when pressure buildup is occurring at the start, and tailoff pressures when the fuel valve is closed. It should also be noted that the high thermal inertia of the gas generator tends to maintain the exhaust gas temperature within a rather narrow band. For example, data from the 10-percent power level, high inertia machine schedule, shows a difference of 1.5 percent between minimum and maximum temperature readings.

In the pressure modulated opeations, fuel flow is throttled and thus result in lower chamber pressures and lower associated exhaust gas temperatures.

Propellant Consumption Comparisons

The tank weighing system allowed the measurement of the total propellant consumed during the performance of each individual pulse mode test. The average fuel consumption per pulse was then computed by dividing the change in tank weight (plus the weight of the compressed nitrogen pressurization gas replacing the expelled N_2H_4 volume) by the total number of pulses performed.

The Appendix A computer program calculates the specific energy per pulse rather than propellant weight, so no direct comparison of the measured versus the calculated quantities was possible.

To compare the computer program weight results with the measured values, it was necessary to time integrate the pressure history of a pulse, and derive an average chamber pressure. The c* relationship was then used to complute the fuel

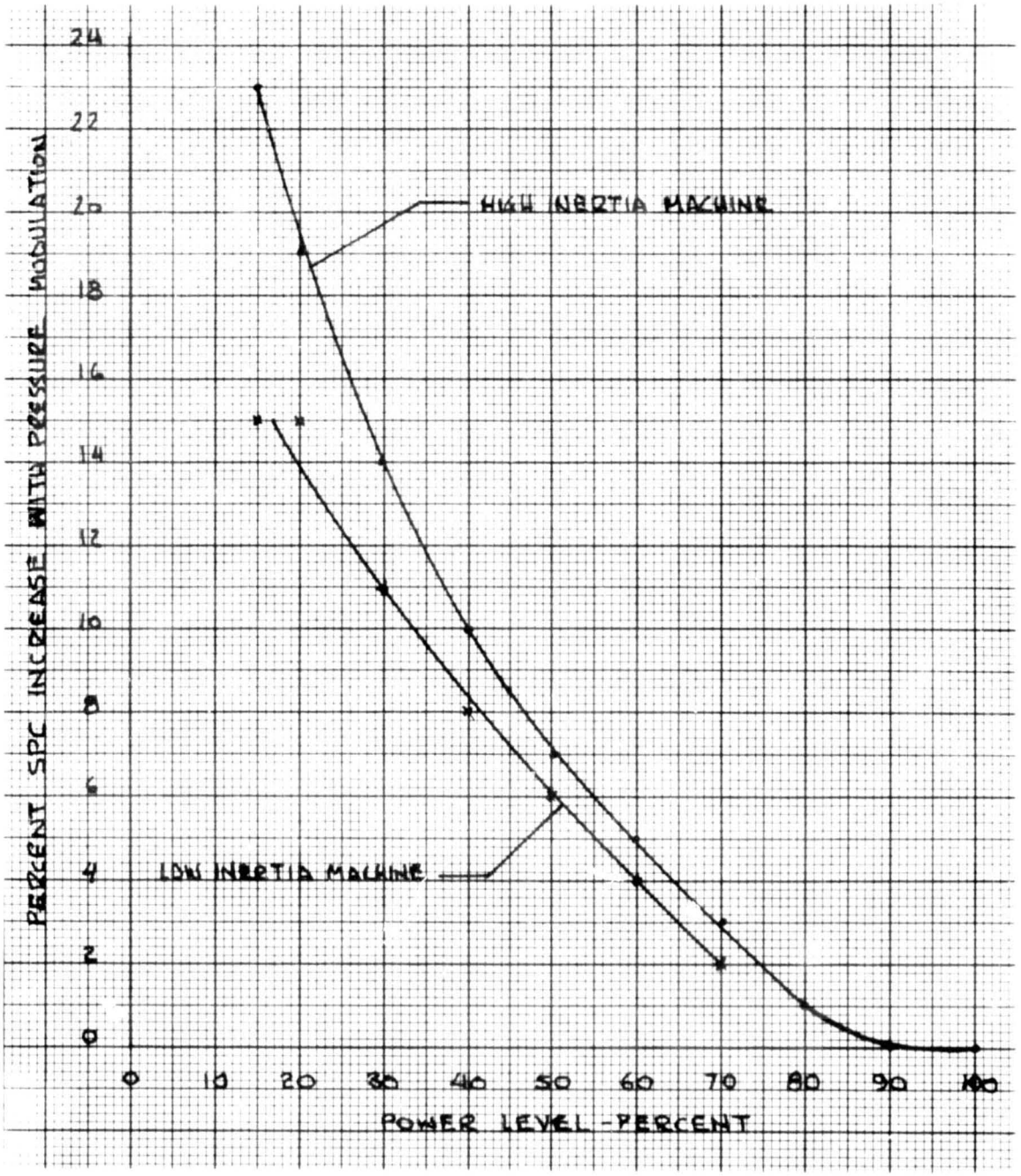

Figure 49. SPC Penalty Associated With Pressure Modulation as a Function of Power Level

flowrate which is required to generate that chamber pressure. For example, for the 60 percent high duty case, measured weight for 86 pulses was 8.551 pounds. Weight per pulse is $\frac{8.551}{86}$ = .0994 pounds. The time-integrated average pressure P = 312.6 psia for a typical pulse. Chamber temperature varied over a range of 1561 to 1598 F during the pulse. Time integrated average temperature was approximately 1585 F which corresponds to a c* of 4265 ft/sec. Then, from the relation

$$\overline{\dot{w}} = \frac{PAg}{\overline{c^*}},$$

average flowrate during the pulse is

$$\frac{312.6 \times 0.0866 \times 32.2}{4265} = 0.2044 \text{ lb/sec.}$$

Pulse duration was 0.5939 second; hence, propellant weight per pulse is 0.2044 x 0.5939 = 0.1214 pounds. This represents a weight consumption 22 percent greater than that indicated by the tank weighing system. Since very carefull and accurate tank measurements were taken, this leads to a conclusion that there was significant varieties in either integrated pressure, throat area, or c* over the 86 pulses to negate use of a single typical pulse.

GAS GENERATOR RESPONSE CHARACTERISTICS

As previously noted, the chamber pressure rise to 90 percent of the full value, required approximately 30 milliseconds after the main valve began to open. The time lag between the injection pressure (P_{1F}) 90 percent point attainment and the corresponding chamber pressure rise was determined to be 15 milliseconds. This time lag is attributable to the void volume of the gas generator system. A calculation, using the General Gas Law (PV=WRT), shows that approximately 22 milliseconds at the design flowrate would be required to provide the mass of gas required to pressurize this void volume. However, since exhaust gas outflow through the nozzle is occurring simultaneously, an even longer P_c rise time might be expected. The much shorter P_c rise time noted (15 milliseconds) results from the higher fuel flow rates which occur with decreased chamber pressure, and some bed temperature readjustments during the valve "OFF" period. The tendency for bed temperature to become more uniform increases the upstream bed temperatures to levels higher than exist at the steady state 100 percent power condition. Consequently, the initial pressure buildup rate is accelerated by virtue of absorption of some of this excess temperature, resulting in higher gas temperatures and pressures than would otherwise exist.

It should be pointed out that the gas generator tested was designed and developed for use with a pressure modulated control system. The ability to operate very stably over a wide range of chamber pressures was an important consideration and resulted directly in the present design. It is very possible that for a pulse mode type of operation, where stability at a rather high chamber pressure would be the sole stability requirements, a smaller chamber might be satisfactory. This would reduce the void volume proportionately and thereby increase the chamber pressure buildup rate.

A gas generator of essentially the same bed configuration as the heater reactor was operated at a bed loading of 0.143 lb/in.^{2}-sec, Ref. 2. The operating chamber pressure in this program was 8000 psia.

This bed loading can be contrasted to the 0.068 lb/in.^{2}-sec bed loading of the subject Space Shuttle APU gas generator. As a first approximation it would appear that the smaller chamber diameter that would be required to increase the bed loading to a similar value would halve the 15 millisecond P_c rise time noted.

HOT RESTARTS

The results of the hot restart tests indicate that propellant manifold temperatures in excess of 550 F are not acceptable. The statistical nature of ignition phenomena is such that a successful start at a 548 F manifold temperature does not guarantee that other attempts at this temperature would not encounter explosions.

It should be noted that the explosion which occurred with the 565 F manifold temperature would not have happened if the firing had been continued. The manifold explosion occurred because the hydrazine velocities were reduced to essentially zero, while the manifold temperature was still high. A longer period of operation would have decreased the manifold temperatures to a safe level. It might be noted that portions of the fuel ignition passages in the Ref. 2 and 3 programs were in the 1100 F temperature range, without causing any apparent problems.

Perhaps the most direct solution to the hot manifold problem would be to monitor the manifold temperature and to maintain propellant flowrate until this temperature decreased to some acceptable level.

THERMAL BED PREHEATING

The ball packed thermal bed pilot gas generator used during part of this program had a previous history of satisfactory operation under somewhat different operating conditions. The Ref. 3 program demonstrated the gas generator operation over a range of chamber pressures of 50 psia to 600 psia. In the Ref. 2 program, chamber pressure conditions in the range of 6,000 psia to 9,000 psia were investigated.

The failures encountered during this program occurred at chamber pressures intermediate between these previously tested ranges. The spiking phenomena encountered would appear to indicate the formation of a relatively low temperature bed zone near the injector, at these particular flowrates, with the possibility of some accumulation of undecomposed hydrazine vapors. The 1/16 inch diameter balls packed in a 1/2 inch I.D. chamber, result in sizeable interstitial void volumes. This would suggest that the use of much smaller balls in the initial portion of the gas generator bed, or the substitution of a fine mesh screen pack for that region would be desirable.

The use of a pilot gas generator for the startup of a larger gas generator was demonstrated in the Ref. 4 program. In this case a catalytic gas generator was used for the pilot stage for the sake of convenience. The pilot gas generator exhaust gases were injected radially into the 1.92 inch I.D. gas generator at four equally spaced ports. The plane of injection was as close to the injector face as was possible.

The time between initiation of the pilot gas generator flow and the point where the main gas generator operation was completely self-sustained was reduced to a total of 18 seconds. Operations with shorter heatup times were not attempted, so the minimum startup time probably would be somewhat shorter.

In principle, this startup technique attempted to create a short bed zone near the injector that was preheated to the temperature condition that would exist under steady state operating conditions for the N_2H_4 flowrate which would be used on start. In addition, of course, the four hot gas injection ports would act as igniters during the period of time that both gas generators were operating simultaneously.

The Space Shuttle APU gas generator was not designed to be compatible with this injection technique. A single 3/16 inch diameter tube, which led the hot gases through the injector body, was used. This resulted in the necessity for the entire injector to become heated to rather high temperatures before effective heating of

the thermal bed could start. In addition, the single port entry of the hot gases resulted in rather slow diffusion of the heat in the radial directions. These factors result in a longer heatup time than for the Ref. 4 system.

It is not believed that the startup time with pilot gas generator preheat system in the configuration employed during the present program could be reduced appreciably below ten minutes. This is in contrast with the demonstrated 18 second startup in the somewhat smaller gas generator used for the Ref. 4 tests.

The use of the pilot gas generator preheat system resulted in a deterioration of the S/N 1 gas generator. The heater-reactor output gas temperatures were in the order of 1600 F. These temperatures were sufficiently high to result in localized temperatures, in the vicinity of the hot gas injector port, that reduced the strength of the "Ni-Oro" braze joints between the injector body and the propellant feed tubes.

Test No. 9, with the S/N 1 gas generator, was aborted when it was noted that at high chamber pressures a small amount of propellant leakage was apparent at the injector. This was the result of the braze porosities that had developed. Further testing was conducted with the S/N 2 gas generator.

CONCLUSIONS

As noted above, the S/N 1 gas generator is still functional, but seepages now occur at a number of tube braze joints. Prior to its use in the present program phase, this gas generator had accumulated 2.48 hours of use, with the last operation on 10/22/73. The present total accumulated time of operation is 3.78 hours.

The S/N 2 gas generator was used to complete the Phase III program. Its accumulated operating time was 18.3 hours, and its last use was on 6/12/73. The gas generator was stored without any special effort to maintain control of humidity or other environmental factors. Its next use, in the present program, was on 11/23/74.

The total accumulated operating time for the S/N 2 gas generator is now 21.9 hours. This includes 4790 "ON-OFF" pulses of varying durations accumulated during the pulse mode tests. The gas generator performance does not show any change relative to its last use in preceding phases of the gas generator demonstration program. In addition, there is no indication of any deterioration which would preclude the probability of meeting a 1000 hour life requirement.

REFERENCES

1. Pressurization Systems Design Guide, Volume III, "Pressurant Gas Solubility in Liquid Propellants," prepared for NASA Contract NAS7-548, McDonnell Douglas Report No. DAC-60510-F1, July 1968.

2. NASA Letter, "Review of Rocketdyne Test Plan for Performance Evaluation of the Hydrazine Gas Generator, Contract NAS9-13003, Modification 5S," dated 16 May 1974.

3. Speeds, J. and L. Kusak, "Feasibility of High-Pressure Hydrazine Gas Generator," AFRPL-TR-74-69, November 1974.

4. Kusak, L., "Preliminary Evaluations of Pilot Hydrazine Gas Generators for the Space Shuttle APU Application," Internal Memorandum No. C&P 73-1, 8 January 1973.

5. Kusak, L., "Preliminary Evaluation of Rapid Start System for the Space Shuttle APU Gas Generator," Internal Memorandum No. C&P 73-22, 22 August 1973.

APPENDIX A

PERFORMANCE DEGRADATION OF A MONOPROPELLANT GAS GENERATOR IN A PULSE RATE MODULATED MODE OF OPERATION

INTRODUCTION

An APU gas generator system necessarily incorporates a speed control valve to regulate hydrazine flow in order to match turbine power against the varying APU load. Liquid hydrazine flow to the gas generator is either modulated or pulsed to achieve the required regulation. Continuous flow modulation (throttled operation) results in a performance degradation at reduced APU power due to the reduction in both turbine inlet pressure and inlet temperature. These contribute to an increase in specific propellant consumption (SPC) because of the reduced head of the fluid being furnished to the turbine.

Pulse modulation of hydrazine flow does not suffer from this type of performance degradation, since, under ideal pulse conditions, flow through the turbine only exists at maximum head (maximum inlet temperature and pressure) conditions. The problem arises from the fact that ideal pulse conditions do not exist. The turbine inlet pressure rise and tail off is affected by the chamber capacitance, valve travel time, and hold up volume between valve and injector. The turbine inlet temperature is affected primarily by thermal capacitance of the bed and possibly by a variation in gas properties due to time dependent variation in ammonia dissociation.

DISCUSSION

Evaluation of power level performance degradation due to continuous modulation is straightforward and involves only the ratio of actual turbine head at reduced power to turbine head at maximum power or:

$$\sigma \text{ (performance degradation)} = \frac{\frac{T}{MW}\left(\frac{\gamma}{\gamma-1}\right)\left[1-\left(\frac{P_o}{P}\right)^{\gamma-1/\gamma}\right]}{\frac{T_M}{MW_M}\left(\frac{\gamma_M}{\gamma_M-1}\right)\left[1-\left(\frac{P_o}{P_M}\right)^{\gamma-1/\gamma}\right]}$$

where

T = turbine inlet temperature
P = turbine inlet pressure
γ = ratio of specific heat
MW = mol. weight
P_o - ambient pressure
(subscript M refers to maximum power conditions)

Evaluation of power level performance degradation due to pulse modulation involves knowledge of the time dependent variation of flowrate, gas pressure, temperature, and chemical properties. An example of an ideal and actual pulse characteristic is shown in Fig. A-1. Pulse performance may be defined as the ratio of the energy delivered to the turbine per pulse to the pounds of propellant consumed during a pulse. This ratio is the pulse specific energy.

$$E_{sp} \text{ (Specific Energy)} = E_p/W_p$$

where

E_p = energy content of a pulse, Btu
W_p = propellant consumed, lbs

The energy content of a pulse,

$$E_p = \int_{t=0}^{t=\theta_p} \Delta h \, \dot{w} \, dt$$

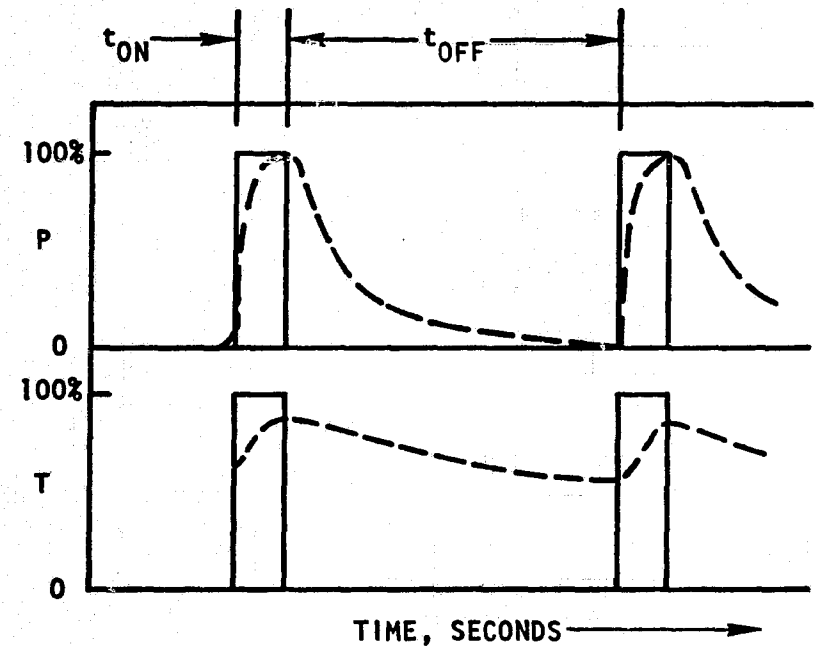

θ_P (PULSE PERIOD) = $t_{ON} + t_{OFF}$

——— IDEAL PULSE

- INSTANTANEOUS VALVE MOTION
- ZERO HOLD UP VOLUME
- ZERO FLUID CAPACITANCE
- ZERO THERMAL CAPACITANCE

– – – – ACTUAL PULSE

Figure A-1. Typical Pulse Performance

where

Δh = instantaneous isentropic head, Btu/lb

$\dot{w}$ = instantaneous flowrate, lb/sec

θ_p = pulse period, secs

The isentropic head,

$$\Delta h = \frac{R}{J} T \left(\frac{\gamma-1}{\gamma}\right) \left[1 - \left(\frac{P_o}{P}\right)^{\gamma-1/\gamma}\right]$$

The flowrate may be calculated as follows, assuming a choked condition

$$\dot{w} = \frac{PA_e}{\sqrt{RT}} \sqrt{g\gamma\left(\frac{2}{\gamma+1}\right)^{\gamma-1/\gamma}}$$

where

$$R = \frac{R' \text{ (universal gas constant)}}{\text{Molecular weight}}$$

A_e = effective turbine inlet nozzle area

Pulse performance degradation is defined as the ratio of the pulse specific energy, E_{sp} to the ideal pulse specific energy $(E_{sp})_i$. The ideal pulse specific energy assumes a square wave in turbine inlet pressure, temperature and flowrate (see Fig. 1); then

$$(E_{sp})_i = \frac{\Delta h_i \dot{w} t_{ON}}{\dot{w} t_{ON}} = \Delta h_i = \frac{R}{J} T_i \left(\frac{\gamma_i - 1}{\gamma_i}\right) \left[1 - \left(\frac{P_o}{P_i}\right)^{\gamma-1/\gamma}\right]$$

where the subscript, $_i$ denotes ideal square wave conditions.

If it is assumed that during a pulse, the deviation from ideal exit gas conditions does not result from a significant variation in ammonia dissociation, then

the gas properties may be considered time independent. Assuming, also that the turbine inlet nozzle effective area is time independent. Then

$$E_{sp} = \frac{\int_{t=0}^{t=\theta_p} \Delta h \dot{w}\, dt}{\int_{t=0}^{t=\theta_p} \dot{w}\, dt} = \frac{\frac{R}{J}\left(\frac{\gamma-1}{\gamma}\right) \int_{t=0}^{t=\theta_p} P\sqrt{T}\left[1 - \left(\frac{P_o}{P}\right)^{\gamma-1/\gamma}\right] dt}{\int_{t=0}^{t=\theta_p} \frac{P}{\sqrt{T}}\, dt}$$

Finally, the pulse perfomrance degradation may be written:

$$\sigma_P = \frac{\int_{t=0}^{t=\theta_p} P\sqrt{T}\left[1 - \left(\frac{P_o}{P}\right)^{\gamma-1/\gamma} dt\right]}{T_i\left[1 - \left(\frac{P_o}{P_i}\right)^{\frac{\gamma-1}{\gamma}}\right] \int_{t=0}^{t=\theta_p} \frac{P}{\sqrt{T}}\, dt}$$

Computer Program

A computer program was written for the GE Timesharing system in order to evaluate the pulse degradation function (θ_p) given above. A listing of the program is included in this report as Table A-1.

The variables listed in the line 160 "Read" statement are defined as follows:

- P - atmospheric pressure for GG exhaust, psia
- P1 - chamber pressure, ideal (steady state), psia
- T1 - exhaust gas temperature, ideal (steady state), F
- G - Gamma function
- S - "ON" time - sec
- SO - Total time (cycle period) - sec

X - For an input of 0, program calcualtes a uniform time increment between data points, utilizing other input information

For an input other than 0, a variable time interval between data points is assumed and these intervals are entered along with the other data

Y - Number of data points

TABLE A-1. PULSE DEGRADATION COMPUTER PROGRAM

```
RUN
PULSE

100  PRINT "APU GG PULSE PERFORMANCE DEGRADATION"
110  PRINT
120  PRINT "UNITS OF INPUT PRESS AND TEMP ARE PSI ABS AND DEG F"
130  PRINT "MAX NO. OF DATA POINTS IS 800"
140  PRINT
150  PRINT
160  READ P,P1,T1,G,S,S0,X,Y
170  LET G0=(G-1)/G
180  LET P=(T1+460)*(1-(P/P1)↑G0)
190  PRINT "P ATM","P IDEAL","T IDEAL","GAMMA"
200  PRINT P,P1,T1,G
210  PRINT
220  PRINT "ON TIME","TOTAL TIME","INCREMENT","POINTS"
230  IF X=0 THEN 260
240  PRINT S,S0,"VARIABLE",Y
250  GO TO 280
260  LET S1=S0/(Y-1)
270 PRINT S,S0,S1,Y
280 PRINT
290 DIM P(800),T(800),S(800),N(800),D(800)
300 FOR I=1 TO Y
310 READ P(I)
320 NEXT I
330 FOR I=1 TO Y
340 READ T(I)
350 LET T(I)=T(I)+460
360 LET N(I)=P(I)*SQR(T(I))*(1-(P/P(I))↑G0)
370 LET D(I)=P(I)/SQR(T(I))
380 NEXT I
390 LET Q=0
400 LET R=0
410 FOR I=1 TO Y-1
420 IF X=0 THEN 450
430 READ S(I)
440 GO TO 460
450 LET S(I)=S1
460 IF I>1 THEN 490
470 LET M=(N(2)-N(1))/S(1)
480 LET N=(D(2)-D(1))/S(1)
490 LET Q=Q+S(I)*(N(I)+(N(I+1)-N(I))/3+M*S(I)/6)
500 LET R=R+S(I)*(D(I)+(D(I+1)-D(I))/3+N*S(I)/6)
510 LET M=2*(N(I+1)-N(I))/S(I)-M
520 LET N=2*(D(I+1)-D(I))/S(I)-N
530 NEXT I
540 LET E=Q/(8*R)
550 PRINT "PULSE PERFORMANCE DEGRADATION ="E
560 GO TO 140
```

APPENDIX B

THERMAL BED PACKING PROCEDURE

Bed Compaction

Early IR&D and contract tests, conducted with various screen packs, resulted in compaction of the screen pack during operation of the gas generator. In some instances it was observed that compaction increased with successive firings. The most extensive compaction was observed after a successful series of tests with the same gas generator. In this case, a 2-inch void had formed at the injector end of the gas generator. Although the test was successful, changes in the bed are undesirable since a gap at the injector end could be hazardous and performance might become unpredictable.

Packing Procedure

To eliminate bed compaction during operation, a packing technique was developed that has eliminated bed compaction even after 10 MDC's, acceptance tests and a 500 sec full power burn, (18 hrs of operation).

This procedure consists of mounting the gas generator in a tensil tester and applying a predetermined load to the screens as they are packed. The load applied to the bed is a function of contact area between screens and screen settling load and spring rate. Yield was established experimentally at 30,000 lb_f, settling load at 3000 lb_f and spring rate at 527,000 lb/in. Based on stress-strain curves and anticipated thermal expansion, the gas generator Model 268-560 was packed using a 3000 lb applied force with a "not to exceed" 5000 lb limit. The actual bed packing dimensions for gas generator Model 268-560 S/N 02 are shown in Table B-1. These dimensions were established as follows:

$$p.f. = \frac{L_I}{L_A}$$

where:

$p.f.$ = packing factor

L_I = length ideal

L_A = length actual

for regular weave,

$$L_I = 2\,(D_w)(n)$$

$$p.f. = \frac{2\,(D_w)(n)}{L_A}$$

where:

D_w = wire diameter

n = number of screens

For 16 mesh x 0.035 in. dia. screen

$$L_A = \left[\frac{2(0.035)}{0.95^*}\right]n = (0.0737)n$$

*p.f. is based on experimental data

Therefore, for a 4-inch bed with 16 x 0.035 screens

$$n = \frac{L_A}{0.0737} = 54 \text{ screens}$$

It should be noted that bed length (L_A) is measured after the load has been released.

TABLE B-1. BED PACKING DIMENSIONS

		Design	Measured	
Screen Size, in.	Screen Quantity	Screen Stacking Height, in.	Stacking Height, in.	Applied Load, lb.
16 by .035	10	0.74	1.300	3000
	20	1.48	2.060	3000
	30	2.22	2.800	3000
	40	2.96	3.560	3000
	50	3.70	4.300	3000
	53	4.00	4.530	3000
26 by .015	20	4.61	5.130	3000
	40	5.22	5.730	3000
	60	5.83	6.330	3000
	80	6.44	6.940	3000
	100	7.05	7.580	3000
	120	7.66	8.120	3000
	128	8.03	8.340	3000

APPENDIX C

GAS GENERATOR DESIGN EVOLUTION

The initial design of the gas generator for this program consisted of a 1.89 in. diameter bed by 8 inches long with a stand-off showerhead injector. This gas generator was used to evaluate initiation methods. Three different methods were investigated.

1. Internal electric heater
2. External electric heater
3. Hot gas supply

INTERNAL ELECTRIC HEATER

Successful initiation of a flight-type gas generator was demonstrated. Utilizing 500 watt electric power, the upper portion of the bed rose to 810 F in 10 minutes; see Fig. C-1. This is sufficiently high to start hydrazine flow. The injector face rose to a maximum of 250 F in that time and the chamber wall to 500 F. The problem associated with this initiation approach involves gas generator steady-state operating characteristics over the power range. Installation of the heater and fins caused the front bed section to be ineffective by inhibiting hydrazine decomposition. This resulted in a very low bed pressure drop and instability as well as high exit gas temperatures. A number of tests were conducted that exhibited chugging. After the final test, during start of purge, hydrazine detonated in the upper end of the chamber. Based on the poor operational characteristics of the gas generator, the internal heater was discarded.

EXTERNAL ELECTRIC HEATER

Based on previous IR&D testing, it had been established that approximately 35% of the electric power is converted into useful heat energy to raise the temperature of a fully insulated gas generator assembly. With respect to a

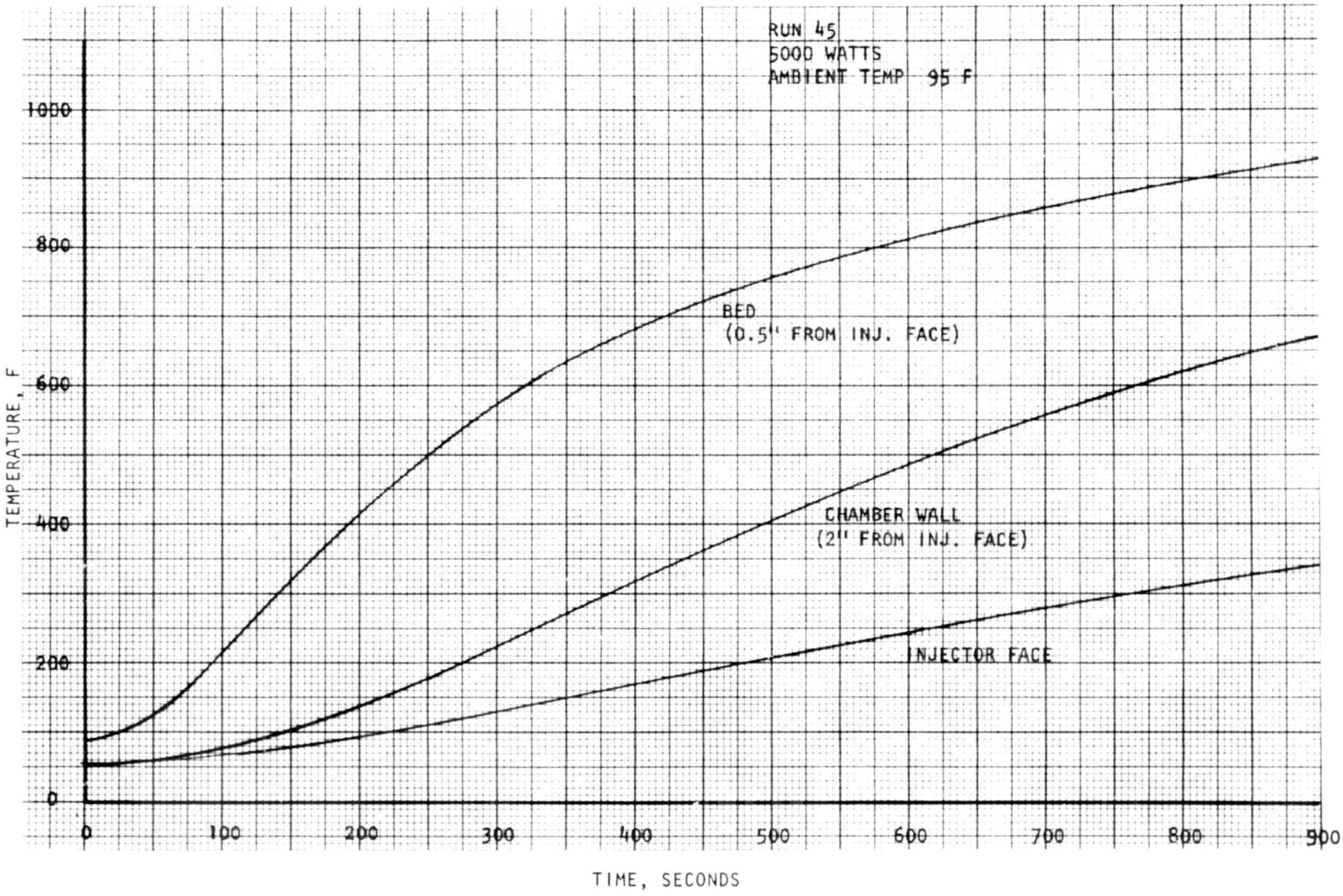

Figure C-1. Electric Heater Initiation Test

flightweight design, it is estimated that approximately 1.25 KW of electric power would be required to raise the bed to 700 F in 15 minutes.

HOT GAS SUPPLY

Initiation of the gas generator through the use of hot gas injection into the bed had been demonstrated during IR&D testing in which heated nitrogen gas was introduced through an opening in the injector. The upper bed section was brought to 670 F in 20 minutes with nitrogen gas heated to 1000 F. Nitrogen flowrate was 0.185 lb/sec. Approximately a 250 to 300 F temperature drop resulted from heat losses prior to reaching the chamber bed. Based on this data a bed time constant of approximately 9.0 minutes was calculated. Using a pilot flow rate of 2% of maximum power flow, i.e., 0.0074 lb/sec, at 1600 F, an upper bed temperature of 700 F can be attained in 12.7 minutes.

Based on the demonstrated initiation technique with heated gas, a 1.91 inch diameter bed by 8 inches long was assembled for MDC* testing. The same style stand-off injector was used with a gas inlet substituted for the internal heater.

The gas generator performed satisfactorily for 4 MDC's. During the fifth MDC, an explosion occurred. During these tests, the screen pack settled (compacted) resulting in a 2-inch void at the injector end of the gas generator. Bed compaction occurs progressively, thus one must conclude that the gas generator operated properly with void spaces ranging up to 2 inches. Therefore, the explosion cannot be attributed solely to bed compaction. This chamber was fabricated with Inconel 600 which is a very ductile material and does not embrittle due to nitriding. It was postulated that progressive bulging of the chamber occurred during test until a sufficient pocket (channel) was formed where undecomposed hydrazine could accumulate and then explosively decompose. Based on these results, the flight-type gas generator described in this report was designed using Haynes 188 as the structural chamber wall.

---

*MDC – Mission Duty Cycle

APPENDIX D

THROTTLE VALVE

The proposed space shuttle APU incorporated a pressure modulated control system. Therefore, the gas generator requirements included operation over a 10:1 turn-down ratio which was achieved by incorporating a throttle valve. Investigation of suitable throttle valves resulted in purchasing two throttle valves from Moog, Inc. under this program and one throttle valve from E-Systems, Inc. for an IR&D effort.

The two Moog throttle valves, delivered with the gas generators to the Air Force, are of the rotary band type. These valves were bench tested while gas generator testing was continuing with the E-System valve. Both valves met all the required specifications. Typical results from these bench tests are shown in Fig. D-1.

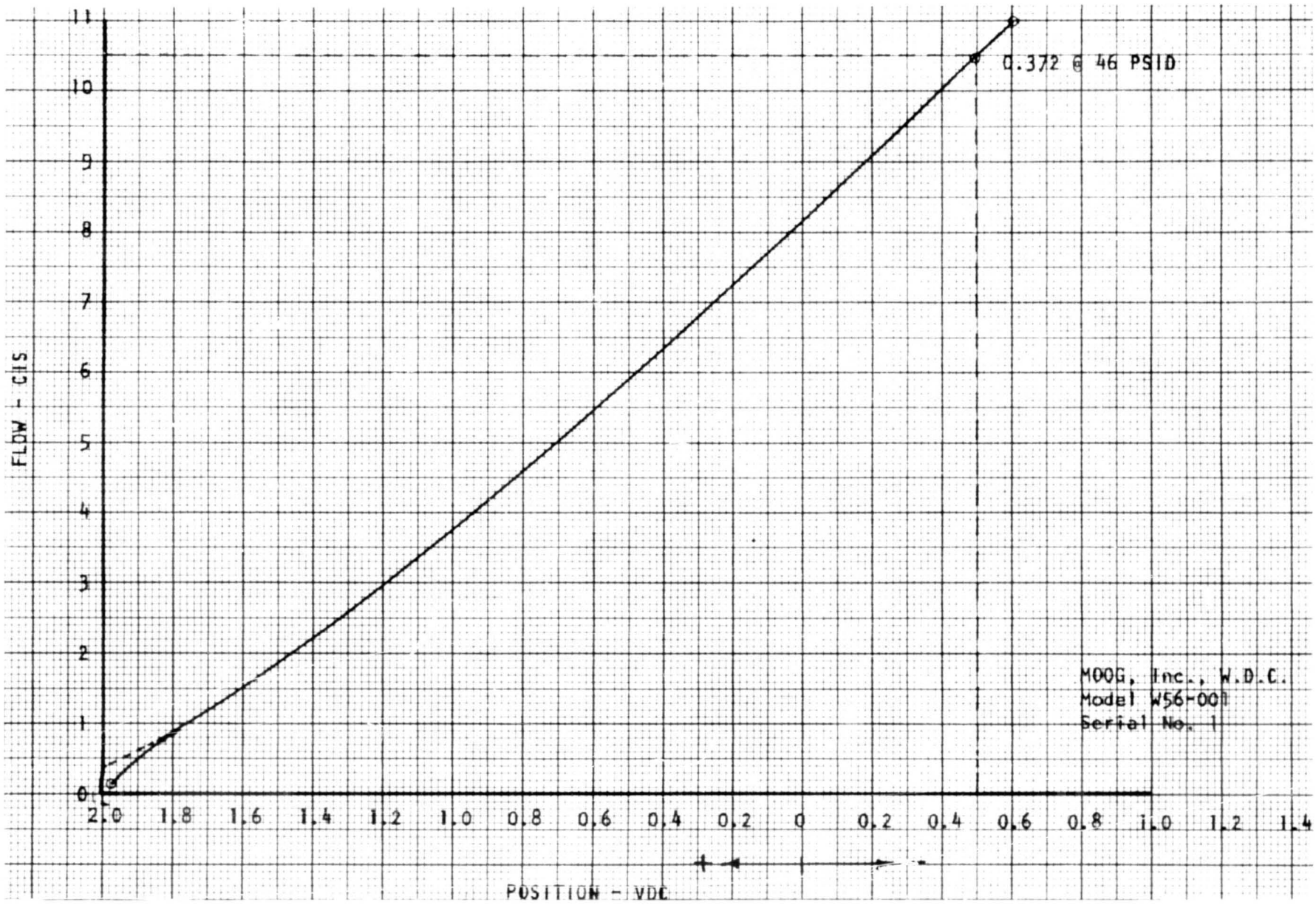

Figure D-1. Rotary Fuel Control Band Valve